DISCOVERING THE GENOMIC ARCHITECTURE OF CELL-TYPE SPECIFIC GENE REGULATION USING GENETICALLY DIVERSE STRAINS OF MICE

by

ADRIANNA MARIA JUREK

A dissertation submitted in partial fulfillment of the
requirements for the degree of

DOCTOR OF PHILOSOPHY IN BIOLOGICAL AND BIOMEDICAL SCIENCES

2025

Oakland University
Rochester, Michigan

Doctoral Advisory Committee:

Randal Westrick, Ph.D., Chair
Gerard Madlambayan, Ph.D.
Shailesh Lal, Ph.D.
Valance Washington, Ph.D.

© Copyright by Adrianna Maria Jurek, 2025
All rights reserved

To my future husband—thank you for constantly pushing me to write my "book", even though I rolled my eyes every time. Your support, encouragement, and constant belief in my capabilities helped me more than you know. Knowing that you speak about me with such pride, even when I'm not around, means the world to me.

To my parents— thank you for bragging about your scientist daughter, even if you still ask me exactly what it is that I do.

To my puppy—thanks for bringing such joy into my life, even if you're sure to give me more grey hair than writing this dissertation ever did.

ACKNOWLEDGMENTS

I would like to express my deepest gratitude to my PhD advisor, Dr. Randal Westrick, for his unwavering support, guidance, instruction, and belief in my abilities. Just over four years ago, Dr. Westrick offered me a PhD position in his lab, which changed the direction of my future, allowing me to accomplish my lifelong goal of becoming a doctor. I would not be here, writing my dissertation, without his steady mentorship, encouragement, and belief in me, even when I doubted myself and my skills. His guidance shaped the course of my research, but also significantly influenced my growth as an independent thinker and problem solver. Both in and out of the lab, Dr. Westrick has helped me grow as a person, and I am forever thankful for the opportunity to work under his leadership. I could not have asked for a better mentor.

I would also like to acknowledge my lab mates, both present and past, who have been with me through it all. Caitlin Schneider, Arina Rodionova, Arina Kozina, Kailey MacFadyen, and Katherine Lichtenberg, thank you for always being there when I needed someone to vent to, to bounce ideas off, and to help with tasks, even if they *probably* could have been done solo. My PhD experience would not have been the same without you.

Lastly, I would like to acknowledge the support I have received from the Department of Biological Sciences, as well as my committee. Without your guidance, your support, and your constant willingness to help in any situation, I would not have been able to make it through the program as smoothly as I did.

This research was supported by the National Institutes of Health, National Heart, Lung, and Blood Institute (NHLBI) Grant R15-HL133907, DAMOS NSF NRT grant #2152007, M-KUHR training grant, TL1DK136046, AHA AIREA Research Grant 23AIREA1055261 and the American Heart Association Strategically Focused Research Network on Inflammation in Cardiac and Neurovascular Disease.

Adrianna Maria Jurek

PREFACE

Ever since I was young, I wanted the title of "doctor". As I approach the end of this journey, I find it appropriate to reflect on how I got here and the challenges I faced along the way. I knew of thrombosis from a relatively young age due to personal circumstances, and I have been interested in genetics for as long as I can remember. Still, I never thought I would be working in a lab investigating the genetic controls of this deadly process.

My research investigating the genomic architecture of cell-type specific gene regulation has been my life for nearly four and a half years, and it has not been without struggles. I've faced experiments that refused to work, ELISA kits that turned out to be faulty, grant rejections for nearly *every* grant I applied for, and the disaster of spilling thousands of freshly autoclaved pipette tips in the elevator. Through it all, I have learned how to confront failure, accept criticism, solve problems creatively, and navigate the consequences of my own questionable choices. Despite the setbacks and roadblocks, I feel proud of the work that I have done. I feel strongly that my work has expanded our understanding of the genetic controls of clotting disorders but also will serve as a steppingstone for more personalized medicine, helping those at risk for and affected by thrombosis. Reaching this point has taken perseverance, growth, determination, and the support of many, and I am deeply grateful.

ABSTRACT

DISCOVERING THE GENOMIC ARCHITECTURE OF CELL-TYPE SPECIFIC GENE REGULATION USING GENETICALLY DIVERSE STRAINS OF MICE

by

Adrianna Maria Jurek

Adviser: Randal Westrick, Ph.D.

In developed nations, thrombosis remains the most common cause of death, with myocardial infarction (MI) and stroke causing the most fatalities in the United States. Hemostasis, the highly regulated process of clot formation and dissolution, involves the complex interactions of diverse cell types and regulatory molecules, including clotting factors, fibrinolytic proteins, as well as components packed into vascular cells such as platelets and endothelial cells. Proper balance of this system is vital to prevent blood loss and unwanted clotting. Although the mechanisms of coagulation have been well characterized, the genetic regulation of essential molecules in the cell types contributing to hemostasis has not been well understood.

To address this gap, I investigated the genetic regulators of three important coagulation and fibrinolysis molecules: Coagulation Factor V (FV), Plasminogen Activator Inhibitor 1 (PAI-1), and Protein C (PC). The appropriate regulation of these molecules is necessary for promoting hemostasis and fibrinolysis (the process of dissolving a clot) in the correct balance to maintain the physiological “status-quo”.

I used inbred mice with natural differences in their antigen levels to generate four genetically informative crosses. I measured the antigen levels for all three proteins in the

plasma and platelets of the strains and received genotyping data using miniMUGA to use in Quantitative Trait Loci (QTL) analyses to discover unique genetic regulators.

This approach revealed a significant locus on Chromosome 1 when analyzing the plasma FV in one cross, and one significant and one suggestive locus when sex was included as a covariate for platelet FV. For platelet PAI-1, a major locus on Chromosome 5 was identified in all 4 crosses with suggestive loci identified in three crosses. Lastly, a suggestive locus on Chromosome 7 when using sex as an additive covariate was found when analyzing PC levels in the plasma.

My findings offer improved insight into the cell-type specific regulatory pathways of these essential coagulation molecules. Enhanced understanding of physiological and pathogenic regulatory pathways may lead to future novel therapeutic strategies for humans.

TABLE OF CONTENTS

TABLE OF CONTENTS—Continued

TABLE OF CONTENTS—Continued

TABLE OF CONTENTS—Continued

LIST OF TABLES

LIST OF FIGURES

LIST OF ABBREVIATIONS

129S1	129S1/SvImJ Mouse Strain
APC	Activated Protein C
aPTT	Activated Partial Thromboplastin Time
B6	C57BL/6J Mouse Strain
BALB	BALB/cJ Mouse Strain
BCA	Bicinchoninic Acid
BCP	B- Cell Progenitors
BSGC	Buffered Saline Glucose Citrate
cDNA	Complementary DNA
CAST	CAST/EiJ Mouse Strain
Chr	Chromosome
CVD	Cardiovascular Disease
DBA	DBA/2J Mouse Strain
DIC	Disseminated Intravascular Coagulation
DEPC	Diethyl Pyrocarbonate Treated Water
ELISA	Enzyme-Linked Immunosorbent Assay
EPCR	Endothelial Protein C Receptor
F1	First Filial Generation
F2	Second generation of offspring from cross-breeding (F1 x F1)
FIX	Coagulation Factor IX
FV	Coagulation Factor V

FVa	Active Coagulation Factor V
FVIIIa	Active Coagulation Factor VIIi
FVL	Factor V Leiden
FXa	Active Coagulation Factor X
FXIIIA	Coagulation Factor FXIII Subunit A
HSC	Hematopoietic Stem Cell
IACUC	Institutional Committee on Use and Care of Animals
LOD	Logarithm of the Odds
miniMUGA	Mini Mouse Universal Genotyping Array
PA	Plasminogen Activator
PAI-1	Plasminogen Activator Inhibitor 1
PC	Protein C
pPAI-1	Platelet Plasminogen Activator Inhibitor 1
$Proc^{-/-}$	Protein C Deficiency
PS	Protein S
PT	Prothrombin Time
QTL	Quantitative Trait Loci
RIPA	Radioimmunoprecipitation Assay Buffer
SPF	Specific Pathogen Free
SNP	Single Nucleotide Polymorphism
TAD	Topologically Associated Domain

TFPI	Tissue Factor Pathway Inhibitor
TFPIα	Tissue Factor Pathway Inhibitor Alpha
TMB	3,3′,5,5′-Tetramethylbenzidine
tPA	Tissue Plasminogen Activator
uPA	Urokinase Plasminogen Activator

CHAPTER ONE

INTRODUCTION

1.1 Cell-Type Specific Gene Regulation and Hemostasis

Thrombosis is the most common cause of death in developed countries, with myocardial infarction (MI) and cerebrovascular accidents accounting for the majority of deaths in the United States[1]. Under physiological conditions, the formation of a blood clot is a tightly regulated process essential for hemostasis, which prevents bleeding following vascular injury. The pathways responsible for clot formation and dissolution are extremely complex, comprised of numerous regulatory molecules, including clotting factors and fibrinolytic proteins. These molecules work in harmony to tightly control the process of coagulation, ensuring that blood clots are formed where necessary and dissolved when the blood loss has ceased[2,3]. Alterations in the normal levels of these factors alter the body's ability to regulate this complicated system, leading to thrombosis or hemorrhage[4].

In addition to these molecular regulators, several cell types play critical roles in the hemostatic response. Hepatocytes, platelets (and their precursors, megakaryocytes), and endothelial cells contribute to different aspects of clot formation and regulation. Hepatocytes play a major role in both the synthesis and clearance of vital circulating hemostatic proteins, and alteration of liver function can induce both pro- and anti-coagulant changes to the hemostatic system[5,6]. Platelets are derived from megakaryocytes, and their accumulation at the site of injury is one of the first steps in the

formation of a blood clot[7,8]. Platelets are also vital to the coagulation cascade, contributing to platelet adhesion, activation, aggregation, and thrombin generation[7]. Endothelial cells function in the coagulation cascade in both a pro- and anti-coagulant manner upon vascular injury, helping to localize clotting to injured areas while preventing the spread of clots to areas of the body where they are not needed.[9] Disruption of any of these cellular functions can affect the hemostatic balance and increase susceptibility to hemorrhage or thrombosis.

As these cell types are the key players in the coagulation cascade, understanding the nuances of gene regulation and expression for each cell type is vital for unraveling both normal hemostatic control and pathogenic thrombosis. There have been many recent advances in genomics and transcriptomics that have provided insight into how gene regulation varies by cell type in the context of hemostasis and thrombosis. Several studies have begun to uncover these genetic regulatory mechanisms and their association with thrombotic phenotypes. For example, eQTL variants, including one linked to arterial thrombosis [10] and a regulator of platelet activation [11,12] have been identified. Another example includes the *Mvwf1* mutation in mice, which causes *B4galnt2* expression to switch from the intestinal epithelium to the vascular epithelium due to a cis-regulatory switch. von Willebrand Factor, a critical protein in hemostasis, was found to be abnormally glycosylated due to this switch, causing rapid clearance[13].

There have been multiple studies showing the effect of MicroRNAs (miRNA) on the expression of coagulant and anticoagulant proteins in the vascular endothelium. Abherent expression of these miRNAs can lead to alterations in the coagulation cascade, and both promote and inhibit the formation of thrombotic clots[14].

The sex-linked disease Hemophilia B Leyden is characterized by a severe hemorrhagic phenotype early in life due to extremely low factor IX (FIX) levels but exhibits increased FIX levels and subsequent normal coagulation function after puberty. Due to the presence of increased functional FIX levels later in life, Hemophilia B Leyden is not caused by a structural deficit or a modification to the structural gene and instead could be a result of altered regulatory elements affecting the early expression of FIX[15].

Additional studies have shown just how complex transcriptomic regulation is in hemostasis. Kida et al. characterized transcription factor binding sites in a regulatory region upstream of the coagulation factor XIII subunit A (FXIIIA) gene which controls the expression levels of FXIIIA in megakaryocytes and monocytes[16]. Multiple sites playing key roles in the expression of FXIIIA were found within the promotor region, as well as more nuanced control due to transcription factor binding in an enhancer/silencer region[16]. Another study shows that the three distinct expression levels of FXIIIA protein in leukemic B-cell progenitors (BCP) seen in patients with BCP-acute lymphoblastic leukemia are each associated with a distinct gene expression pattern. The differential expression of FXIIIA corresponds with differential expression of multiple other genes, suggesting there are common transcription factors regulating both FXIIIA and these genes' expression within BCPs[17].

Analysis of regulatory elements involved in the megakaryocyte-specific expression of the thrombopoietin receptor gene reveals multiple factors that coregulate this cell-type-specific expression. Important elements include GATA and ETS nuclear factor binding sites; however, those elements alone are not enough to completely isolate

expression to megakaryocytes, and other factors are also required to cause total cell-type specificity[18].

A similar complexity in regulation is observed in other megakaryocyte-specific genes, such as α_{IIb}, part of a surface receptor protein complex involved in the activation of platelets. Block et al. characterized the impact that nuclear factor binding sites in the 5' flanking region of the α_{IIb} gene have on its expression and proposed a model by which the factors immediately upstream of the gene, specifically SP1, ETS, and GATA elements, interact with each other and other proteins to promote transcription[19].

Together, these findings show how cell-type specific gene regulation contributes to maintaining hemostatic balance, and how disruption to these regulatory networks can lead to thrombosis or hemorrhage. However, many of the regulatory elements influencing proteins involved in the coagulation cascade remain genetically uncharacterized. To address this, my research focuses on three proteins with known roles in thrombosis: Coagulation Factor 5 (*F5,* FV), Plasminogen Activator Inhibitor 1 (*Serpine1,* PAI-1), and Protein C (*Proc,* PC) to investigate their cell-type-specific genetic control. To investigate the genetic regulation of these proteins, we turned to inbred mouse strains with natural variations in their protein levels. Due to their shared ancestry, the availability of sequencing information[20] and the novel combination of alleles due to meiotic recombination, inbred mouse strains are extremely useful for this type of analysis. By using F2 crosses of these mice, quantitative trait locus (QTL) analysis, genotyping data, and measured antigen levels in F2 mice, we can better understand how these important proteins are regulated and how they contribute to thrombosis. The workflow is shown in Figure 1.

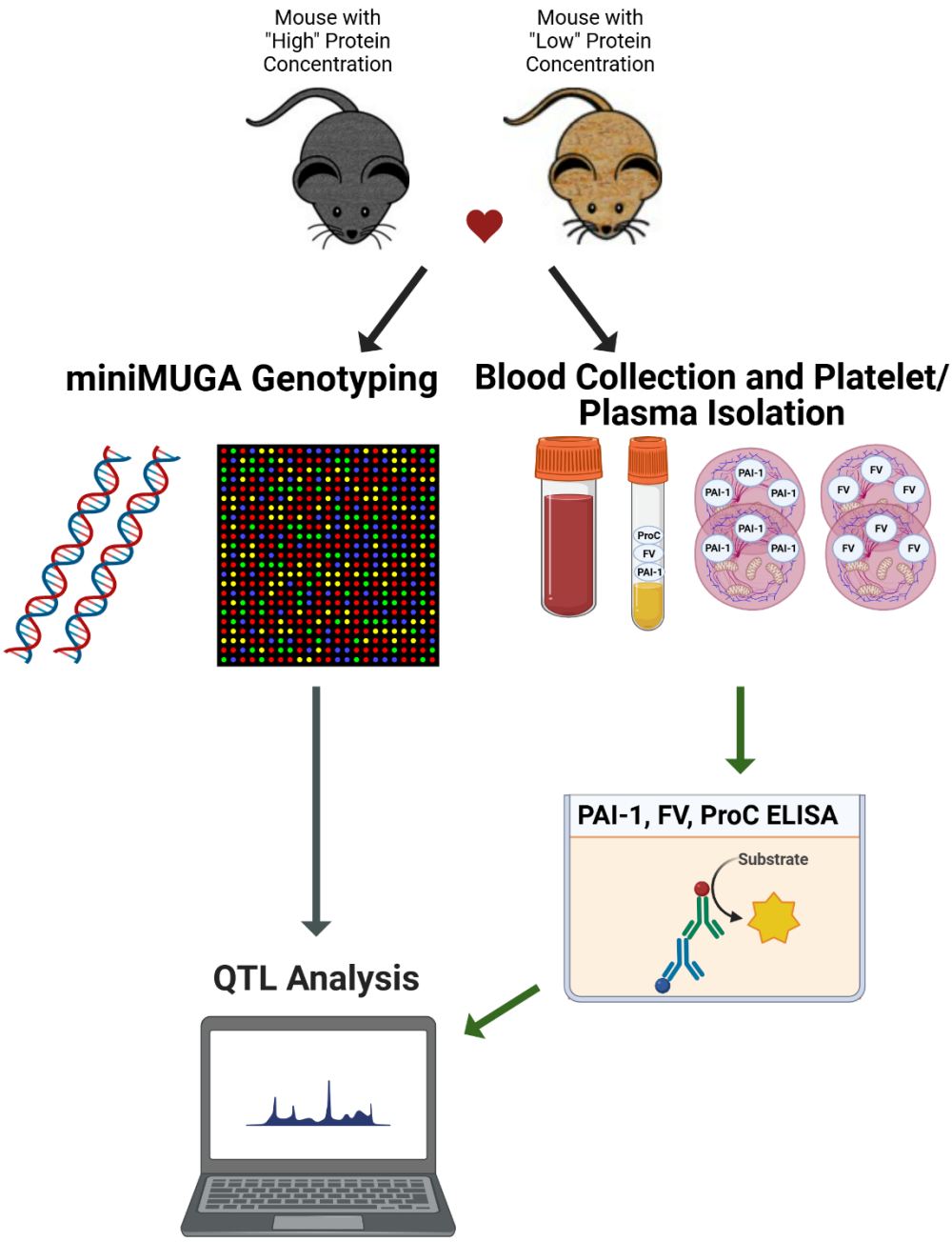

Figure 1: Workflow of Dissertation.

CHAPTER TWO

IDENTIFICATION OF SIGNIFICANT REGULATORY LOCI FOR MEGAKARYOCYTE AND HEPATOCYTE COAGULATION FACTOR V EXPRESSION IN MICE

2.1 Introduction

FV is a critical protein in the coagulation cascade. In its active form (FVa), FV is a necessary cofactor for activated factor X (FXa) in the prothrombinase complex, which produces thrombin and amplifies coagulation[21]. FV is also active in an anti-coagulant manner with Protein S (PS) as a cofactor for activated protein C (APC), inhibiting coagulation factor VIIIa (FVIIIa)[22] for tissue factor pathway inhibitor (TFPI) to inhibit FXa[23]. In blood, FV is present in two compartments: 80% circulating in the plasma and 20% sequestered in the platelet alpha-granules[24,25]. In humans, FV is produced by the liver hepatocytes, contributing to the FV circulating in the plasma pool. The plasma FV is endocytosed by megakaryocytes and stored in platelet alpha granules[26,27]. This differs in mice, with the hepatocytes producing the circulating plasma FV[24], and the megakaryocytes producing platelet FV directly[28]. Platelet FV is prothrombotic and increasing levels of platelet FV lead to decreased time to occlusion in a carotid artery injury mouse model [29]. Deficiency in FV causes mucosal lining and post-trauma bleeding, and complete FV loss is incompatible with life[30].

Studies have shown that APC cleaves and inactivates FVa[31] and TFPIα binds with partially cleaved FV or platelet FV to prevent assembly of the prothrombinase complex[30,32]. Additionally, the FV Leiden (FVL) mutation, which is associated with thromboembolic diseases and APC resistance[31] is well documented[33]. Recently, *PLXDC2*

has been shown to correlate with the modulation of FV expression[34] and *PSKH2* has been found to play a role in the variability of FV activity[35], but otherwise little is known about the genomic regulation of this critical procoagulant and anticoagulant protein, which is positioned at the center of coagulation. Here, we identified natural variations in platelet and plasma FV levels of inbred mice and then used QTL mapping to identify genomic loci regulating FV expression.

2.2 Methods

2.2.1 Mouse Strains

Five mouse strains were acquired from The Jackson Laboratory. C57BL/6J (B6, Stock Number 000664), DBA/2J (DBA, Stock Number 000671), A/J (Stock Number 000646), CAST/EiJ (CAST, Stock Number 000735), and 129S1/SvImJ (129S1, Stock Number 002448).

2.2.2 Generation of F2 Mice

Female DBA mice were outcrossed to male CAST mice to generate CASTD2F1 (F1) mice. Male and female F1 mice were intercrossed to generate the CASTD2F2 (F2) generation. The F2 mice were then used in subsequent experiments. All experiments with these mice follow the guidelines of Oakland University's Institutional Committee on Use and Care of Animals (IACUC).

2.2.3 Isolation of Plasma

Whole blood was collected via cardiac puncture from 15 B6, 15 DBA, 17 A/J, 14 129S1, 12 CAST, 19 F1, and 61 F2 mice and diluted 9:1 in 3.2% buffered sodium citrate

(Medicago, Aniara Diagnostica) using the techniques detailed in Brake et al[36]. Briefly, blood samples were centrifuged at 5000 x g for 10 minutes at room temperature. The plasma supernatant was transferred to a new tube and then centrifuged for 10 minutes at 5000 x g at room temperature. Platelet Poor Plasma was stored at -80 °C until required for experiments. An approximately equal number of males and females was used for each strain (26 M and 35 F F2s).

2.2.4 Isolation of Platelets

Platelets were isolated from 18 B6, 14 DBA, 12 A/J, 17 129S1, 13 CAST, 20 F1, and 85 F2 mice. Whole blood was diluted 20:1 with acid citrate dextrose/prostaglandin E1 (1mM cocktail) during exsanguination by cardiac puncture[36]. Blood was diluted 1:1 with buffered saline glucose citrate (BSGC, 129 mM NaCl, 13.6 mM Na3 citrate, 11.1 mM glucose, 1.6 mM KH2PO4, and 8.6 mM NAH2PO4; pH 7.3). The diluted blood was centrifuged at 180 x g for 5 minutes at room temperature. Platelet Rich Plasma was removed and centrifuged at 1000x g for 8 minutes at room temperature to pellet the platelets. The supernatant was discarded, and platelets were lysed in radioimmunoprecipitation assay buffer (RIPA; 50 mM Tris-HCl, 150 mM NaCl, 1.0% Triton X-100, 0.25% sodium deoxycholate, 5.0 mM EDTA) and 10 µL/mL HALT protease inhibitor cocktail (Thermo Fisher Scientific). Platelets were fully lysed and resuspended by pipetting up and down gently until no platelet particles remained. The lysed platelet samples were stored at -80°C until required for experiments. An approximately equal number of males and females were used for each strain (40 M and 45 F F2s).

2.2.5 Genotyping by Mouse Universal Genotyping Array

Tail biopsies from all F2 mice, two DBA females, and two CAST males were collected and stored at -80°C. The tail biopsies were sent in a 96-well plate to TransnetYX to be genotyped using their Mini Mouse Universal Genotyping Array (MiniMUGA, Cordova, TN)[37].

2.2.6 Measurement of FV Levels in Plasma and Platelets

Total FV protein concentration was measured by enzyme-linked immunosorbent assay (ELISA) for plasma and platelets. Platelets were diluted 20x in RIPA buffer, and platelet protein concentration was determined by the Pierce bicinchoninic acid protein assay (Thermo Fisher Scientific). Platelet protein concentration was normalized to 25 µg/mL using blocking buffer (1X PBS, 0.05% Tween-20, 6% Bovine Serum Albumin solution). Plasma was serially diluted with blocking buffer, 1:10 and then 1:25 for a final dilution of 1:250. A Nunc Maxisorp (Thermo Fisher Scientific) 96 well plate was coated with 50 µL of 1 µg/mL solution of GMA-755 Rat Anti-Murine monoclonal FV antibody (Green Mountain Antibodies) in coating buffer (0.1M Carbonate pH 9.2) and left at 4°C overnight. The plate was washed 3 times using a Biotek T50 plate washer, with 200 µL/well wash buffer (0.01% Tween-20 in 1X PBS) the next morning. 200 µL blocking buffer was added to all wells and incubated at room temperature for 2 hours, then washed. 50µL of samples and standard curve of recombinant FV purified from BHK-21 fibroblasts (obtained as a gift from Dr. Rodney Camire at Children's Hospital of Philadelphia) were added in duplicate to the plate and incubated for 1 hour at 37 °C. The wells were then washed, and 100 µL of tagged detection antibody (Rat Anti- Murine FV

GMA-752 antibody (100 μg/mL) (Green Mountain Antibodies) tagged using HRP Conjugation Kit-Lightening Link-Abcam, diluted 1:4000 in blocking buffer) was added to all wells and incubated at 37°C for 1 hour. The wells were then washed and 50 μL of 3,3′,5,5′-Tetramethylbenzidine (TMB) was added to all wells in the dark and incubated for 10 minutes at room temperature. The reaction was quenched with 25 μL 1N H_2SO_4. The absorbance of each well was read immediately using the Biotek Synergy H1 plate reader at 450 nm and standards were plotted on a log scale. Final measurements for the platelets were calculated out to ng/μg of platelet protein, and plasma values were multiplied by the dilution factor to obtain plasma levels.

2.2.7 Quantitative Trait Loci Analysis

Separate genome scans of platelet and plasma FV mice were performed on separate groups of F2 mice using the r/qtl package [38] to determine the presence of regulatory loci controlling both platelet and plasma FV levels. Genotyping data were received from TransnetYX MiniMUGA, with 3,825 and 3,885 informative markers identified and used to discern DBA and CAST inheritance used for the plasma and platelet QTL analysis respectively. A genome-wide scan was performed using *scanone* with Hailey-Knott regression and an error rate of 0.001[38]. Biological sex was considered as both an interactive and additive covariate. Significance thresholds were determined for the logarithm of the odds (LOD) with 1000 permutations, and LOD scores over 50% and 95% of the permutation distribution were considered suggestive and significant, respectively[39,40]. QTL positions were determined using Bayesian 95% credible intervals. Initial analysis was performed using the GRCm38 mouse build, and chromosome

positions were converted to the GRCm39 build using UCSC LiftOver (https://genome.ucsc.edu/cgi-bin/hgLiftOver).

2.2.8 Statistical Analyses

The graphed results are shown as mean ± SEM. Graphs were generated using GraphPad Prism (GraphPad Software), and statistical analysis was performed using a 1 or 2-way analysis of variance adjusted for multiple comparisons for groups 3 or larger, and Welch's or Student's t-test were used for groups of two. A P value of <0.05 was considered significant.

2.3 Results and Discussion

2.3.1 FV Antigen Levels

Plasma analysis (Figure 2A) revealed that CAST mice (132.6 μg/mL) had significantly higher FV antigen levels than the 129S1 (86.67 μg/mL), and B6 (91.53 μg/mL) strains ($p = 0.0065, 0.0168$, respectively). Although CAST and DBA (119.2 μg/mL) strains had plasma FV levels that were not significantly different when analyzed with both males and females in a single group, we analyzed F2 mice of this cross for QTLs regulating plasma levels due to the sex-specific differences and found significant differences in the DBA strain as well as the significant difference in FV antigen levels between the female CAST and female DBA mice (Figure 2B).

FV antigen levels were highly variable in the platelets from the five strains (Figure 2C). The two strains, DBA and CAST, used in our F2 cross had mean FV levels of 4.814 and 3.277 ng/μg platelet protein, respectively ($p=0.0033$). Prothrombin Time

(PT) and Activated Partial Thromboplastin Times (aPTT) were not significantly different between any of the strains, despite the significant differences in FV antigen levels[41].

When analyzing the F1s vs F2s, there were no significant differences observed between the strains in plasma or platelet FV. There was also no significant difference between the males and females of the F1 and F2 mice in the plasma. Interestingly, there was no sex difference in the parental platelet FV levels, but a sex difference appeared upon examination of the offspring generated by a cross between the parentals (F2s, $p<0.0001$).

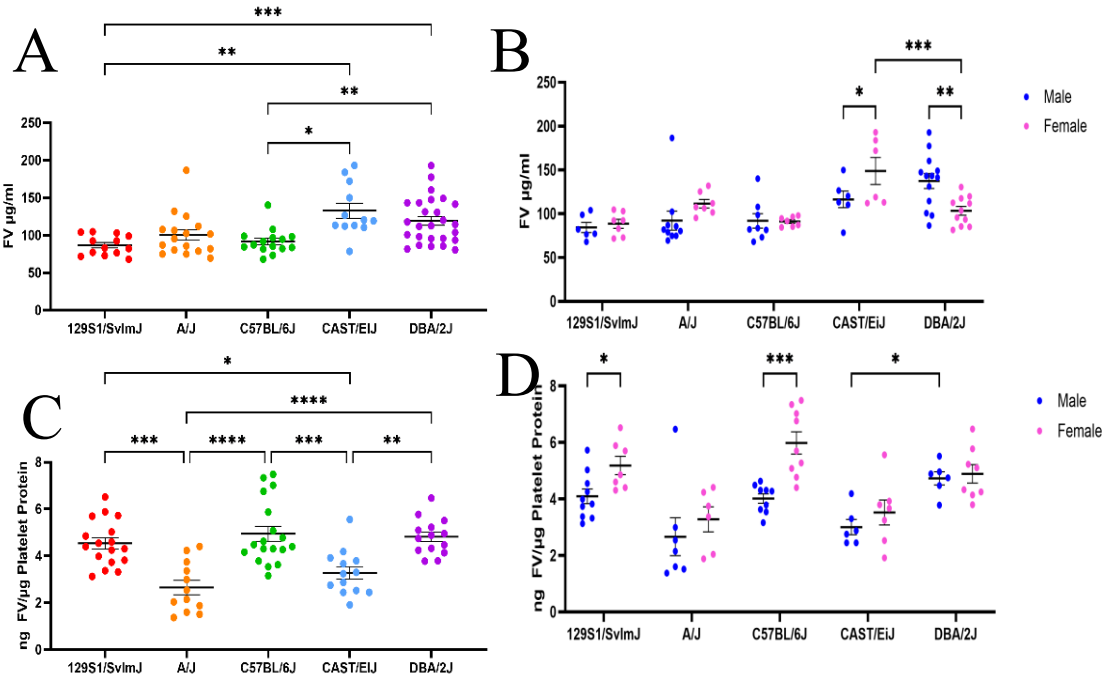

Figure 2: Factor V Levels in Plasma (A) and Platelets (C) from Five Mouse Strains. A) Plasma FV levels were significantly different in 129S1 and CAST ($p=0.0065$) and B6 and CAST ($p=0.0168$). B) Plasma FV levels were significantly different between the males and females in the DBA strain ($p=0.0011$). There is also a significant difference between the DBA females and the CAST females ($p=0.0004$). C) Platelet FV levels were significantly different in 129S1 and A/J ($p=0.0001$), 129S1 and CAST ($p=0.0166$), A/J and B6 ($p<0.0001$), A/J and DBA ($p<0.0001$), B6 and CAST ($p=0.0005$), and CAST and DBA ($p=0.0033$). D) Platelet FV levels in females are significantly higher in the 129S1 ($p=0.0322$) and the B6 ($p=0.0001$) strains. We also see a significant difference between the male CAST and male DBA mice ($p=0.0336$).

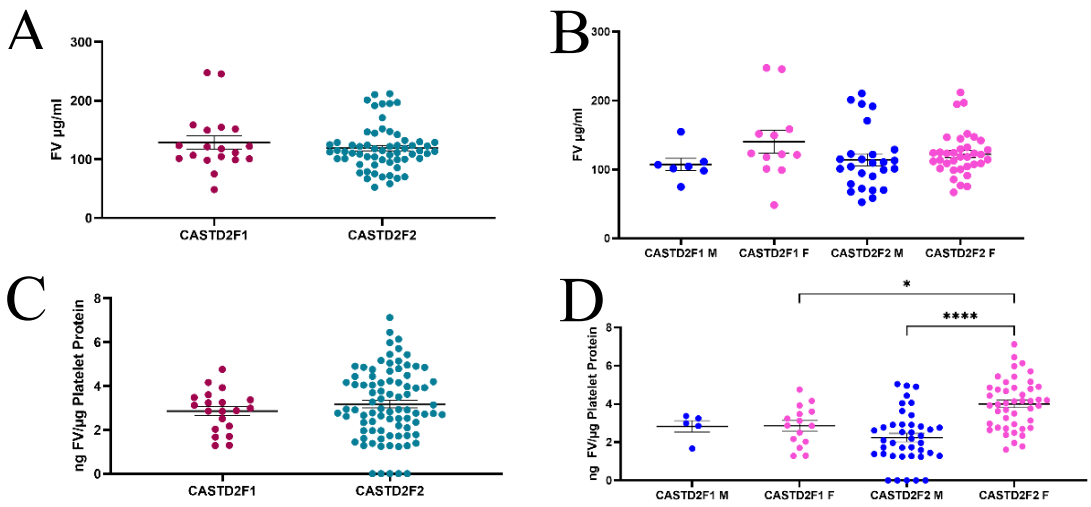

Figure 3: FV Antigen Levels in F1 and F2s in the Plasma and Platelets. A) FV plasma levels in the F1 and F2 mice. There was no significant difference between the strains. Mean antigen levels for the F1 and F2s: 128.3 and 118.8 µg/ml respectively. B) There was no significant sex difference within the strains. C) FV platelet levels in the F1 and F2 mice. There was no significant difference between the strains. Mean antigen levels for the F1s and F2s: 2.856 and 3.176 ng/µg Platelet Protein, respectively. D) There is a significant difference in FV platelet antigen levels between the F2 males and females ($p<0.0001$) and between he F1 females and the F2 females ($p=0.0177$).

2.3.2 Identification of a Significant Chromosome 1 Regulatory Locus for Plasma FV

To identify genomic regions regulating plasma FV levels, a QTL analysis was performed on 61 F2 mice. A significant peak was observed on Chromosome (Chr) 1 (LOD 5.24, significance threshold 4.21, $p=0.00641$, Figure 4A (Black graph)) from 95,095,725-166,889,809. At the maximum peak on Chr 1 (main peak: 151,294,711 marker gUNC1944082, range: 144,425,337-153,204,726), mice homozygous and heterozygous for the DBA allele were associated with lower plasma FV when compared to those homozygous for the CAST allele ($p<0.0001$ and $p=0.0006$, respectively, Figure 4C). Considering sex as either an additive or interactive covariate had little impact on the strength of the QTL on Chr 1 when considered independently, but when taken together in a full model (LOD_F), we see an increase in the LOD score at the Chr 1 peak. The more

significant peak is located at the Bayesian interval 95,095,725-166,889,809, with position 106,272,710 having the highest LOD score (max range: 106,272,710-116,168,330, LOD 6.789316, significance threshold 6.34, p=0.0246, Figure 4A (Blue Graph)). At the maximum peak in the full model, mice homozygous and heterozygous for the DBA allele were associated with significantly lower FV levels than those homozygous for the CAST allele, ($p<0.0001$), similar to the results from initial QTL analysis. Unlike the initial QTL run, we observed a significant difference between the males and the females of the mice heterozygous for CAST/DBA (p=0.0416, Figure 4E). Interestingly, the initial QTL run identified the significant peak at Chr 1 without including sex as a covariate, despite our initial findings of sex specificity in the parentals. This could be due to the female CAST vs DBA strain difference we observed in Figure 2B. When including sex as a covariate, the peak strengthened, which was expected given our initial findings.

In mice, the FV gene is located on Chr1:163,979,407-164,047,846 (MGI, GRCm39), which is included in the Bayesian-identified QTL region. However, the main significance peak identified in the full model is in a transcriptionally rich region 57,706,697 bp upstream of the gene. It is highly unlikely that a Topologically Associating Domain (TAD) regulating gene expression within their boundaries is responsible for regulating plasma FV, given that the typical size of a TAD is 0.1-2 Mb[42].

Although the region is large, we located a serpin cluster in the minimal significant recombinant interval of the full QTL model. This serpin cluster includes *Serpinb2* (PAI-2), which is a known component of the coagulation cascade[43,44]. While no direct linkage to FV has been reported, serpins generally bind and inhibit serine proteases[45] such as FXa and XIa[46] clearing them from the plasma and affecting their antigen levels. This

interaction could potentially occur with FV or FVa in the prothrombinase complex or some other similar mechanism, increasing its clearance from the plasma. Due to the large number of potential causative variants located in the significant range, additional studies are required to identify the precise genetic regulator.

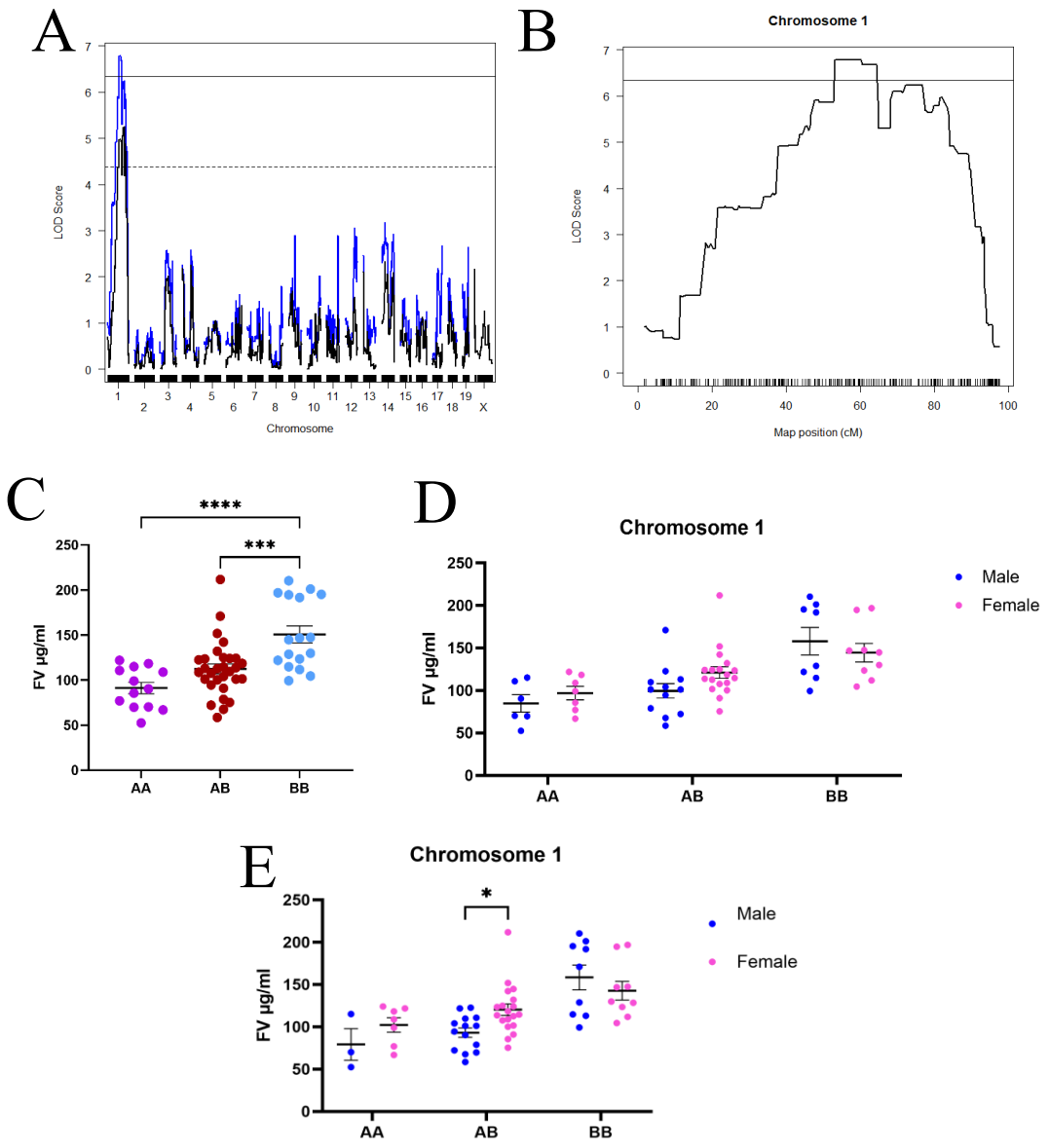

Figure 4: Plasma CASTD2F2 QTL Results. A) Initial QTL and LOD_F QTL with a significant peak identified on Chr 1 with a LOD score 5.24, significance threshold 4.21, p=0.00641 (initial) and LOD 6.789316, significance threshold 6.34, p=0.0246 (Full Model). No suggestive peaks were seen. B) Zoomed in view of Chr 1 peak from full model with significance threshold. C) Effect plot demonstrating that individuals homozygous for CAST (BB) at marker gUNC1944082 have significantly higher plasma FV when compared to those homozygous for DBA (AA, p<0.0001) and heterozygous (AB, p=0.0006). D) There were no significant differences seen regarding sex in the initial QTL model. E) In the full model, we saw a significant difference in the mice heterozygous for CAST/DBA (p=0.0416) at the most significant marker gJAX00007709.

2.3.3 Identification of Sex Specific Platelet Regulatory Loci on Chromosomes 14 and 15

To identify genomic regions regulating platelet FV levels, a QTL analysis was performed on 85 CASTDBAF2 mice. While no significant or suggestive peaks were detected with the initial QTL scan, after using sex as an interactive covariate a significant peak was observed on Chr 14 at position: 21,755,369-23,755,370 (LOD 3.52, significance threshold 2.32, p=0.00641), with the most significant peak located at position 22,728,735 (Figure 5A & 5B). A suggestive peak was seen on Chr 15 at position: 4,029,482-7,086,683 (LOD 1.64, suggestive 20% threshold 1.58, p value= 0.17844, Figure 5C), with the highest peak marker located at 4,758,870. On Chr 14, male mice homozygous for DBA and CAST had lower platelet FV levels than females of the same genotype for this marker ($p<0.0001$, Figure 6A). At Chr 15, the same trend was seen, as well as the heterozygous females also had significantly higher FV than their male counterparts (heterozygous: $p=0.0068$, homozygous DBA: $p<0.0001$, homozygous CAST: $p=0.0013$, Figure 6B). When sex was used as an additive covariate (Figure 5D), a suggestive Chr 2 peak at position: 25,299,872-181,438,313 was also present (LOD 3.66, suggestive threshold 2.78, p=0.113, Figure 5E). The highest LOD score in the region was marker gUNC4139799, located at position 143,901,800 (range:143,502,220-146,651,920). The same trend from the interactive covariate scan is seen here. The male mice had significantly lower FV levels than the females for all genotypes as shown in the effect plots in Figure 6C (homozygous DBA: $p=0.0011$, heterozygous: $p=0.0009$, homozygous CAST: $p=0.0003$). The known coagulation gene TFPI[47] is located on Chr 2 from 84,263,199-84,307,119 (MGI, GRCm39). Additionally, *PLXDC*2, a gene that plays a role in the variability of plasma FV[34], is also located on Chr 2: 16,361,115-16,760,650

(MGI, GRCm39). However, these genes are located at a significant distance from our mapped region, suggesting that any potential effects of these loci would be due to higher order interactions of the type precipitated by the spatial organization of chromatin[48]. Since these platelet regulatory loci were identified when investigating sex as a covariate due to the significant sex difference seen in our F2s, a potential role of sex hormones like estrogen in platelet FV level variation may be present.

Our study is the first to demonstrate strain-dependent differences in FV expression among laboratory mice. Future work aimed at fine mapping and identifying the regulatory elements controlling platelet and plasma-specific FV expression will increase our understanding of cell type–specific gene regulation and may reveal novel targets or strategies for modulating FV in humans.

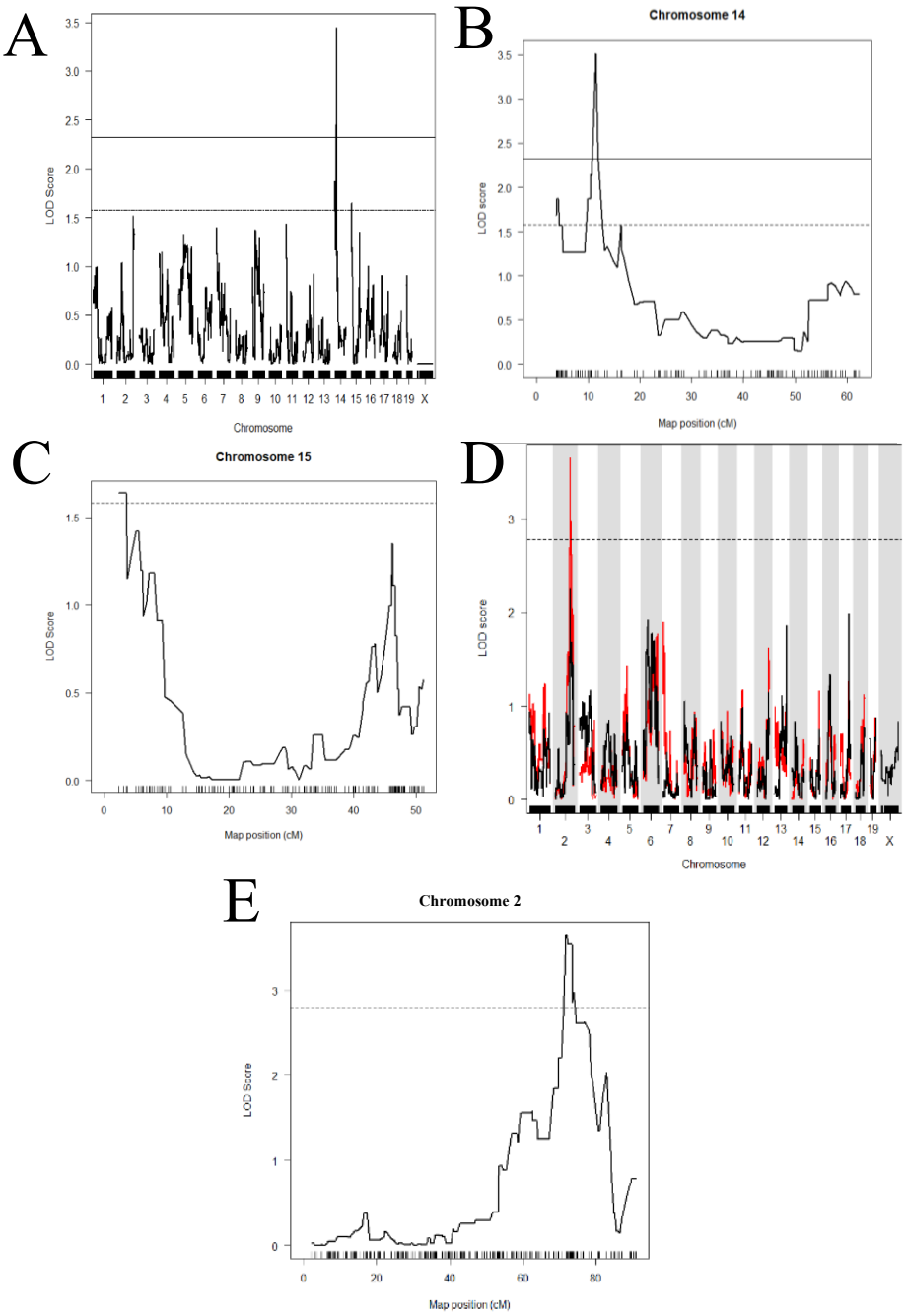

Figure 5: Platelet CASTD2F2 Whole QTL with Sex as an Interactive Covariate (A), and QTL Output with Sex as an Additive Covariate (D). A) Whole platelet QTL with sex as an interactive covariate. A significant peak was seen on Chr 14, and a suggestive peak was found on Chr 15. B) Zoomed in Chr 14 peak, LOD 3.52, significant threshold 2.32, p=0.00641. C) Zoomed in Chr 15 peak, LOD Score 1.64, suggestive 20% threshold 1.58, p value= 0.17844. D) Whole QTL with sex as an additive covariate with a suggestive peak on Chr 2 E) Zoomed in Chr 2 peak, LOD 3.66, suggestive threshold 2.78, p=0.113.

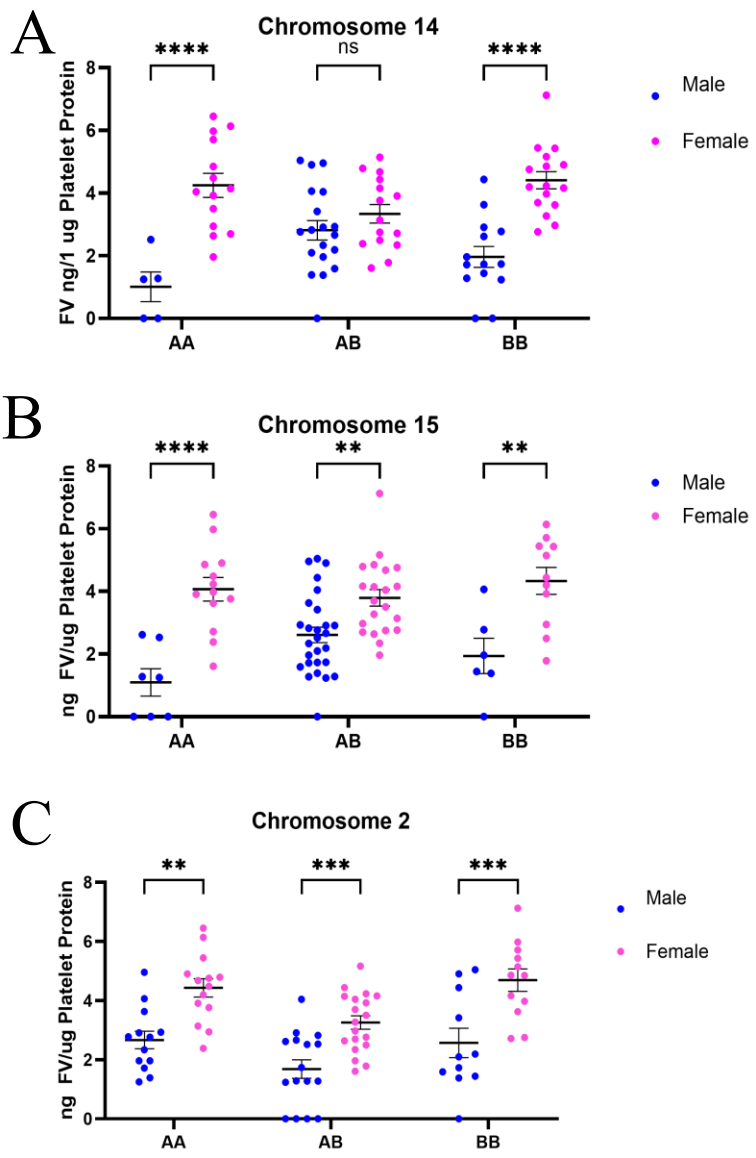

Figure 6: FV Effect Plots at Chr 14 (A), 15 (B) and 2 (C). A) Individuals homozygous for DBA (AA) and CAST (BB) at marker gUNC23694515 on Chr 14 showed a significant difference in sex ($p<0.0001$). B) The same difference was seen at Chr 15 marker gUNC24956990 (AA $p<0.0001$, BB $p=0.0013$) but the significant sex difference was seen in heterozygous individuals as well (AB $p=0.0068$). C) At marker gUNC4139799 on Chr 2, the same trend is seen, with males having statistically lower FV levels than the females at each genotype (AA $p=0.00117$, AB $p=0.0009$, and BB $p=0.0003$).

CHAPTER THREE

IDENTIFICATION OF SIGNIFICANT LOCI CONTROLLING PLASMINOGEN ACTIVATOR INHIBITOR 1 LEVELS IN THE PLASMA AND PLATELETS OF INBRED MOUSE STRAINS

3.1 Introduction

3.1.1 PAI-1 and Hemostasis

Intravascular blood clotting is due to many varying interactions between the vasculature and several distinct components in blood, including plasma, platelets, and other blood cells[36]. After an injury, this clotting system activates to minimize the loss of blood from the body. The developing clot depends on an equilibrium between platelets and coagulation factors that favor clot formation, and the fibrinolytic system that opposes clot formation[49]. The main mediator of clot dissolution is plasmin, a fibrinolytic protease that is produced from its inactive form plasminogen[49]. Plasminogen is converted to plasmin by tissue plasminogen activator (tPA) and urokinase plasminogen activator (uPA)[50]. When inhibiting the fibrinolytic system to promote blood clot formation, regulation can occur at either the plasmin level or the plasminogen activator (PA) level. PAI-1 (gene name *Serpine1*) plays a significant role in fibrinolysis by inhibiting the production of plasmin[51]. PAI-1 is a major PA regulator, inhibiting both tPA and uPA to prohibit clot dissolution[50,52]. Low levels of PAI-1 cause a mild bleeding disorder first discovered in Amish individuals[53]. In contrast, high levels of PAI-1 have been associated with MI risk[54] as well as deep venous thrombosis[55]. PAI-1 and other fibrinolytic molecules play a major role in diseases such as diabetes[56], acute and chronic renal diseases[57], and thrombosis[58]. PAI-1 expression is constitutive or inducible in many cell

types and has been identified as a major participant in multiple disease processes[59]. In addition, PAI-1 is expressed in adipose tissues[60] and is one of the key molecules studied in diabetes and obesity[56]. At a cellular level, PAI-1 regulates cell motility[61], affecting tumorigenesis[62], hematopoiesis[63], and the formation of bone marrow niches[64]. Many conditions where PAI-1 plays a role have a high component of heritability, but little is known about how the diseases are controlled genetically. Cell-type specific regulation of PAI-1 could be an important missing piece of the puzzle for understanding these diseases[65]. Brogren et al. show that platelets *de novo* synthesize active platelet PAI-1 (pPAI-1) during thrombin stimulation, suggesting that pPAI-1 plays an important role in inhibiting fibrinolysis[66]. Therefore, PAI-1 has a demonstrably important effect in maintaining hemostasis, though little is known about the genetic regulation of pPAI-1.

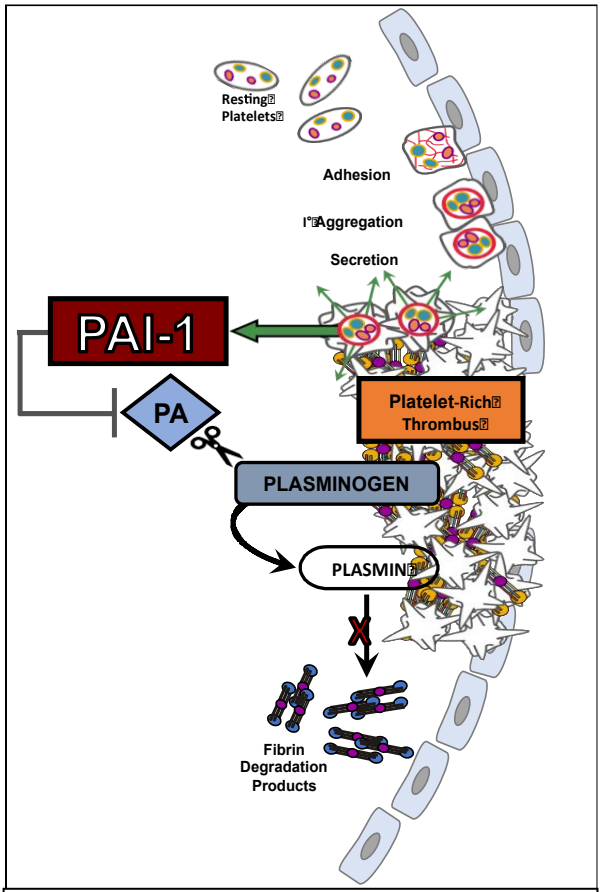

Figure 7: Platelets Secrete Abundant Amounts of the Fibrinolysis Inhibitor, PAI-1

3.1.2 The Plasma and Platelet PAI-1 Pools

PAI-1 circulates in two distinct pools: 10% circulates in a cell free manner in the plasma and 90% is

sequestered in the platelet alpha granules[67] (Figure 7). Interestingly, this configuration is the opposite of FV, which has 20% in the platelets and 80% in the circulation[24,25]. PAI-1 expression in the megakaryocyte is responsible for producing the pPAI-1[68]. Megakaryocyte PAI-1 is packaged in the platelet alpha granules. Platelets are then shed from the megakaryocytes into the circulation. Genetic defects such as gray platelet syndrome (caused by NBEAL2 deficiency), resulting in severe platelet alpha granule deficiencies, would presumably also dramatically reduce the total amount of alpha granular contents in the platelets[68], such as PAI-1 and other proteins. Reductions in pPAI-1 in gray platelet syndrome could play a role in the bleeding phenotype of this disease by increasing the rate of fibrinolysis at injury sites where platelets are actively contributing to the growing blood clot.

Multiple cell types may contribute to plasma PAI-1 expression. This contribution may differ under normal conditions and conditions of acute or chronic illness such as respiratory infections[52] or obesity/type 2 diabetes[56]. PAI-1 is a glycosylated serine protease inhibitory protein, based on variable glycosylation patterns[51], it is possible to determine the cellular source of PAI-1 in the overall plasma pool. This was assessed for adipocyte PAI-1 in humans[69].

PAI-1 has a very unstable reactive center loop, so PAI-1 in circulation is rapidly transformed into the inactive version, with an active half-life of 1-2 hours[51,70]. This also occurs when PAI-1 binds to its target serine protease, forming a 1:1 stoichiometric complex with the serine protease[51]. Thus, PAI-1 is known as a suicide inhibitor[71]. However, most of the plasma PAI-1 circulates in a complex with vitronectin, which doubles its half-life to approximately 4 hours[51,72]. Vitronectin is one of the most abundant

proteins in the circulation[73]. In addition to binding with PAI-1, vitronectin acts as an opsonin and is also called the complement S protein, serving as a main inhibitor of the complement membrane attack complex[74].

3.1.3 Physiology and Pathophysiology and PAI-1

During normal physiological conditions, PAI-1 is maintained in the plasma in low levels (5-20ng/ml) and is responsible for maintaining the hemostatic and fibrinolytic balance in blood[75]. When the body experiences blood loss, PAI-1 works to prevent the clot necessary for stopping the bleeding from breaking down, keeping the blood inside the body and maintaining hemostasis. While significantly higher or lower than average PAI-1 levels can be the cause of disease, PAI-1 could potentially be used in the treatment of individuals with bleeding disorders, enabling clots to form and remain intact more easily. In addition, mutagenesis studies of PAI-1 have yielded PAI-1 molecules that are extraordinarily more stable than the native PAI-1. These have been shown to inhibit fibrinolysis more effectively[76].

The levels of PAI-1 are constantly changing in response to stimuli[75] and many pathophysiological conditions exhibit PAI-1 levels above or below the threshold of normal. PAI-1 is linked to cardiovascular disease (CVD), cancer, inflammation, neurodegenerative diseases (and more), and circulating levels can predict worse outcomes in patients with these diseases[52]. Increased levels of PAI-1 create a hypofibrinolytic (prothrombotic) state, and this can lead to CVD including venous thrombosis, ischemic heart disease, and stroke[52]. Additionally, PAI-1 is elevated in

individuals with type II diabetes, potentially due to obesity and insulin resistance[56]. Increasing adipose tissue, or adipogenesis, allows for inducers of PAI-1 to act more readily on adipocytes, enhancing PAI-1 production from fat[77]. In addition to adipose production of PAI-1, insulin, proinsulin, and insulin-like growth factor 1 were found to increase PAI-1 expression in HepG2 hepatocytes[56]. Since these proteins are increased in individuals with type 2 diabetes with insulin resistance, PAI-1 expression from the liver is enhanced, and in conjunction with adipose production, further elevates plasma PAI-1 levels. These increased levels of PAI-1 put obese individuals with diabetes at higher risk for MI compared to their unaffected peers[78].

3.1.4 General Hematology Relevance

While PAI-1 plays a major role in thrombosis, high levels of this molecule have implications for hematopoietic stem cell (HSC) regeneration[63]. In mice fed a high-fat diet, the adipocyte population of the bone marrow expands, altering fibrinolysis by increasing the levels of PAI-1[63]. The expansion of adipocytes in the hematopoietic cell bone marrow niche[79,80] negatively impacts the process of hematopoietic regeneration[81,63]. In obese mice that underwent myeloablation and subsequent HSC transplant, inhibition of PAI-1 increased the regeneration of the HSC[64]. While these treatments appear to be effective in strengthening regeneration, we do not know the impact that inhibiting extracellular PAI-1 will have on intracellular PAI-1 (which is important for the localization of hematopoietic stem progenitor cells[63]). Understanding the genetic regulation of PAI-1 will enable us to find new mechanisms for reducing PAI-1 in obese

patients undergoing treatment of malignant hematological conditions, potentially increasing the likelihood of a successful outcome for the patient[63].

3.1.5 PAI-1 as a Drug Target

PAI-1 is a versatile molecule produced by multiple cell types and plays prominent roles in physiological and pathophysiological processes. Thus, there has been intense interest in targeting PAI-1 therapeutically to reduce diseases such as CVD, diabetes, cancer, etc. However, because of the multitude of functional effects PAI-1 has, fully characterizing these is very important for any therapy targeting PAI-1 to prevent deleterious side effects. In addition, a preferred strategy may be to target PAI-1 from a particular cell type for maximum benefit. For example, in diabetes, targeting adipocyte PAI-1 may be a superior strategy, as it is likely a large amount of the excess PAI-1 in the plasma in these cases is coming from the adipocytes. Prior research has found that pharmacological inhibition of PAI-1 in obese mice results in weight loss, as well as a decrease in adipose volume[82]. Specifically inhibiting this pool of PAI-1 may have greater success for sustained weight loss, without impacting the overall pool of PAI-1 that is needed for normal physiological functioning.

In the experiments described here, we use mouse genetics to map regulatory loci for platelet and plasma PAI-1. We identify the major Chr 5 locus controlling pPAI-1 in several additional inbred mouse strains, as well as several new PAI-1 regulatory loci.

3.2 Methods

3.2.1 Mouse Strains

Five inbred mouse strains were obtained from the Jackson Laboratory: 129S1 (stock number 002448), A/J (stock number 000646), CAST (stock number 000928), B6 (stock number 000664), and DBA (stock number 000671). Additionally, 3 outcrosses were obtained from the Jackson Laboratory: B6129SF1 (stock number 101043), B6AF1 (stock number 100002), and B6D2F1 (stock number 100006).

3.2.2 Generation of F2 Mice

Multiple crosses were performed to generate genetically informative F2 mice. B6129SF1/J, B6AF1/J, and B6D2F2/J mice were intercrossed to produce the B6129SF2, B6AF2, and B6D2F2 progeny. Additionally, CAST males were crossed with DBA females to produce the CASTD2F1 generation, and these F1 progeny were intercrossed to produce CASTD2F2 mice. All protocols and care of these mice were approved by the IACUC at Oakland University and comply with the principles of Laboratory and Animal Care established by the National Society for Medical Research.

3.2.3 Isolation of Platelet Protein

Platelets were isolated from whole blood from the 5 inbred mouse strains, B6, 129S1, A/J, CAST, and DBA, as well as our F1 and F2 mice. Blood was collected via cardiac puncture following the methods described by Brake et al.[36] BSGC (129 mM NaCl, 13.6 mM Na3 citrate, 11.1 mM glucose, 1.6 mM KH2PO4, and 8.6 mM NAH2PO4; pH 7) was added to whole blood in a 1:1 ratio and was then centrifuged at

180 x g for 5 minutes at room temperature to separate the platelet rich plasma from the red and white blood cells. Platelet rich plasma was obtained and centrifuged at 800 x g for 8 minutes at room temperature to pellet the platelets. For future analysis, platelets were lysed in RIPA buffer (50 mM Tris-HCl, 150 mM NaCl, 1.0% Triton X-100, 0.25% sodium deoxycholate, 5.0 mM EDTA) with 10uL/mL HALT protease inhibitor cocktail (Thermo Fisher Scientific) and mixed until no platelets remained visible. This process is also explained in Brake et al[36]. 20x dilutions were then prepared by placing 5ul of the freshly lysed platelets into 95ul of RIPA buffer.

3.2.4 Isolation of Plasma

Plasma was isolated from whole blood from the 5 inbred mouse strains, B6, 129S1, A/J, CAST, and DBA, as well as CASTD2F1 and CASTD2F2 strains. Whole blood was collected as described in Brake et al [36] with a 9:1 ratio of 3.2% buffered sodium citrate solution (Medicago, Aniara Diagnostica). Blood was centrifuged at 5000 x g for 10 minutes, and platelet poor plasma was collected. This plasma was centrifuged again at 5000 x g for 10 minutes to remove any lingering platelets/cells. The collected plasma was stored at -80 °C until needed for further experiments. [36]All plasma was collected between 8 and 11 AM Eastern Standard Time to minimize any variation due to the time of day[83].

3.2.5 Measurement of PAI-1 Levels by ELISA

The 20x platelet dilutions were used to perform the Pierce™ bicinchoninic acid (BCA) protein assay to determine the protein concentration of each individual platelet sample. The output values from this assay were then multiplied by 20 to determine the concentration of protein in each stock sample. These values were then used to normalize the platelet samples to 150 µg/ml of platelet protein. Plasma samples were diluted 1:5 in 3% bovine serum albumin (w/v) in Tris Buffered Saline (pH 7.4). The Mouse PAI-1 Total Antigen Assay (Innovative Research) was used to determine the PAI-1 antigen levels in each sample. The manufacturer's protocol was followed for the assays, and the plate was read at 450 nm on the Synergy H1 plate reader (BioTek). Each sample was assayed in duplicate and the average for each sample was calculated using Gen5 software with nonlinear regression parameters. The raw plasma PAI-1 levels were multiplied by the dilution factor of 5. Platelet PAI-1 levels were calculated to pg/µg of platelet protein. Males and females were assayed approximately equally for each strain.

3.2.6 Mouse Universal Genotyping Array Genotyping: Plasma

To locate areas in the genome that control PAI-1 levels, we genotyped DNA samples from the parental strains, F1, and the genetically informative F2 mice. Tail biopsies were prepared and sent to the company Transnetyx for DNA extraction and subsequent genotyping. For the mice used for plasma PAI-1 QTL mapping, 1 CAST/EiJ (M), 1 DBA/2J (F) and 57 CASTD2F2 (34 F, 23M) DNA samples from distinct mice were genotyped using the MiniMUGA genotyping array[37].

3.2.7 Mouse Universal Genotyping Array Genotyping: Platelets

Following the same procedures as above, tail biopsies were prepared and sent to TransnetYX for DNA extraction and subsequent genotyping of 1 CAST/EiJ (M), and 2 DBA/2J (F), 3 C57BL/6J (F), 1 A/J (M), and 1 129S1/SvImJ (M), 82 CASTD2F2 (46 F, 36 M), 88 B6129SF2 (45 F, 43 M), 88 B6D2F2 (42 F, 46 M), and 88 B6AF2 (42F, 46M). These mice were then genotyped using MiniMUGA[37].

3.2.8 QTL Analysis: Plasma

To discover loci regulating plasma PAI-1 levels in the CAST x DBA cross, 3,505 informative markers where the CAST and DBA mice had differing alleles were used to perform a QTL analysis using R/qtl. A single locus QTL scan with sex as an interactive covariate was performed with the *"scanone"* function using Haley-Knott regression and an error rate of 0.001[38]. To determine the significance threshold for the logarithm of the odds (LOD) score, 1,000 permutations were performed and scores over 95% and 50% of the distribution were significant and suggestive for linkage, respectively. These thresholds have been recommended by Lander and Kruglyak [40] and Abiola et al[39]. Position intervals were determined using LOD support intervals and 95% Baysian credible intervals. The analyses were performed using positions from the CRCm38 mouse build, then converted to the GRCm39 build using the UCSC LiftOver Tool (https://genome.ucsc.edu/cgi-bin/hgLiftOver).

3.2.9 QTL Analysis: Platelet

The same analysis using the R/qtl package was performed on the 4 platelet crosses, but the significance and suggestive thresholds were determined by running permutations in each individual case. The number of informative markers used for each cross are as follows: 3,534 for CAST x DBA, 3,133 for B6 x DBA, 3,282 for B6 x A/J, and 3,011 for B6 x 129.

3.2.10 Mouse FM Analysis

For additional information and fine mapping, we ran the R/MouseFM package [84]. This package uses data from the Mouse Genomes Project database (https://www.sanger.ac.uk/data/mouse-genomes-project/). Mouse strains with low pPAI-1 values (B6, CAST, WSB/EiJ, KK/HiJ [85]) and strains with high pPAI-1 values (DBA, A/J, 129, LEWES/EiJ [85]) were input as the strains for comparison, with the impact set as "High", "Moderate", and "Low". B6 was used as the reference strain. The output of this analysis was single nucleotide polymorphisms (SNPs) that were the same in the "low" strains but different in the "high" strains.

3.2.11 Statistical Analyses

The results of the analyses were presented as mean +- SEM. GraphPad Prism (GraphPad Software) was used to create the graphs. To determine significance between groups, a 1-way, 2-way and Brown-Forsythe/Welch's analysis of variance adjusted using Tukey's, Šídák's and Dunnett's post hoc tests were used, as well as Welch's and Students

t-test for comparisons between two groups. A P value of <0.05 was considered significant.

3.3 Results

3.3.1 DBA, and 129S1 Mouse Strains have Significantly Increased pPAI-1 Expression Compared to Other Mouse Strains

PAI-1 was measured from the platelet lysates from 5 inbred mouse strains (B6, 129, DBA, A/J, and CAST) to identify any variation in pPAI-1 levels (Figure 8A). Two of the strains, DBA and 129, had very high levels of pPAI-1 (13.58 and 15.16 pg/µg platelet protein, respectively), while B6 and CAST had very low levels of pPAI-1 (0.6910 and 0.5473 pg/µg platelet protein, respectively). The A/J mouse strain had intermediate levels of pPAI-1 compared to the other 4 strains (5.669 pg/µg platelet protein). There were significant differences between 129S1 and AJ ($p=0.0004$), 129S1 and B6, 129S1 and CAST, A/J and B6, A/J and CAST, A/J and DBA, B6 and DBA, and CAST and DBA ($p<0.0001$). Additionally, there was a significant sex difference in the A/J and B6 strains, with females having higher pPAI-1 in both cases, as shown in Figure 8B ($p= 0.0286$ and 0.0306, respectively).

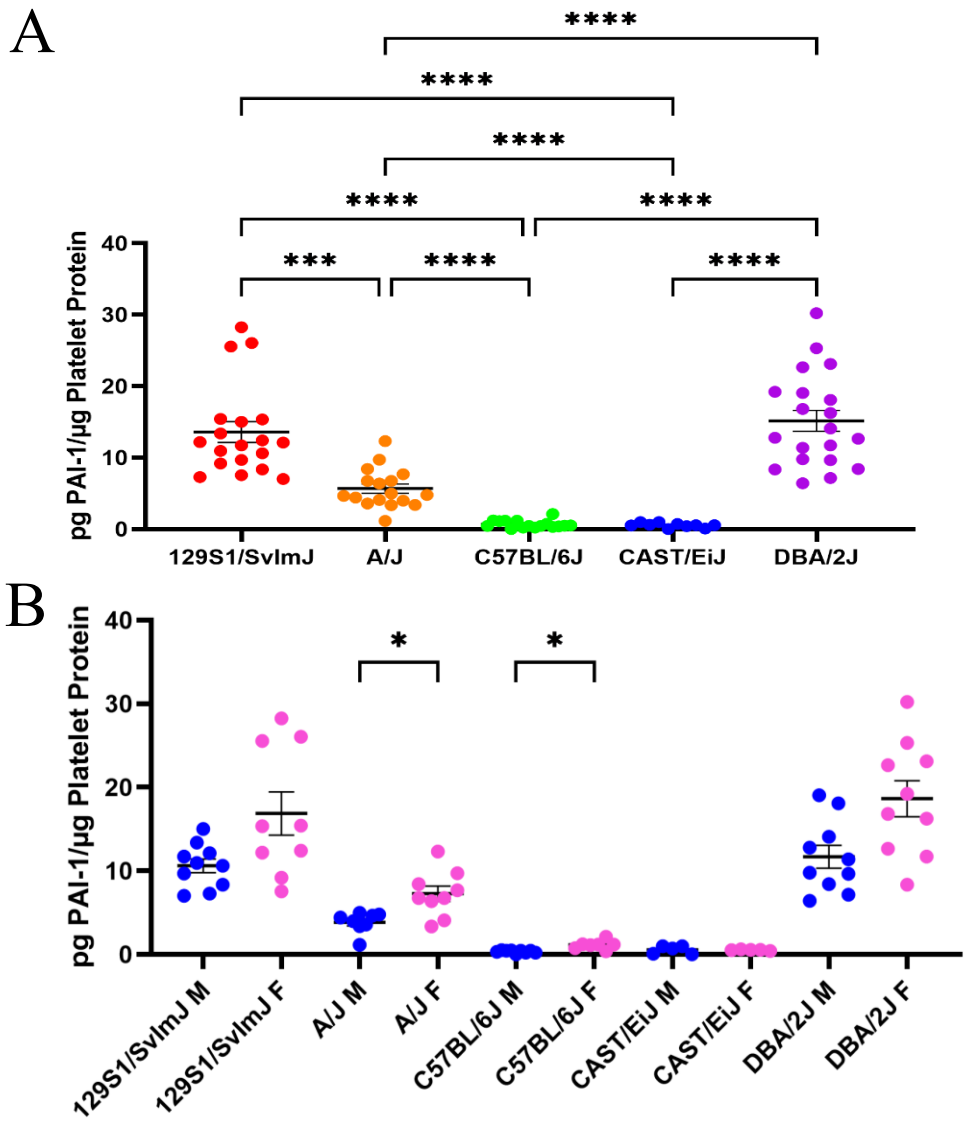

Figure 8: Platelet PAI-1 Levels in Five Mouse Strains. A) Mean pPAI-1 levels are as follows: 129S1: 13.58 pg/µg platelet protein, A/J: 5.669 pg/µg platelet protein, B6: 0.6910 pg/µg platelet protein, CAST: 0.5473 pg/µg platelet protein, and DBA: 15.16 pg/µg platelet protein. There is a significant difference between, 129S1 and B6, 129S1 and CAST, A/J and B6, A/J and CAST, A/J and DBA, B6 and DBA, CAST and DBA ($p<0.0001$), and A/J and 129S1 B6 ($p=0.0004$). B) Sex difference in platelet PAI-1 levels in 5 mouse strains. A significant difference was observed in the A/J and B6 strains, with females having higher pPAI-1 in both cases ($p=0.0.0286$ and 0.0306 respectively).

3.3.2 CAST Expresses Significantly Less Plasma PAI-1 Compared to the Other 4 Strains

PAI-1 was measured from the plasma of 5 inbred mouse strains (B6, 129, DBA, A/J, and CAST) to identify any variation in plasma PAI-1 levels. We saw significant differences in B6 (3.438 ng/ml) and A/J (5.216 ng/ml, $p=0.0171$). CAST plasma PAI-1 antigen levels were significantly lower than the other 4 strains (129, A/J, DBA, B6: $p<0.0001$, Figure 9A).

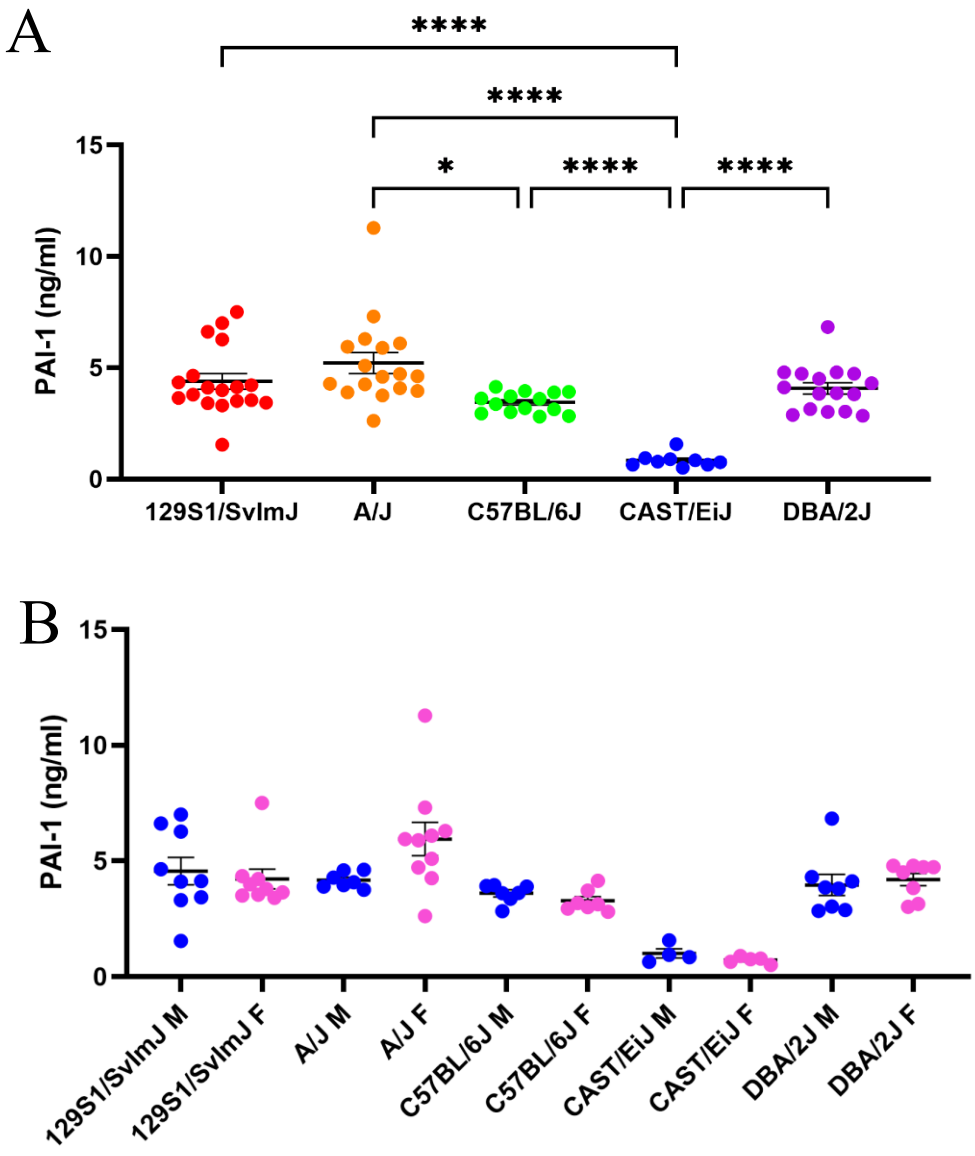

Figure 9: Plasma PAI-1 Levels in Five Mouse Strains. A) Mean PAI-1 levels are as follows: 129S1/SvImJ: 4.389 ng/ml, A/J: 5.216 ng/ml, 3.438 ng/ml, CAST/EiJ: 0.8428 ng/ml, DBA/2J: 4.076 ng/ml. There are significant differences between: 129S1/SvImJ and CAST/EiJ, A/J and CAST/EiJ, DBA/2J and CAST/EiJ $p<0.0001$, A/J and C57BL/6J: $p=0.0171$, C57BL/6J and CAST/EiJ: $p<0.0001$. B) Sex differences in plasma PAI-1 levels with no significant sex difference identified

3.3.3 pPAI-1 Levels in F2 Crosses

To discover if the differences in pPAI-1 levels in our inbred strains were genetic, we ordered B6D2F1, B6129SF1, and B6AF1 mice, which are crosses of our "low" pPAI-1 level (B6) mice and our "high" and "intermediate" pPAI-1 level (DBA, 129, A/J) mice. Additionally, we crossed the CAST strain ("low" pPAI-1) with the DBA strain ("high" pPAI-1) to generate the CASTD2F1 strain. We then proceeded to cross our F1 mice to generate B6D2F2, B6129SF2, B6AF2, and CASTD2F2, which are genetically informative due to meiotic recombination. The F1s had intermediate pPAI-1 levels when compared to the parentals (B6D2F1: 4.595 pg/µg platelet protein, B6AF1: 3.284 pg/µg platelet protein, B6129SF1: 4.228 pg/µg platelet protein, CastD2F1: 10.91 pg/µg platelet protein). All four F2 strains had pPAI-1 levels that fell into a trimodal distribution (Figures 10A, 11A, 12A, and 13A), suggesting a semidominant Mendelian inheritance pattern. The B6D2F2 (6.016 pg/µg platelet protein) had a highly segmented, trimodal distribution. In comparison, the B6129SF2 (3.292 pg/µg platelet protein), B6AF2 (2.544 pg/µg platelet protein), and CASTD2F2 (14.05 pg/µg platelet protein) exhibited a greater spread of values. Interestingly, the B6129SF2 distribution fell almost entirely below the level of the 129S1 strain, unlike the others. Additionally, the CASTD2F2 strain had pPAI-1 antigen levels that exceeded the maximum antigen levels seen in the DBA strain.

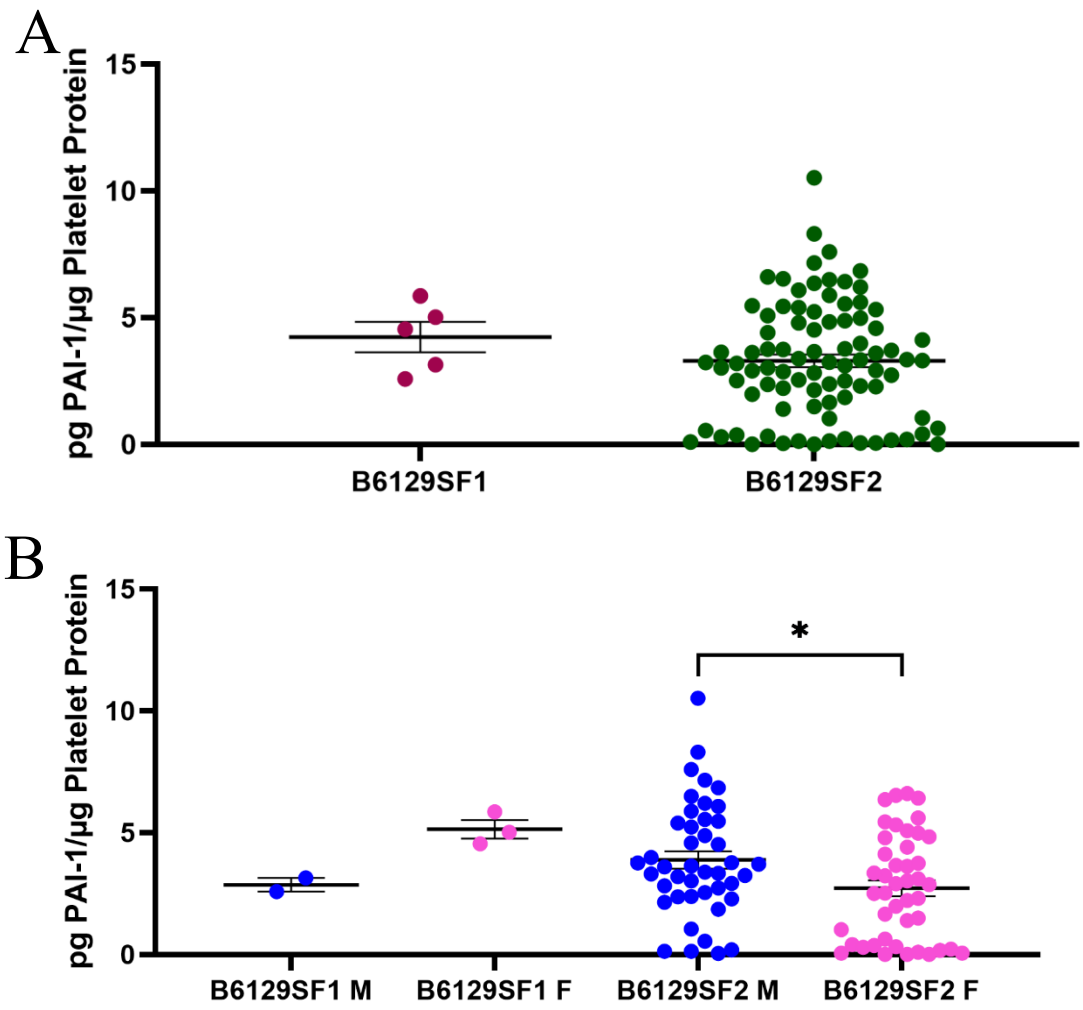

Figure 10: C57BL/6J x 129S1/SvImJ F2 Platelet PAI-1 Levels and Sex Differences. A) Levels in the F1s, and F2s. Mean antigen levels are as follows: F1: 4.595 pg/µg platelet protein, F2: 3.292 pg/µg platelet protein. There is no significant difference between the F1s and F2s. B) A significant sex difference is seen within the F2s, with males having significantly higher pPAI-1 levels than the females (p=0.032).

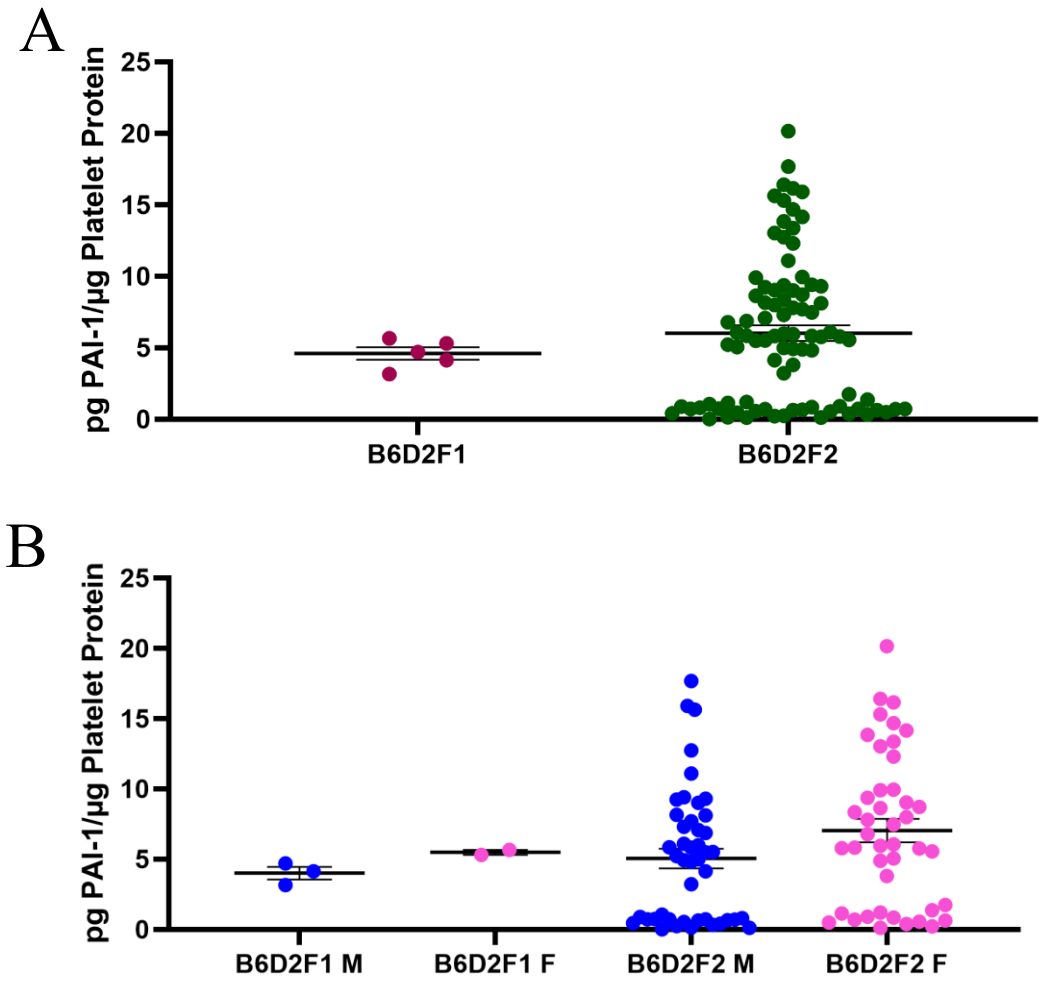

Figure 11: C57BL/6J x DBA/2J Platelet PAI-1 Levels and Sex Differences. A) F1s and F2s. Fairly distinct groupings are seen in the F2 strain, indicating potential Mendelian inheritance. Mean antigen levels are as follows: F1: 4.595 pg/µg platelet protein and F2: 6.016 pg/µg platelet protein. No significant difference was seen between the strains. B) Sex differences in the strains, with no significant differences identified.

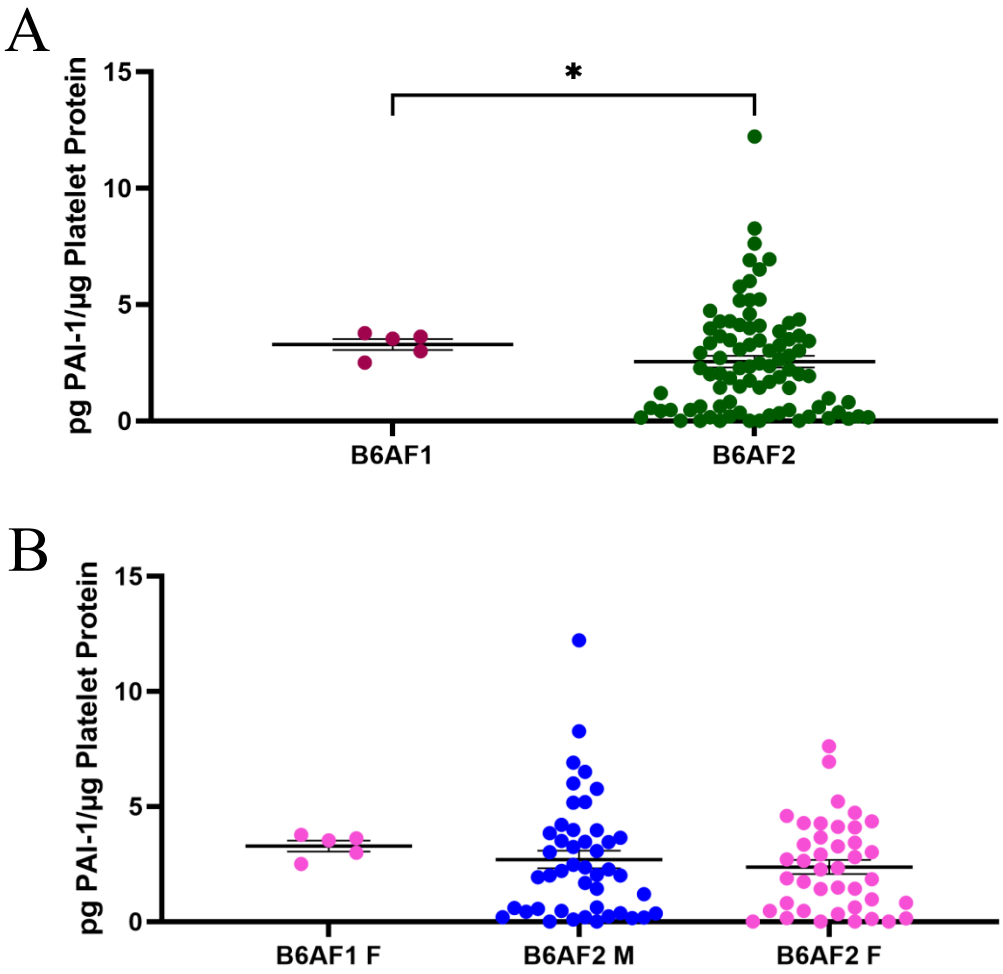

Figure 12: C57BL/6J x A/J Platelet PAI-1 and Sex Differences. A) F1 and F2s, with a trimodal distribution seen in the F2's. There is more of a spread of values and the levels span the range of the B6 and A/J parental strains. Mean antigen levels are as follows: F1: 3.284 pg/µg platelet protein andF2: 2.544 pg/µg platelet protein (p=0.0443). B) Sex differences in the strains, with no significant difference seen within the F2s.

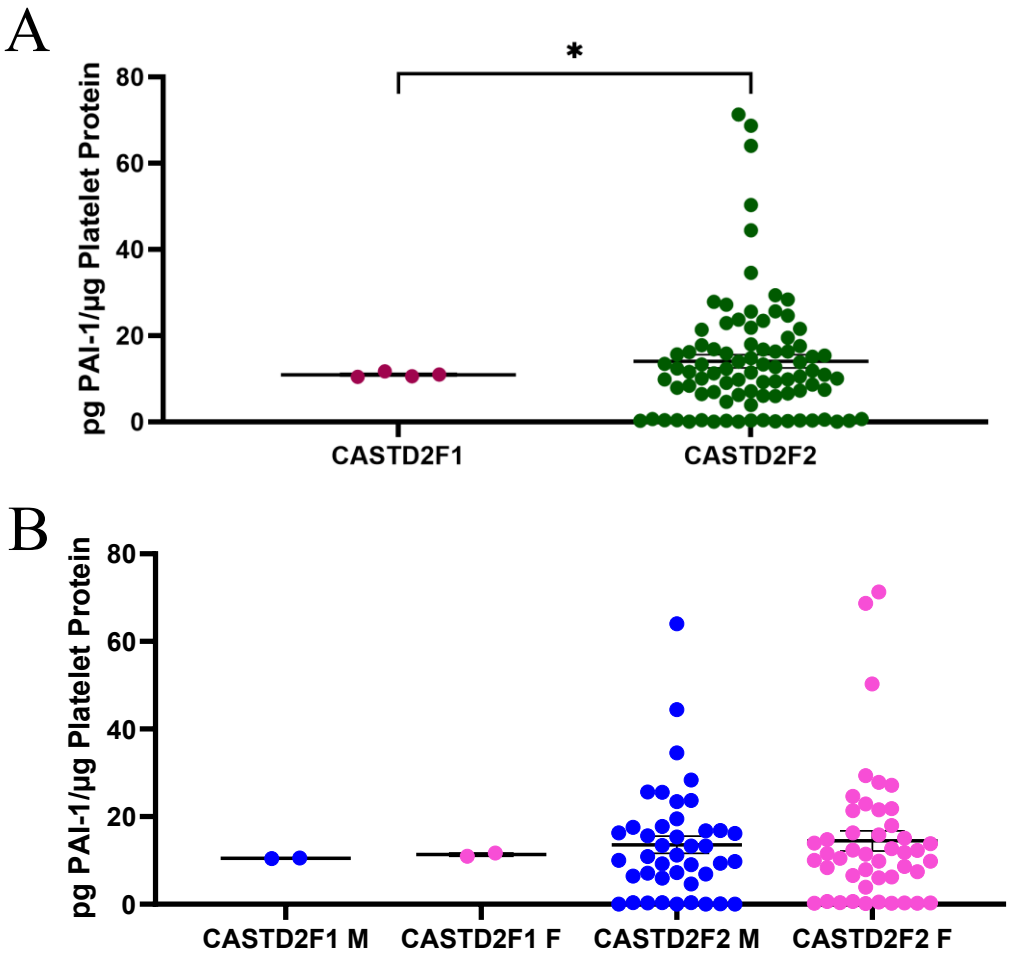

Figure 13: CAST/EiJ x DBA/2J: Platelet PAI-1 and Sex Differences. A) F1s and F2s with F2 levels exceeding the DBA range. A trimodal distribution is less striking than in the DBA x B6 cross but still present here. Mean pPAI-1 antigen levels are as follows: F1: 10.91 pg/µg platelet protein and F2: 14.05 pg/µg platelet protein. A significant difference is seen between the strains (p=0.0458). B) Sex differences in the strains, no significant difference observed.

3.3.4 Plasma PAI-1 Levels in CASTD2F2 Cross

To discover if there were genetic factors controlling the levels of plasma PAI-1, we crossed our "low" plasma PAI-1 strain (CAST) with the DBA strain to produce CASTD2F1 mice. These F1 mice had an average plasma PAI-1 level of 5.077 ng/ml. To generate genetically informative F2 mice, we crossed a male and a female CASTD2F1 mouse to create the CASTD2F2 generation. These F2 mice had an average plasma PAI-1 level of 5.001 ng/ml, with multiple values exceeding the levels of DBA. There were no significant sex differences observed between males and females in any strain, as shown in Figure 14B.

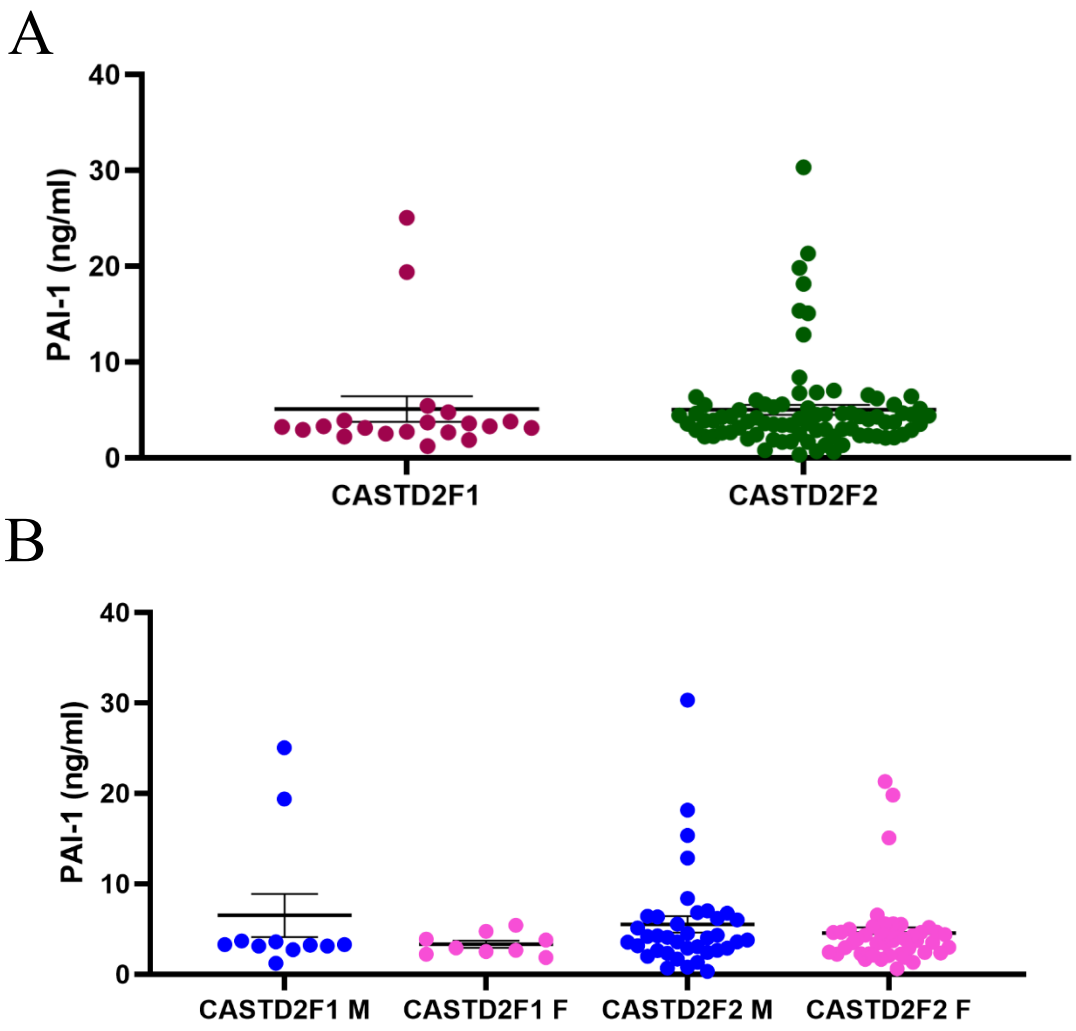

Figure 14: CAST x DBA: Plasma PAI-1 Levels and Sex Differences. A) Plasma PAI-1 levels in the F1 and F2 were seen to exceed levels of the DBA parent. Mean antigen levels are as follows: F1: 5.077 ng/ml and F2: 5.001 ng/ml. B) No significant sex differences were seen in either of the strains.

3.3.5 Identification of a Significant Locus Controlling pPAI-1 Levels by Analysis of B6D2F2 Mice

To determine the genetic regulators of PAI-1 in the platelets, we began by analyzing 88 B6D2F2 mice. We identified a highly significant peak on Chr 5, position 132,347,199-139,851,575 (LOD 30.24572, significance threshold 4.14, $p<0.0001$, Figure 15A). The most significant peak was seen at 135,957,994 (range 135,957,994-137,141,954). At the most significant position on Chr 5 (Figure 15B), individuals homozygous for B6 (AA) had low pPAI-1, heterozygous (AB) individuals had an intermediate level of pPAI-1, and those homozygous for DBA (BB) had a high level of pPAI-1 ($p<0.0001$, Figure 15C). These levels mirror the results seen in Figure 8A. When including sex as an interactive covariate two significant peak were found, one on Chr 2 (max peak 28,890,012, marker S2J021157890, LOD 2.64, significance threshold 2.55, $p=0.0363$) and the other on Chr 5 in the same position as the initial QTL (LOD 2.62, $p=0.0395$). Multiple suggestive peaks were identified on Chr 1 (LOD 2.07, 20% suggestive threshold 1.69, $p=0.1233$), Chr 6 (LOD 2.18, $p=0.1053$), Chr 9 (LOD 2.35, $p=0.0756$), and Chr 15 (LOD 2.09, $p=0.1159$). At Chr 2, there is a significant sex difference between the males and females heterozygous for CAST/DBA ($p=0.01$, Figure 15E).

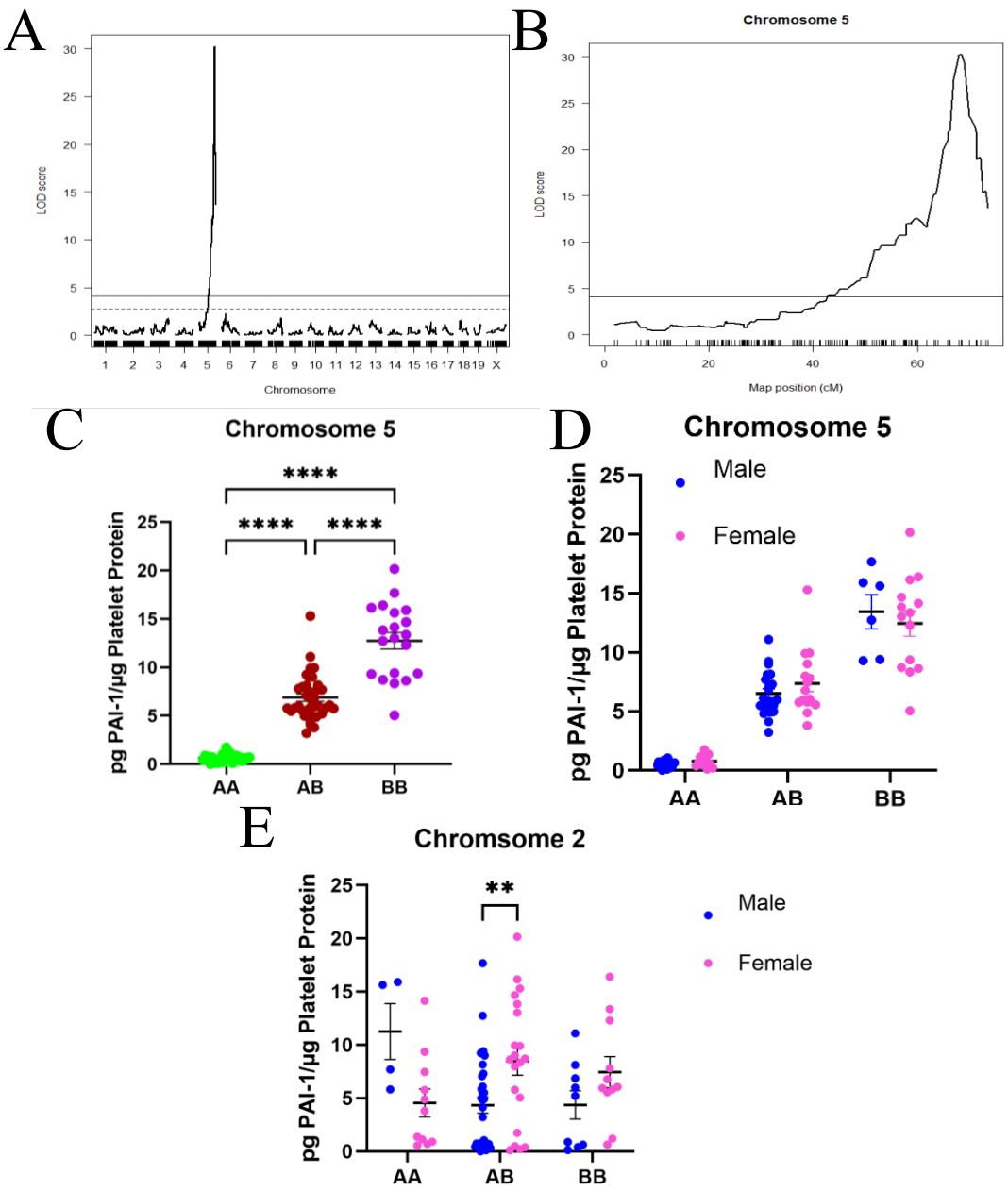

Figure 15: QTL Results from B6 x DBA Cross. A) Whole QTL for the B6 x DBA cross, with a highly significant peak on Chr 5 (LOD 30.24572, significance threshold 4.14, $p<0.0001$). B) Zoomed in Chr 5 peak, with the most significant point towards the end of the chromosome around the 135,929,140 bp range. C) Effect plot showing pPAI-1 differences for individuals homozygous for B6 (AA), heterozygous (AB), and homozygous for DBA (BB). pPAI-1 levels increase in mice with 1 or 2 DBA alleles, consistent with semi dominance ($p<0.0001$ in all comparisons). D) No sex differences were seen at any genotype. E) Significant sex difference is seen in the heterozygous mice (AB, $p=0.01$).

3.3.6 Identification of Significant and Suggestive Loci by QTL Analysis: B6AF2 Platelet

To determine if there are any significant or suggestive loci responsible for controlling the pPAI-1 levels in the B6AF2 mice, 86 mice were used to perform QTL analysis (Figure 16A). We identified a significant peak on Chr 5 position 132,140,479-140,991,055 (LOD 16.18556, significance threshold 4.03, $p<0.0001$, Figure 16B) with the most significant peak located at position 137,141,894 (range 135,957,994-137,927,402). We also identified a suggestive peak on Chr 7, position 4,785,973-144,627,107 (LOD: 3.187459, suggestive threshold: 2.67, $p=0.23$, Figure 16C). The most significant peak was seen at 143,113,393 (range 142,698,225-144,609,243). When examining sex as an interactive covariate, we identified a significant peak on Chr 8, Bayes range 13,175,534- 33,479,184 (LOD 3.09, $p=0.0278$) and a suggestive peak on Chr 14, range 19,364,360-124,693,448 (LOD 1.79, $p=0.1871$). There were no additional peaks when examining sex as an additive covariate. When examining the effect plot seen in Figure 17A, we see that at Chr 5, those homozygous for B6 (AA) have extremely low pPAI-1 and those homozygous for DBA (BB) have high pPAI-1 ($p<0.0001$), mirroring the results from the original parental strain antigen levels. When comparing those results to the effect plot for Chr 7, we see an opposite trend, with individuals homozygous for DBA having lower pPAI-1 levels than the homozygous B6 mice ($p=0.0045$). In Figures 17C and 17D, effect plots for Chrs 8 and 14 have similar pPAI-1 levels for all genotypes, but males homozygous for B6 have significantly higher pPAI-1 than females at Chr 8 ($p=0.0024$).

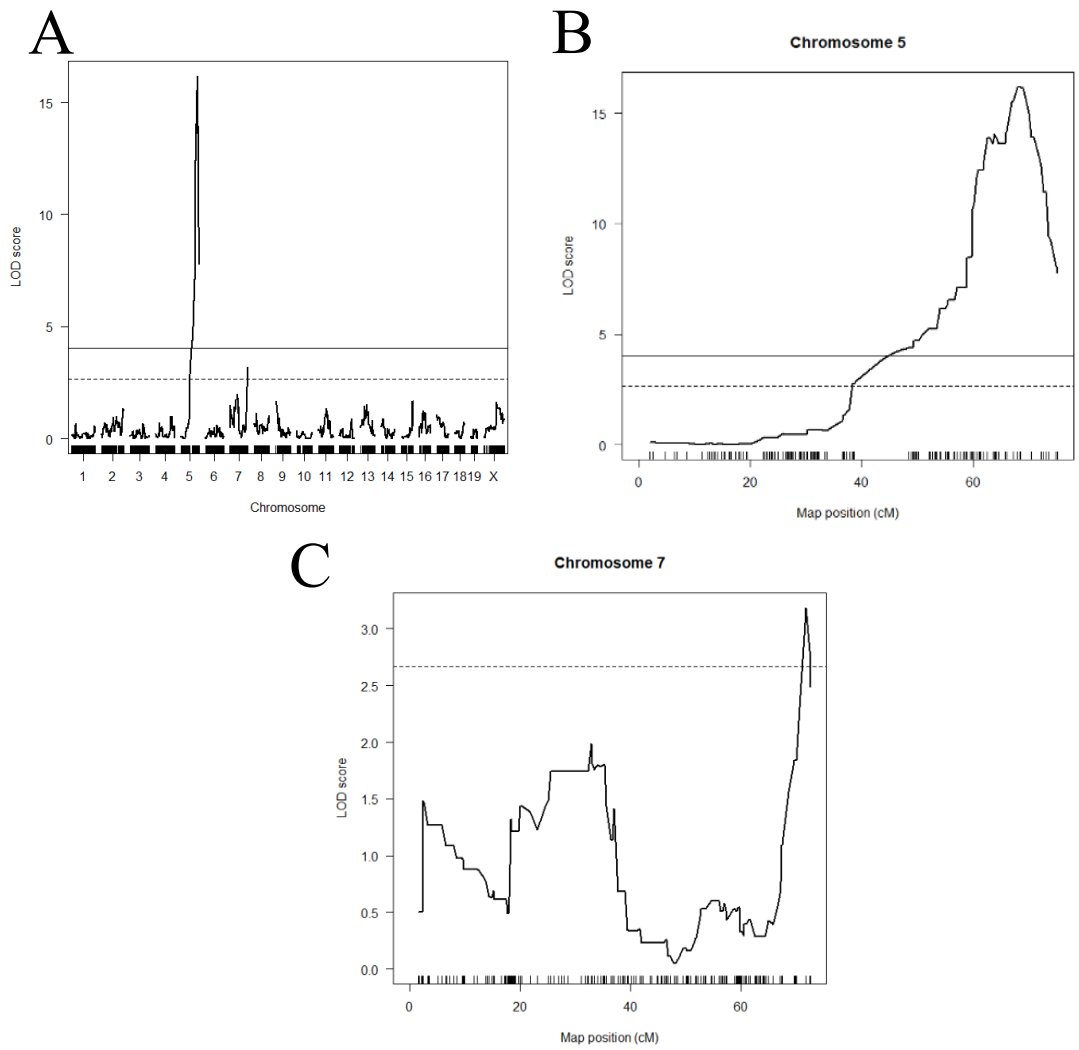

Figure 16: QTL Results for B6 x AJ Cross. A) Whole QTL from the B6 x AJ cross with a highly significant peak on Chr 5 (LOD: 16.18556, p<0.0001) and a suggestive peak seen on Chr 7 (LOD: 3.187459, p=0.23). B) Zoomed in Chr 5 peak, with maximum at position 137,141,894. C) Zoomed in Chr 7 peak, with most significant peak located at position 143,113,393.

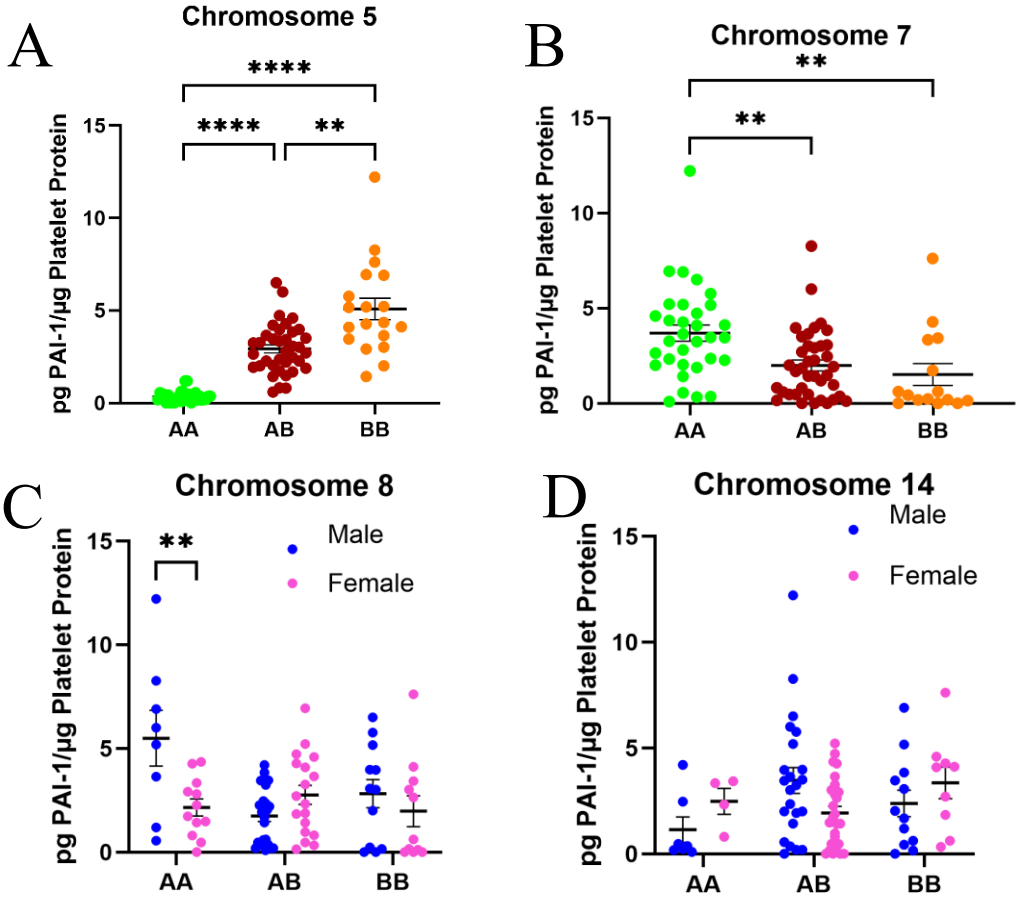

Figure 17: Effect Plots for Chr 5 (A), 7 (B), 8 (C), and 14 (D) for the B6 x A/J Cross. A) At the significant locus at Chr 5, individuals homozygous for B6 (AA) have low levels of pPAI-1, heterozygous individuals (AB) have intermediate levels of pPAI-1, and those homozygous for A/J (BB) have highest levels of pPAI-1 (AA vs AB & AA vs BB, $p < 0.0001$, AB vs BB $p=0.0058$). B) An opposite trend is seen at Chr 7, with those homozygous for B6 having higher pPAI-1 levels than those homozygous for A/J ($p=0.0045$). Heterozygous mice had pPAI-1 levels significantly less than mice homozygous for B6 ($p=0.0034$). C) At the Chr 8 locus, there is not much difference seen in the levels of pPAI-1, though the males have higher levels in the mice homozygous for B6 ($p=0.0024$). D) At Chr 14, there is little difference in mean pPAI-1 regardless of the genotype or sex.

3.3.7 Identification of Significant and Suggestive Loci by QTL Analysis: B6129SF2 Platelet

Eighty-Seven B6129SF2 individuals were used to run a QTL analysis to identify loci responsible for controlling pPAI-1 levels (Figure 18A). We observed a highly significant peak on Chr 5 (LOD 18.79, significance threshold 4.10, $p<0.0001$, Figure 18B) from position 137,141,834-137,197,019, with the most significant peak seen at position 137,141,834. A suggestive peak was found on Chr 3, position 10,193,334-128,424,439 (LOD 2.75, suggestive threshold 2.73, $p=0.479$, Figure 18C), with the peak position located at 11,505,930 (Range 10,193,334-14,592,100). Another suggestive peak was found on Chr 10 position 57,665,056-91,831,182 (LOD 3.934802, $p=0.0767$, Figure 18D), with the peak location at 82,454,554 (range 79,629,912-82798,816). The last suggestive peak was found on Chr 13, position 3,611,536-51,414,126 (LOD 2.779797, $p=0.4575$) with a maximum peak at position 31,461,951 (range 30,974,649-32,825,519). When examining sex as an additive covariate, no additional peaks were found. When investigating sex as an interactive covariate, two additional significant peaks were identified. The first was located on Chr 1 position 3,479,313-151,155,360 with a maximum position of 25,737,069 (LOD 2.85, significance threshold 2.38, $p=0.0448$). The second was located on Chr 18, position 3,745,244-46,378,685 with a maximum peak at position 15,116,711 (LOD 2.62, $p=0.0288$). Two suggestive peaks ($alpha < 0.2$) were also seen when investigating sex as an interactive covariate, Chrs 2 (LOD 1.73, $p=0.1392$), and 17 (LOD 1.52, $p=0.1994$). The effect plot seen in Figure 19A shows similar trends to the original parental antigen levels at Chr 5, with those homozygous for B6 (AA) having no pPAI-1 and those homozygous for DBA (BB) having high pPAI-1

antigen levels (AA vs AB and AA vs BB, $p<0.0001$, AB vs BB, $p=0.0003$). In Figure 19B, DBA homozygotes have significantly higher pPAI-1 than heterozygotes ($p=0.0043$) at Chr 3. At Chr 10, heterozygous mice have significantly higher pPAI-1 than B6 homozygotes ($p<0.0001$, Figure 19C). At Chr 13, DBA homozygotes have significantly higher pPAI-1 levels than heterozygotes and B6 homozygotes ($p= 0.0097$ and 0.0026 respectively, Figure 19D). There were no significant differences between genotypes at Chrs 1 and 18, but males had significantly more pPAI-1 in the DBA homozygotes at Chr 1 ($p=0.0003$) and B6 on Chr 18 ($p=0.0003$). These Chrs could be potential modifiers of the B6129SF2 mice, making their antigen levels lower than the 129S1 strain.

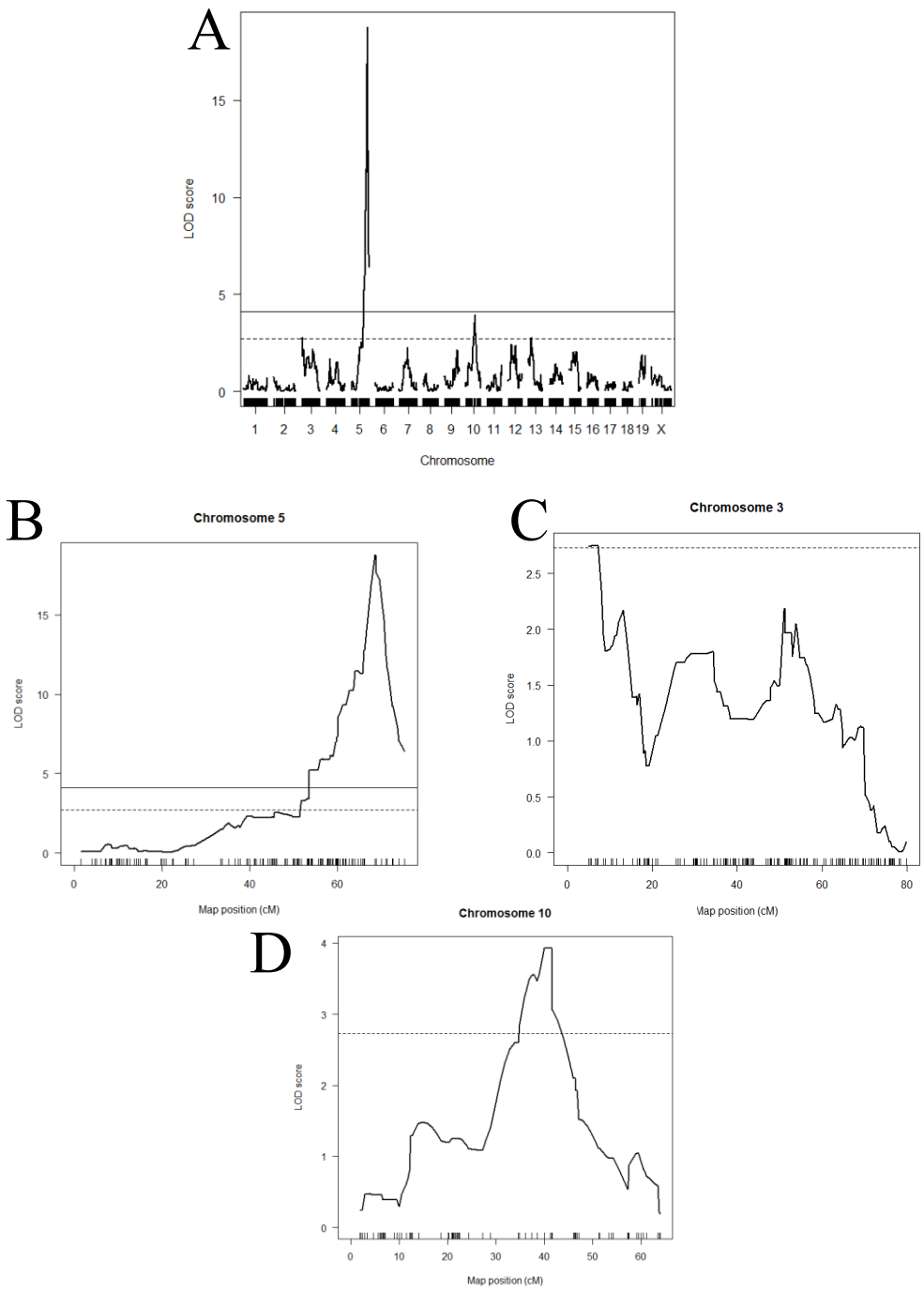

Figure 18: Results from QTL Run on B6 x 129S1 Cross. A) Whole QTL from B6 x 129S1 cross with peaks on Chrs 5, 3, and 10. B) Zoomed in peak on Chr 5 with threshold, most significant peak is located at position 137,141,834 (LOD 18.79, significance threshold 4.10, $p<0.0001$). C) Zoomed in Chr 3 peak with thresholds, with largest peak located at position 11,505,930 (LOD 2.75, suggestive threshold 2.73, $p=0.479$). D) Zoomed in Chr 10 peak with thresholds, with maximum peak located at position 82,454,554 (LOD 3.934802, $p=0.0767$).

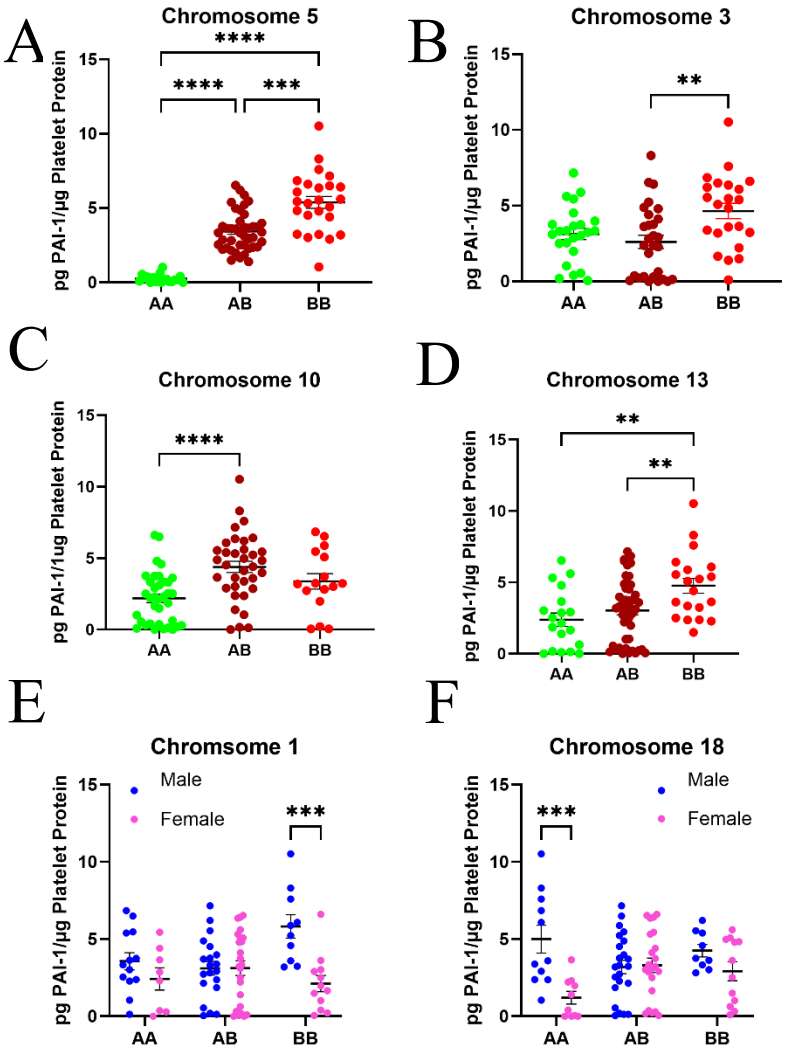

Figure 19: Effect Plots for the B6 x 129 Cross. A) Chr 5 contribution of pPAI-1 levels at Chr 5 locus. Those homozygous for B6 (AA) have the lowest amount of pPAI-1, the heterozygous mice (AB) had intermediate levels of pPAI-1, and the mice homozygous for DBA had the highest levels of pPAI-1 (AA vs AB and AA vs BB, $p<0.0001$, AB vs BB, $p=0.0003$). These results mirrored the results seen in the parental strains. B) pPAI-1 levels at Chr 3, with pPAI-1 levels higher in the DBA homozygotes than the heterozygotes ($p=0.0043$). C) pPAI-1 levels at Chr 10, with the heterozygous mice having the highest levels of pPAI-1, significantly higher than those homozygous for B6 ($p<0.0001$). D) pPAI-1 levels at Chr 13, with those homozygous for DBA having significantly higher pPAI-1 levels than those with AA and AB genotypes ($p=0.0026$ and 0.0097 respectively). E) pPAI-1 levels at Chr 1, with little variation in pPAI-1 levels between genotypes. A significant sex difference was seen in the mice homozygous for DBA ($p=0.0003$) F) pPAI-1 levels at Chr 18, with similar pPAI-1 levels between the genotypes. Males had significantly more pPAI-1 in the mice homozygous for B6 compared to females ($p=0.0003$).

3.3.8 Identification of Significant and Suggestive Loci by QTL Analysis: CASTD2F2 Platelet

To determine the genetic loci responsible for controlling the levels of PAI-1 in the platelets of the CASTD2F2 mice, we performed a QTL analysis on 88 individuals (Figure 20A). We identified one significant locus on Chr 5 (Figure 20B) position 134,521,494-139,851,535 (LOD 12.30, significance threshold 4.17, $p<0.0001$) with the most significant peak located at position 136,055,994 (Range 136,055,994-138,188,122). We also identified two suggestive peaks, one on Chr 11 (LOD 2.95, suggestive threshold 2.64, p=0.332, Figure 20C) position 3,305,458-112,932,044 with a main peak at position 9,305,458 (Range 3,376,486-10,546,636) and Chr 12 (LOD 2.76, p=0.422, Figure 20D) 11,349,537-73,485,148, maximum peak at position 26,773,871 (Range 26,339,041-27,290,391). When investigating sex as an interactive covariate, we identified a peak at Chr 6 (LOD 1.99, Suggestive alpha <.2 threshold LOD 1.78, p=0.145) position 4,204,842-137,304,850 with a maximum peak at position 4,204,824. There were no new peaks identified when including sex as an additive covariate. In Figure 13A, we see that there are CASTD2F2 mice with pPAI-1 antigen levels exceeding the level of the DBA parental strain. When using those mice with a CAST allele at the Chr 5 locus as an interactive covariate, the peak from Chr 11 became significant. At Chr 11, the maximum peak at position 23,305,456 (LOD 13.2, Significance threshold LOD 9.97, p=0.00427). Additionally, the peak seen on Chr 6 when running sex as an interactive covariate was also seen when using the CAST allele as an interactive covariate. The main peak on Chr 6 was seen at position 32,321,915 and had a LOD score of 10.5 (p=0.04056). When investigating these peaks further, we identified the same trend as seen in the parental

antigen levels at Chr 5 (Figure 21A), with the mice homozygous for DBA (AA) having variable and high pPAI-1, and those homozygous for CAST (BB) having extremely low pPAI-1 levels (AA vs AB, $p=0.0032$, AA vs BB and AB vs BB, $p<0.0001$).). The opposite outcome is shown in Figure 21B at the Chr 11 peak, with mice carrying two CAST alleles having higher pPAI-1 than those with two DBA alleles ($p=0.0010$). pPAI-1 antigen levels for hetrozygous mice at Chr 12 were significantly lower ($p=0.0379$) than mice homozygous for DBA, as shown in Figure 21C. There were no significant sex differences on Chrs 5, 11, or 12 within any genotype.

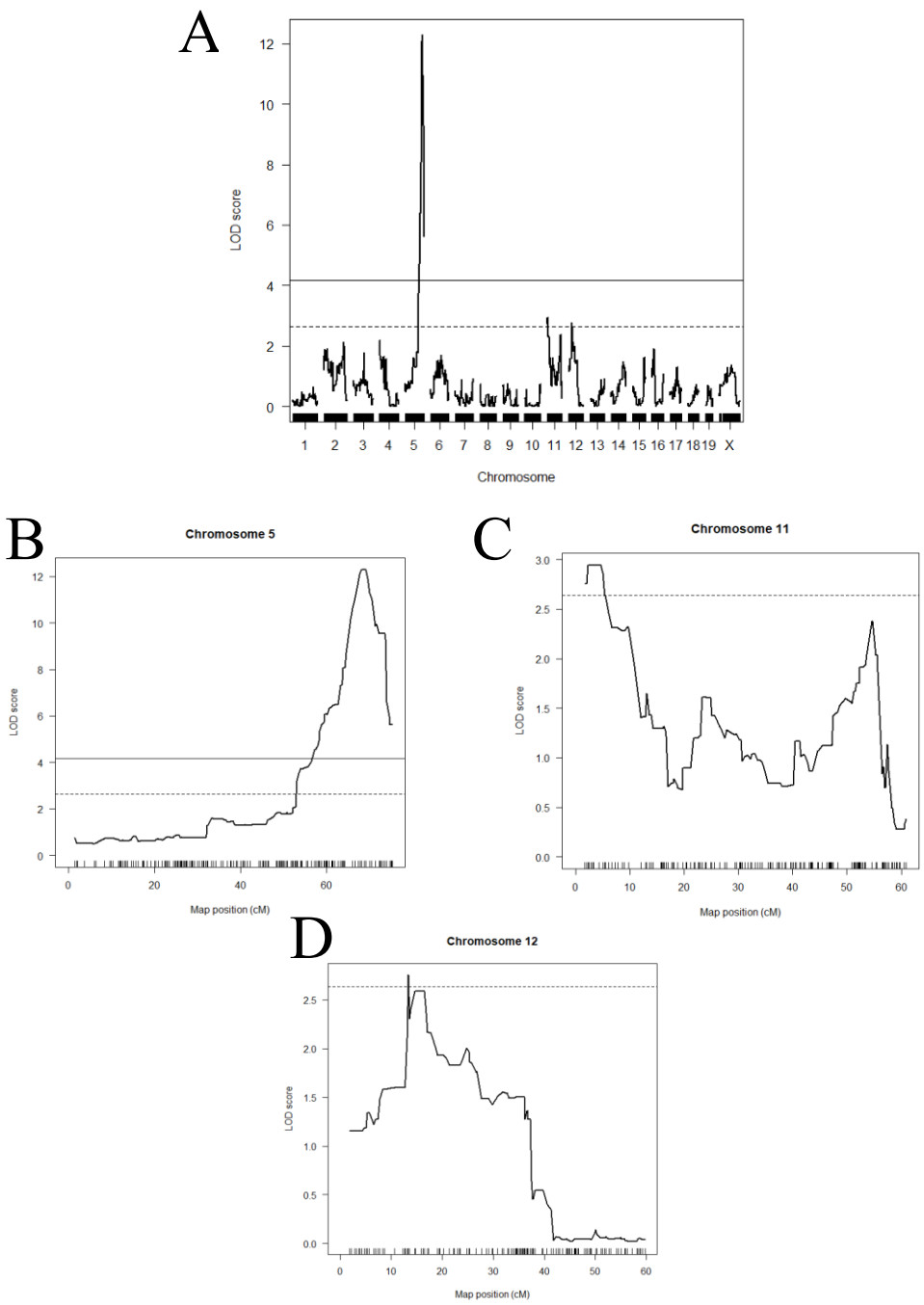

Figure 20: CASTD2F2 Platelet PAI-1 QTL Results. A) Whole QTL from CAST x DBA cross with thresholds. Peaks were seen at Chrs 5, 11 and 12. B) Chr 5 Peak with thresholds, maximum peak at position 136,055,994 (LOD 12.30, significance threshold 4.17, $p<0.0001$). C) Chr 11 peak with thresholds. Most suggestive peak found at position 9,305,458 (LOD 2.95, suggestive threshold 2.64, $p=0.332$). D) Chr 12 peak with thresholds. Most suggestive peak was located at position 26,773,871 (LOD 2.76, $p=0.422$).

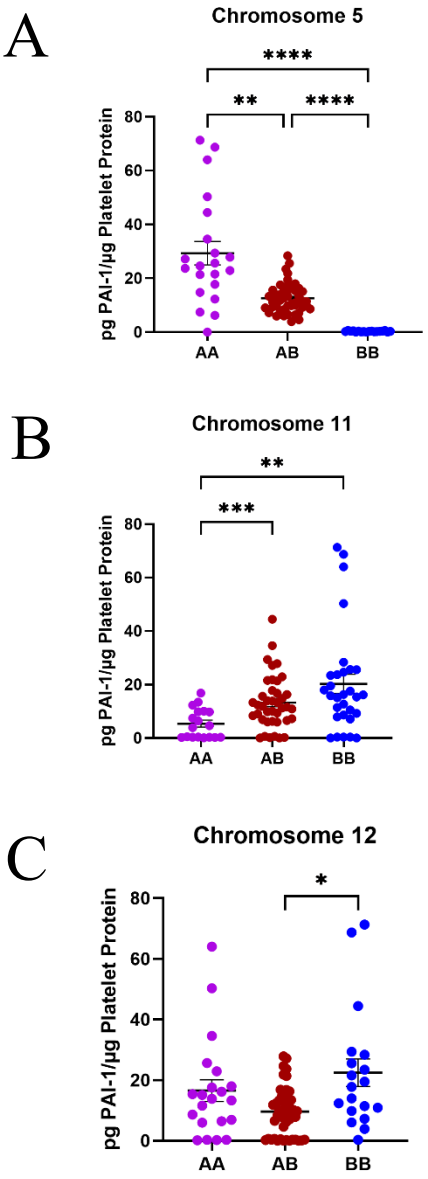

Figure 21: CASTD2F2 Platelet PAI-1 Expression Levels. A) pPAI-1 levels at Chr 5. When mice are homozygous for DBA (AA), we see the highest antigen level, when heterozygous (AB) we observed an intermediate antigen level, and when homozygous for CAST, we observed the lowest pPAI-1 levels (AA vs AB, p=0.0032, AA vs BB and AB vs BB, p<0.0001). This mirrored the levels seen in the parental strains. B) pPAI-1 levels at Chr 11 peak. We observed the opposite trend at this peak, with those homozygous for DBA (AA) having the lowest pPAI-1 levels, the heterozygous mice (AB) had an intermediate amount, and those homozygous for CAST had the highest amount of pPAI-1 (BB) (AA vs BB p=0.0010 & AA vs AB, p=0.0009). C) pPAI-1 levels at Chr 12. Similar pPAI-1 levels were observed between the homozygous genotypes, with the heterozygous mice having significantly lower pPAI-1 levels when compared to CAST homozygotes (p=0.0379).

3.3.9 Identification of Suggestive Loci by QTL Analysis: CASTD2F2 Plasma

In order to determine the genetic regulators of plasma PAI-1, 60 CASTD2F2 mice were used for QTL analysis (Figure 22A). We identified three suggestive peaks on Chrs 5, 6 and 16. The first peak was identified on Chr 5 (LOD 3.27, Suggestive Threshold 2.74, p=0.257, Figure 22B) at position 119,006,045-150,335,225, with the most significant peak position at 143,145,835 (Range 142,488,289-144,293,742). The next peak was identified on Chr 6 (LOD 3.60, p=0.163, Figure 22C) position 129,801,463-148,829,618, with main peak at position 145,930,906 (Range 145,930,898-148,829,608). The last suggestive peak was found at Chr 16 (LOD 2.77, p=0.483, Figure 22D) position 4,275,270-24,903,974 with the main peak at position 10,838,422 (Range 10,143,610-10,656,286). When sex as an additive and interactive covariate was considered, no new loci were identified. The effect plots shown in Figure 23A-B display a similar finding to the QTL analyses of many of the other crosses seen in this paper, with one effect plot mirroring the parentals (Figure 23A) and the other having the opposite trend (Figure 23B). The third effect plot (Figure 23C) shows plasma PAI-1 antigen levels similar to Chr 5 seen in Figure 23A.

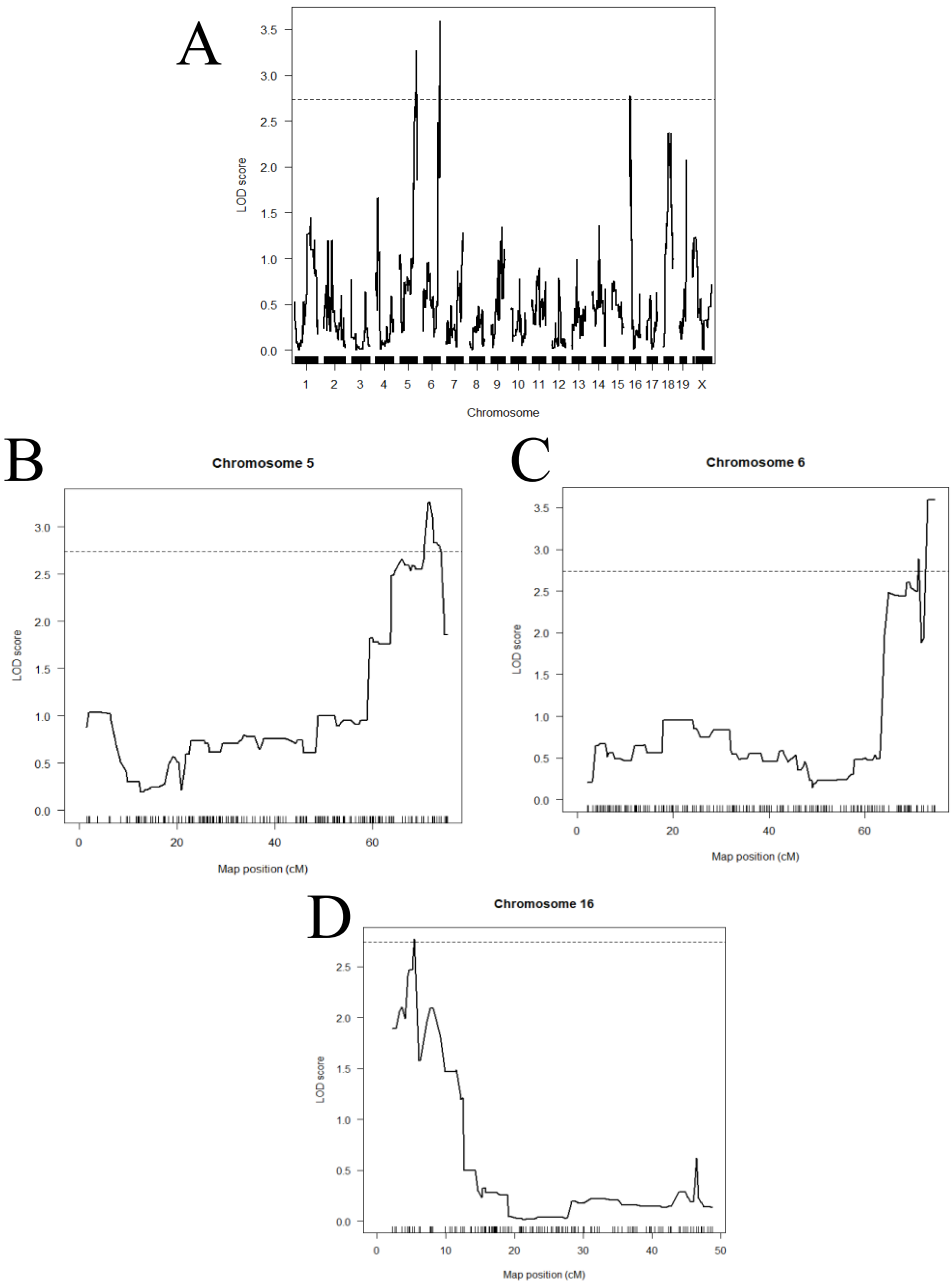

Figure 22: Results from CASTD2F2 Plasma QTL. A) Whole QTL from CAST x DBA cross with thresholds. Suggestive peaks are seen at Chrs 5, 6, and 16. B) Suggestive peak seen at Chr 5. Maximum peak located at position 143,145,835 (LOD 3.27, suggestive threshold 2.74, p=0.257). C) Suggestive peak seen at Chr 6. Highest peak location at position 145,930,906 (LOD 3.60, p=0.163). D) Suggestive peak seen at Chr 16. Maximum peak located at position 10,838,422(LOD 2.77, p=0.483).

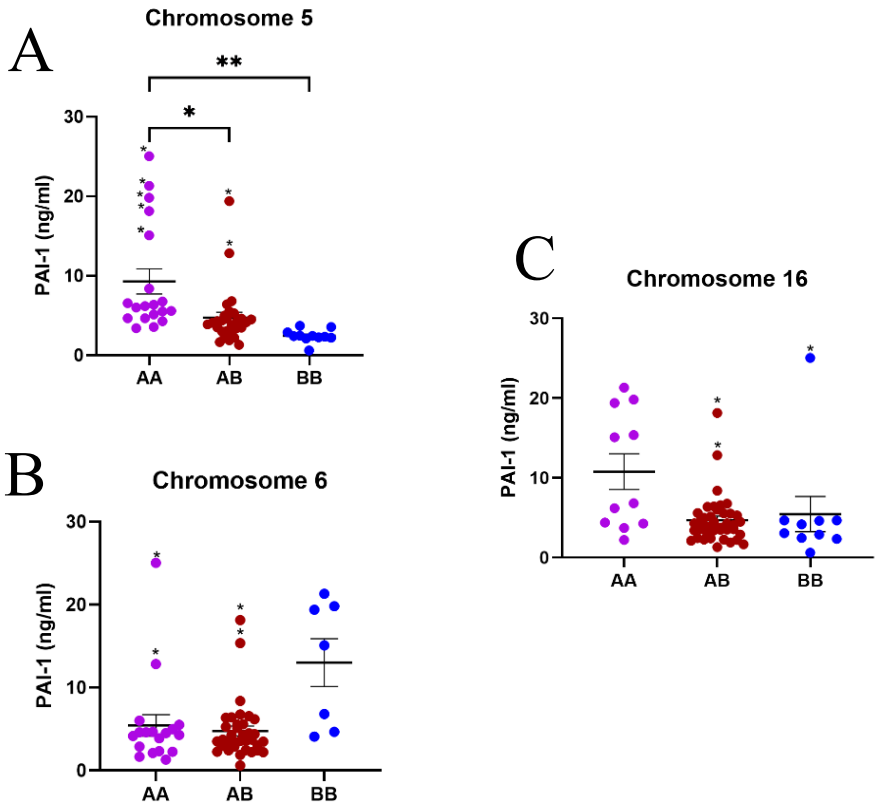

Figure 23: Effect Plots for Plasma CASTDBA QTL at the Identified Suggestive Loci * indicates an outlier from ROUT outlier test. A) Plasma PAI-1 levels at Chr 5 peak. Those homozygous for DBA (AA) had the highest PAI-1 levels, those heterozygous (AB) had intermediate levels, and those homozygous for CAST (BB) had the lowest levels of PAI-1 (AA vs AB p=0.0382, AA vs BB p=0.0011, BB vs AB p=0.0101). This mirrored the plasma PAI-1 levels in the parental strains. Five outliers were seen in AAs and 2 were seen in ABs. B) Plasma PAI-1 level at the Chr 6 locus. An opposite trend from Chr 5 was observed here, with those homozygous for DBA having a lower PAI-1 antigen level than those homozygous for CAST, though this difference is only trending in significance (p=0.1071). Heterozygous mice had lower PAI-1 than CAST homozygotes as well, but this was also only trending towards significance (p=0.0808). Two outliers were seen in AAs and 2 outliers were seen in ABs. C) Plasma PAI-1 levels at the Chr16 locus. The levels of plasma PAI-1 were similar to those seen at Chr 5 for all 3 genotypes. We observed a single data point for a male CAST homozygous mouse that is an outlier. There are also 2 outliers in the AB strain.

3.3.10 Fine Mapping of the Chr 5 Locus Reveals Candidate SNPs for Controlling pPAI-1 Expression

Using the data from our previous publication[85], comparative sequence analysis of the LEWES and the five "B6-like" mouse strains in the 1.6 Mb interval on Chr 5 revealed 511 known SNPs unique to LEWES, which are putative candidates for increased pPAI-1 expression[86]. This same region was identified in my crosses. This region contains the *Serpine1* gene, suggesting that a platelet/megakaryocyte specific *Serpine1* cis eQTL is predominantly responsible for expression differences between LEWES and B6 mice as well as B6 vs DBA, B6 vs 129S1, B6 vs A/J, and CAST vs DBA. As shown in the phylogenetic tree (Figure 24), we used the haplotype relationships between the mouse strains and used the strains that we fully characterized for pPAI-1 levels for fine mapping analysis using the mouse fine mapping QTL program called MouseFM[87] to identify and return a variant list of potential candidates. This analysis yielded two primary candidate SNPs responsible for pPAI-1 regulation within the Chr 5 locus, both of which are located within the congenic fragment (Table 1). These SNPs are predicted to control splicing, so the differential regulation of splicing leading to nonsense mediated decay may be one mechanism by which cell-type specific regulation of PAI-1 expression (and other genes) is governed.

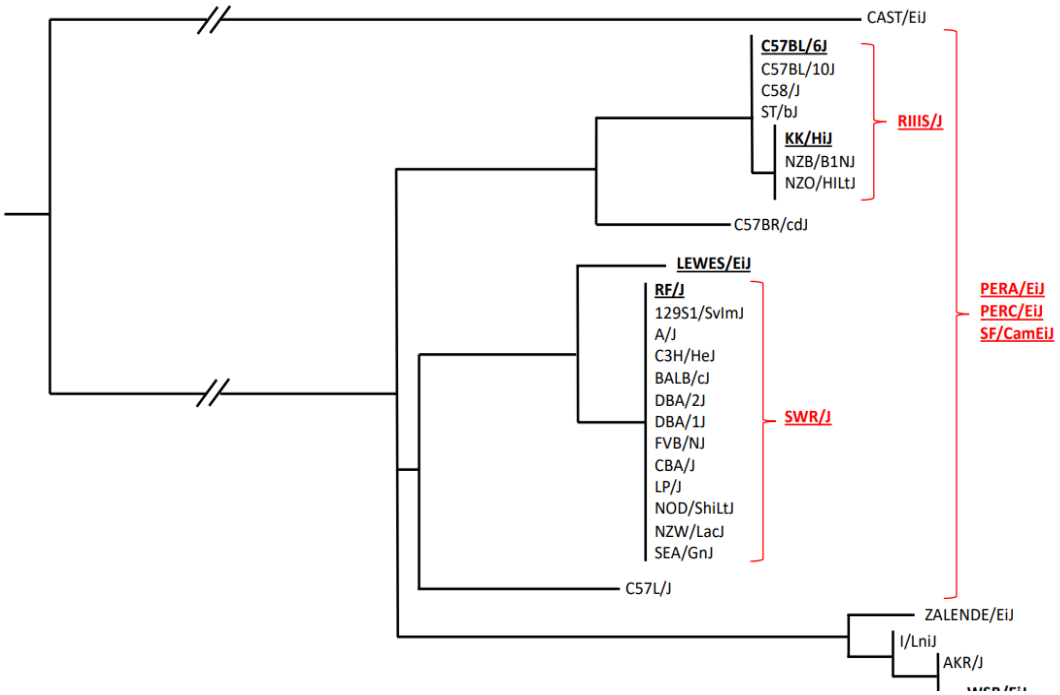

Figure 24: Phylogenetic Tree for the *Serpine1* Locus on Chr 5. DBA, 129S1, A/J mice are distantly related to the B6 strain at this locus. DBA is also distantly related to CAST at this locus.

Chr 5 Nucleotide Position, Build 39 (bp)	dbSNP Name	Reference Genotype	Variant Genotype
137,096,765	rs49619335	T	G
138,190,092	rs29778434	A	C

Table 1: Putative SNV's Responsible for Chr 5 pPAI-1 "ON/OFF" Switch

3.4 Discussion

Plasma or Platelet	Cross	Chromosome	Bayes Range	LOD Score	p value	Significant/Suggestive?	QTL Type
Platelet	B6 x DBA	5	132,347,199-139,851,575	30.24572	p<0.0001	Significant	Initial
Platelet	B6 x A/J	5	132,140,479-140,991,055	16.18556	p<0.0001	Significant	Initial
Platelet	B6 x A/J	7	4,785,973-144,627,107	3.1874589	p=0.23	Suggestive	Initial
Platelet	B6 x A/J	8	13,175,534- 33,479,184	3.09	p=0.0278	Significant	Sex Interactive Covariate
Platelet	B6 x A/J	14	19,364,360-124,693,448	1.79	p=0.1871	Suggestive	Sex Interactive Covariate
Platelet	B6 x 129S1	5	137,141,834-137,197,019	18.79	p<0.0001	Significant	Initial
Platelet	B6 x 129S1	3	10,193,334-128,424,439	2.75	p=0.479	Suggestive	Initial
Platelet	B6 x 129S1	10	57,665,056-91,831,182	3.934802	p=0.0767	Suggestive	Initial
Platelet	B6 x 129S1	13	3,611,536-51,414,126	2.779797	p=0.4575	Suggestive	Initial
Platelet	B6 x 129S1	1	3,479,313-151,155,360	2.85	p=0.0448	Significant	Sex Interactive Covariate
Platelet	B6 x 129S1	18	3,745,244-46,378,685	2.62	p=0.0288	Significant	Sex Interactive Covariate
Platelet	CAST x DBA	5	134,521,494-139,851,535	12.3	p<0.0001	Significant	Initial
Platelet	CAST x DBA	11	3,305,458-112,932,044	2.95	p=0.332	Suggestive	Initial
Platelet	CAST x DBA	12	11,349,537-73,485,148	2.76	p=0.422	Suggestive	Initial
Platelet	CAST x DBA	6	4,204,842-137,304,850	1.99	p=0.145	Suggestive	Sex Interactive Covariate
Platelet	CAST x DBA	11	Max : 23,305,456	13.2	p=0.00427	Significant	CAST Allele Interactive Covariate
Platelet	CAST x DBA	6	Max: 32,321,915	10.5	p=0.04056	Significant	CAST Allele Interactive Covariate
Plasma	CAST x DBA	5	119,006,045-150,335,225	3.27	p=0.257	Suggestive	Initial
Plasma	CAST x DBA	6	129,801,463-148,829,618	3.6	p=0.163	Suggestive	Initial
Plasma	CAST x DBA	16	4,275,270-24,903,974	2.77	0.483	Suggestive	Initial

Table 2: Summary of Significant and Suggestive Peaks from PAI-1 QTL Scans

In this chapter, I described studies of PAI-1 antigen levels in 5 inbred mouse strains, and the use of mouse genetics for mapping loci controlling PAI-1 expression. My findings are summarized in Table 2. We mapped a significant QTL peak on Chr 5, similar to the results seen in our previous paper[85], seen in the pPAI-1 QTL of all four F2 crosses. These Chr 5 peaks overlapped each other, with the absolutely most significant Chr5 peaks all within 1,180,000 bp of each other. Taking advantage of the relatedness of the mouse strains, we constructed a phyologenetic tree of the relationships of the strains specifically at the Chr 5 locus, and then used the MouseFM program to deliver a list of putative causative variants. These variants were not associated with areas of open chromatin, but rather potentially affected splicing, so we hypothesize that aberrent splicing leading to nonsense mediated decay is the mechanism for lowering platelet PAI-1 at this locus. However, this is yet to be investigated.

While a peak was identified on Chr 5 in the CASTD2F2 QTL in the plasma, it was not significant and the position was not as close to the other peaks identified. This may be due to the smaller sample size, decreasing the power of analysis[88,89] and thus peak significance, or the multiple cellular sources contributing to the total pool of plasma PAI-1[90,91] leading to more complex genetic control.

While Chr 5 is the most significant peak that we indentified in all of our F2 crosses, we identified numerous suggestive peaks, unique to each cross, since the QTL is limited to the gene pool used to generate the mice of interest[92]. If, according to our hypothesis, the Chr5 locus works as an on/off switch for pPAI-1 levels, these additional suggestive loci are likely contributing to the spread of antigen values in mice inheriting 1 or 2 permissive alleles for pPAI-1 expression at the Chr 5 locus, something that is evident in our effect plots. We also noticed a distinct lack of spread in the B6D2F2 pPAI-1 antigen level, as seen in Figure 11A, the antigen values fall into a clear trimodal distribution. The other crosses seen in Figures 10A, 12A, 13A, and 14A have more of a spread of values, while still maintaining the trimodal distribution.

Despite the significant difference in the pPAI-1 levels of these 5 strains, there is comparatively little difference in the plasma PAI-1 levels between the strains we measured. 129S1, DBA, A/J, and B6 all have similar plasma PAI-1 levels. A notable exception is the CAST strain, which has significantly less plasma PAI-1 than all other strains (Figure 9A). B6 also has significantly less plasma PAI-1 when compared to the A/J strain. The findings from this study align with the findings from our previous study, that the PAI-1 structural gene or promoter are not responsible for the variation in the pPAI-1 levels of these mouse strains.

When investigating the CAST x DBA cross, we identified several F2 mice with PAI-1 antigen levels exceeding the level of either of the parental strains. When the effect plots in Figure 21A and 21B are examined, an opposite trend in the pPAI-1 levels emerges. At the Chr 5 locus, the trend mirrors the parental strains while at Chr 11, individuals homozygous for the DBA allele have lower levels of pPAI-1 than those homozygous for the CAST allele. Transgressive segregation as seen here could be explained by epistatic interaction between Chrs 5 and 11, causing these novel pPAI-1 values. This phenomenon is explained in Prows et al and Shockley et al[93,94]. The same novel phenotypes are observed in the CASTD2F2 plasma QTL, with Chr 5 mirroring the measured phenotypes and Chr 6 exhibiting an opposite effect, although neither of these peaks reached statistical significance. Similar trends are observed in the B6AF2 and B6129SF2, although the measured values do not exceed those of either parent.

CHAPTER FOUR

PLASMA PROTEIN C EXPRESSION EXHIBITS SIGNIFICANT VARIABILITY IN MICE, WHILE COMPLETE PROTEIN C DEFICIENCY IS RESISTANT TO GENETIC SUPPRESSION

4.1 Introduction

PC is a vitamin K-dependent zymogen that is an essential negative regulator of blood coagulation. Activation of the PC pathway occurs, generating activated protein C (aPC) at the endothelial surface[95]. aPC subsequently downregulates coagulation by proteolytically inactivating the FVa and FVIIIa bound to the endothelial cell membranes, thereby diminishing additional thrombin generation. aPC activity is increased by the interaction of cofactors such as the endothelial protein C receptor (EPCR) and protein S (PS), which accelerate the degradation of FVa and FVIIIa by 20-fold[96,97]. In synergy with protein S, nonactivated FV also participates as a cofactor for the aPC-mediated degradation of FVIIIa[98].

Defects in the PC pathway are associated with an increased risk of thrombosis, with severe PC deficiency manifesting as disseminated intravascular coagulation (DIC) and purpura fulminans (PF). While rare, untreated complete deficiencies of PC are neonatal lethal in humans, and mice lacking PS and EPCR deficient mice exhibit severe embryonic lethal phenotypes[99-101]. PC heterozygosity occurs at higher frequencies, exhibiting prothrombotic predispositions that can interact with other hemostatic variants to cause severe thrombotic disease[102].

Perturbations of the PC pathway (APC resistance due to the FVL variant) also dynamically interact to reduce bleeding risk[103]. As such, the PC pathway is a promising

therapeutic target for bleeding disorders such as hemophilia[104]. We used mouse genetic techniques to identify loci that control PC expression. We also sought to identify heterozygous loss-of-function mutations that could rescue the PC deficient phenotype by implementing a dominant sensitized ENU mutagenesis screen based on the perinatal lethal *Proc*$^{-/-}$ deficient phenotype. Our results suggest that the *Proc*$^{-/-}$ phenotype is not modifiable by dominant (presumably loss of function) mutations, while heterozygous PC deficiency is sensitive to prothrombotic strain modifier genes that induce lethality in this genotype.

4.2 Methods

4.2.1 Mice

C57BL/6J (stock number 000664), 129S1/SvImJ (stock number 002448), DBA/2J (stock number 000671), A/J (stock number 000646), CAST/EiJ (stock number 000735), and BALB/cJ (BALB, stock number 000651) were purchased from The Jackson Laboratories. *F3* deficient mice were a generous gift of Dr. George Broze[105]. The *Proc* deficient mice were a generous gift from Dr. Francis Castellino[100]. *F3*$^{+/-}$ and *Proc*$^{+/-}$ mice were backcrossed greater than 8 generations to C57BL/6J for these studies.

4.2.2 Effects of Strain Modifier Genes on the *Proc*$^{-}$ Genotype

To investigate the A/J, DBA, and 129S1 strain backgrounds on the *Proc* deficient phenotype, B6 *Proc*$^{+/-}$ were crossed to these purebred strains to create F1 mice. F1 males and females were then intercrossed to create F2 generation mice. All mice were maintained on normal chow in specific pathogen-free (SPF) facilities. All animal care and

experimental procedures complied with the principles of Laboratory and Animal Care established by the National Society for Medical Research and were approved by the Oakland University and University of Michigan Committee on Use and Care of Animals.

4.2.3 Protein C ELISA: Plasma

To discover whether differences exist in the plasma Protein C levels of the pure inbred strains, plasma was collected from 129S1, A/J, B6, CAST, and DBA mice using the methods described in Brake et al[36]. Male CAST mice were outcrossed with female DBA mice to generate CASTD2F1 mice. The F1 mice were then intercrossed to produce genetically informative CASTD2F2 mice. Plasma samples were collected from these F1 and F2 mice as well. These plasma samples were then assayed using the Mouse Coagulation Factor XIV/Protein C ELISA from RayBiotech (Peachtree Corners, GA). Plasma samples were diluted 5000x and added to the ELISA plate in duplicate. The plate was read at 450 nm on the BioTek Epoch Plate Reader/Spectrophotometer.

4.2.4 Genotyping and QTL Analysis

Tail biopsies from 1 CAST, 1 DBA 14 CASTD2F1, and59 F2 mice were collected and sent to TransnetyYX (Memphis, TN) for genotyping by the MiniMUGA genotyping array[37]. QTL analyses were subsequently run using phenotypic data from the Protein C ELISA in conjunction with the genotyping data from MiniMUGA as inputs for the R/qtl program[38] to determine if significant loci responsible for controlling the levels of PC in the plasma could be identified. *Scanone* with Hailey-Knott regression and an error rate of 0.001[38] was used to perform a genome-wide QTL scan. Significance

thresholds were determined using 1000 permutations to determine LOD thresholds, and 95% and 50% of the distribution of permutations were considered significant and suggestive, respectively. Biological sex was used as both an interactive and additive covariate. Chromosome positions were converted using UCSC LiftOver from GRCm38 to GRCm39 (https://genome.ucsc.edu/cgi-bin/hgLiftOver).

4.2.5 RNA Extraction and qPCR

In order to investigate the RNA levels of *Proc* in the inbred strains, heart, lung, and liver samples were collected from 6 129S1, 6 A/J, 13 wildtype (B6), 6 CAST, and 6 DBA mice and preserved in RNA Later (Sigma-Aldrich, St. Louis, MO). RNA was extracted using the RNeasy Plus Universal Mini Kit (Qiagen, Germantown, MD). Quantification of RNA was done using the RNA 600 Nano Kit (Agilent, Santa Clara, CA) and the Agilent Bioanalyzer. Complementary DNA (cDNA) was generated from the collected and quantified RNA by adding 4µL of SuperScript VILO MasterMix (Invitrogen, Waltham, MA), Diethyl pyrocarbonate treated (DEPC) water, and enough RNA to make the final concentration of total RNA 1µg. cDNA was diluted to 1 ng/µL by adding 2 µL of cDNA to 98 µL of RNase-free water and stored at -20°C. To perform the RT-qPCR, 1µL of diluted cDNA, 20 µM primers, 5µL SsoAdvanced supermix (BioRad, Hercules, CA), and DEPC water was added to PCR tubes for a total volume of 10 µL per well (96-well Hard-Shell PCR Plates, BioRad, Hercules, CA). *Proc* was used as the gene of interest, and *GusB* and *Actb* were used as the reference genes for normalization of expression in all tissue types. Additionally, expression of the target gene was scaled to the wildtype B6 mice for improved statistical accuracy. The Bio-Rad CFX Connect

(Hercules, CA) was used to perform the reactions, and data analysis was completed using Qbase+ and GraphPad Prism.

4.2.6 Genotyping and Phenotyping

DNA was isolated from tail biopsies as previously described[106]. Mice were genotyped for *Proc*$^{-}$ using conditions and primers reported in Jalbert *et. al.*[107]. Mice were genotyped for *F3* deficiency as previously reported[108]. Mice were phenotyped by assessing their survival, weight, and gross appearance at weaning age.

4.2.7 ENU Mutagenesis and Breeding

The ENU mutagenesis procedure was conducted as previously reported[108]. 99 *Proc*$^{+/-}$ mice were intraperitoneally injected with three weekly doses of ENU (90 mg/kg) over a period of 3 years. After a 10-week recovery period, each mutagenized *Proc*$^{+/-}$ mouse was bred to *Proc*$^{+/-}$ for the screen (Figure 22) on the B6 genetic background to produce G1 generation offspring. These mice were genotyped at two weeks of age. Mice of the *Proc*$^{-/-}$ genotype surviving greater than three weeks of age were considered to carry one or more suppressor mutations.

4.2.8 Candidate Suppression of *Proc*$^{-/-}$ by *F3*$^{+/-}$ Deficiency

F3$^{+/-}$ mice were crossed with *Proc*$^{+/-}$ mice to generate double heterozygous *Proc*$^{+/-}$ *F3*$^{+/-}$ mice. The double heterozygous mice were then crossed back to *Proc*$^{+/-}$ B6 mice to test the effect of *F3* haploinsufficiency on the *Proc*$^{-/-}$ lethal genotype.

4.2.9 Statistical Data Analysis

All experiments were performed blinded to genotype. Statistical differences among the potential progeny of mouse crosses were determined using the χ^2 test. Statistical differences in the measured PC levels between the different strains were assessed by ANOVA with adjustment for multiple comparisons.

4.3 Results and Discussion

4.3.1 The *Proc*$^{-/-}$ Phenotype is Not Suppressible by Dominant ENU-Induced Mutations

Due to the high prevalence of thrombotic cardiovascular disease, the identification of VTE genetic risk factors is essential for its diagnosis and treatment. Our ENU treated *Proc*$^{+/-}$ male mice (G0 generation) crossed with non-mutagenized *Proc*$^{+/-}$ females were expected to produce one quarter *Proc*$^{-/-}$ G1 conceptuses carrying the *Proc*$^{-/-}$ genotype. These crosses generated a total of 962 weaning age G1 progeny. (Figure 25). We observed no *Proc*$^{-/-}$ offspring at weaning due to previously described perinatal lethal thrombosis[100]. Based on the expected number of *Proc*$^{-/-}$ conceptuses (~321) and our previously observed ENU-induced mutation rate[109] these *Proc*$^{-/-}$ conceptuses were predicted to carry ~20,865 new mutations that altered the coding sense in total (or with an overall total of ~2,086,500 ENU induced mutations)[108,110]. Despite this genome coverage, not a single *Proc*$^{-/-}$ mouse survived to weaning age. In contrast, we previously reported a sensitized ENU mutagenesis screen for dominant suppressors of a different perinatal lethal blood clotting phenotype based on a genetic interaction between FVL homozygosity (*F5*$^{L/L}$) and haploinsufficiency for (*Tfpi*$^{+/-}$)[108]. This screen produced one live *F5*$^{L/L}$ *Tfpi*$^{+/-}$ for every 70-progeny analyzed, (~14 per thousand mice generated). The

increased phenotypic severity of *Proc*$^{-/-}$ was initially regarded as an advantage of the *Proc*$^{-/-}$ phenotype, as suppressors of increased strength would be generated. However, given the approximate 1X whole genome mutation coverage, the results of our sensitized suppressor screen suggested that dominant mutations capable of restoring viability to the *Proc*$^{-/-}$ phenotype would occur rarely or not at all.

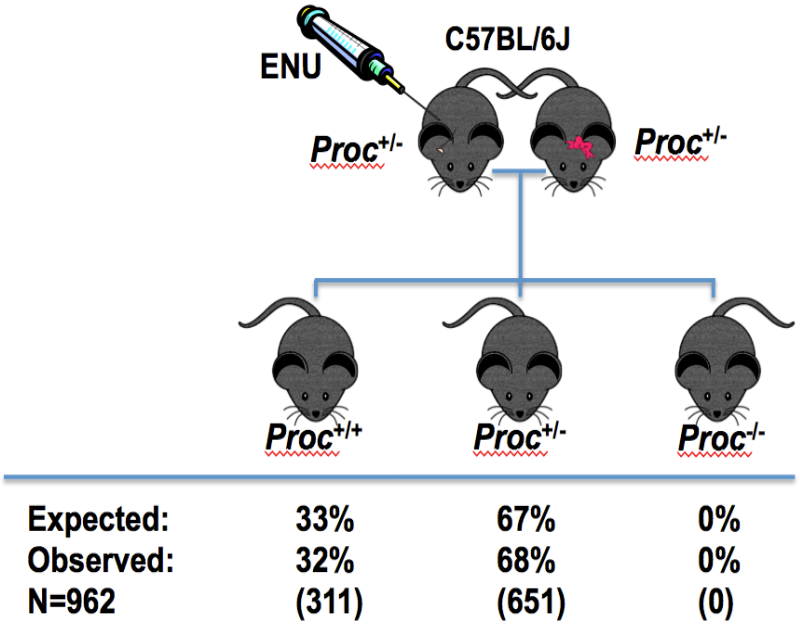

Figure 25: Description of the *Proc* Mutagenesis Screens. The mating scheme and observed distribution of the *Proc* screen. *Proc*$^{+/-}$ male mice were mutagenized with ENU and bred with non-mutagenized *Proc*$^{+/-}$ females. No *Proc*$^{-/-}$ progeny were observed in the 962 progeny analyzed.

4.3.2 *F3* Haploinsufficiency Fails to Suppress *Proc* Deficiency

To test whether $F3^{+/-}$ could similarly suppress $Proc^{-/-}$ lethality, we bred the $F3^{+/-}$ mice onto the $Proc^{-}$ background. As shown in Table 3B, no surviving weaning age $Proc^{-/-}$ $F3^{+/-}$ mice were observed. We previously demonstrated that haploinsufficiency for *F3* suppresses the lethal thrombosis of the $F5^{L/L}$ $Tfpi^{+/-}$ genotype[108]. Our experiment demonstrated that unlike $F5^{L/L}$ $Tfpi^{+/-}$, the $Proc^{-/-}$ phenotype is not responsive to reductions in $F3^{+/-}$.

4.3.3 *Proc* Haploinsufficiency is Thrombotic on a Mixed B6129S1 Genetic Background

We analyzed progeny from F1 $Proc^{+/-}$ matings on 3 mixed genetic backgrounds[102,111]. The resulting *Proc* genotype distribution from the B6A/J and B6DBA intercrosses was consistent with complete lethality of $Proc^{-/-}$ mice, similar to the observations from $Proc^{+/-}$ x $Proc^{+/-}$ on the purebred B6 (Figure 25 and Table 3A). However, analysis of progeny on the background B6129S1 revealed not only an absence of $Proc^{-/-}$ but also a statistically significant reduction of $Proc^{+/-}$ mice ($p<0.05$). Several previous reports have documented enhanced thrombosis for 129S1 compared to other mouse strains, including in the setting of F5 Leiden[112,113].

A.

Parental genotypes

+/-
+/-

B6A/J

***Proc* genotype**	**Expected**	**%**	**Observed**
+/+	22	33.3%	23
+/-	45	66.7%	44
-/-	0	0.0%	0
Total	67	100.0%	40

B6DBA

***Proc* genotype**	**Expected**	**%**	**Observed**
+/+	5	33.3%	6
+/-	11	66.7%	10
-/-	0	0.0%	0
Total	16	100.0%	16

B6129S1

***Proc* genotype**	**Expected**	**%**	**Observed**
+/+	13	33.3%	22
+/-	27	66.7%	18*
-/-	0	0.0%	0
Total	40	100.0%	40

B.

Parental genotypes

***Proc* genotype**	***TF* genotype**
+/-	+/-
+/-	+/+

***Proc* genotype**	***TF* genotype**	**Expected**	**%**	**Observed**	**%**
+/+	+/-	25.4	14.3%	31	17.4%
+/+	+/+	25.4	14.3%	38	21.4%
+/-	+/-	50.9	28.6%	47	26.4%
+/-	+/+	50.9	28.6%	62	34.8%
-/-	+/-	25.4	14.30%	0	0.00%
-/-	+/+	0	0.00%	0	0.00%
Total		178	100.0%	178	100.0%

Table 3: Weaning Age Survival of *Proc*$^{-}$ Progeny. A) Survival of *Proc*$^{+/-}$ weanlings is unaffected on the B6-A/J and B6-DBA mixed genetic backgrounds but significantly decreased the B6-129S1 genetic background ($p<0.01$). B) Survival of *Proc*$^{-/-}$ is unaffected by *F3*$^{+/-}$.

4.3.4 129S1 Exhibits Low Plasma Protein C Antigen Levels

We next analyzed plasma Protein C levels by ELISA and found that the 129S1 strain exhibited the lowest Protein C levels of any strain, with significant differences between 129S1 and DBA ($p=0.0019$), as well as between the CAST and DBA ($p=0.0181$), as seen in Figure 26A. We then analyzed the sex differences within each strain and discovered a significant difference in B6 ($p=0.0037$), CAST ($p=0.0025$), and DBA ($p<0.0001$), with male mice having higher plasma Protein C antigen levels in all three cases, as shown in Figure 26B.

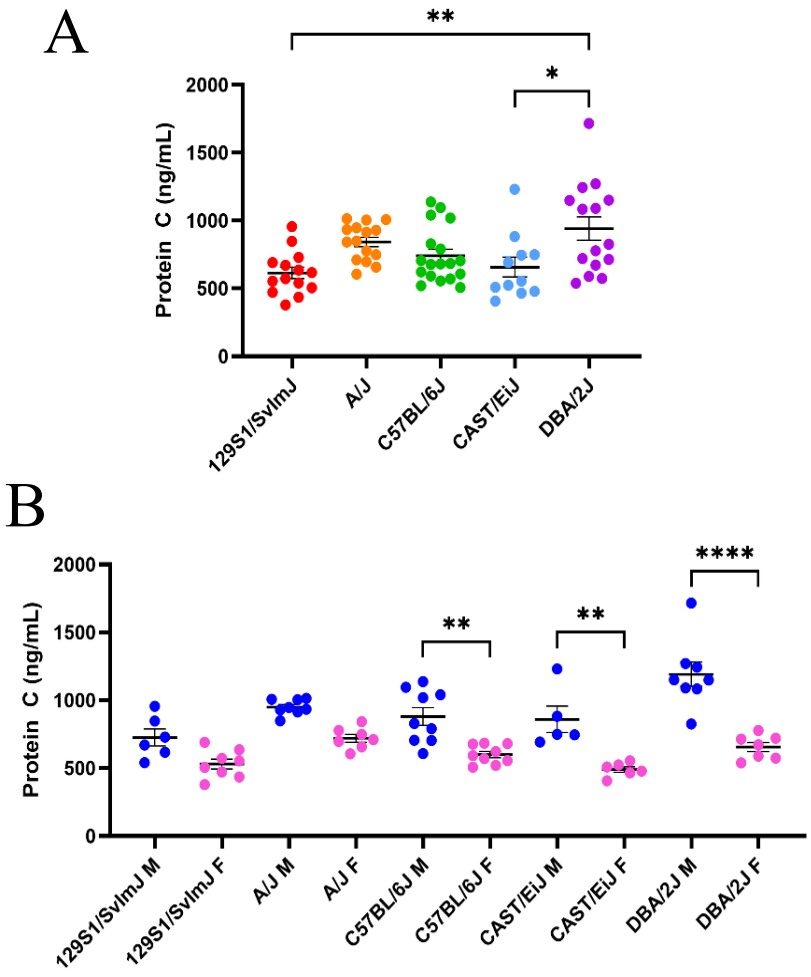

Figure 26: Plasma Protein C Antigen Levels in Five Mouse Strains. A) Plasma Protein C levels in parental mouse strains. Significant differences were seen in the 129S1 and DBA strain (p=0.0019) and the CAST and DBA strain (p=0.0181). B) Sex differences are seen in B6 (p=0.0037), CAST (p=0.0025), and DBA (p<0.0001)

4.3.5 Protein C QTL Analysis Identifies Suggestive Sex Specific Regulatory Locus

QTL analysis of 59 CASTD2F2 individuals with 3,544 total markers was completed using R/qtl[38]. We did not identify any significant or suggestive peaks when running the initial QTL analysis, as seen in Figure 27A. However, when considering sex as an additive covariate, we identified a suggestive peak on Chr 7 (LOD 3.054308, suggestive threshold 2.80, p= 0.339) at marker gJAX00632646. The maximum suggestive position range is 16,231,833-17,733,925. When examining the effect plot seen in Figure 28A, the antigen levels at each genotype are surprising. While our Figure 26A shows DBA individuals having a significantly higher amount of plasma Protein C than the CAST individuals, the opposite is seen here in Figure 28A. Individuals homozygous for the CAST allele (BB) have a higher plasma PC level than those homozygous for the DBA allele (AA), though the effect is not significant. This finding could be due to biological sex being a strong covariate, confounding the effects of the Chr 7 locus until sex is considered as a covariate. We may be seeing a "purer" allelic effect when controlling for sex. This means the CAST allele could increase the PC levels, despite having a lower mean antigen concentration when compared to the DBA strain. When investigating sex as an interactive covariate, no significant peaks were observed. When using the suggestive threshold of $p<0.5$, nearly all Chrs have a suggestive peak. This could be due to the increased complexity of our model being penalized for not increasing the fit of the model[114].

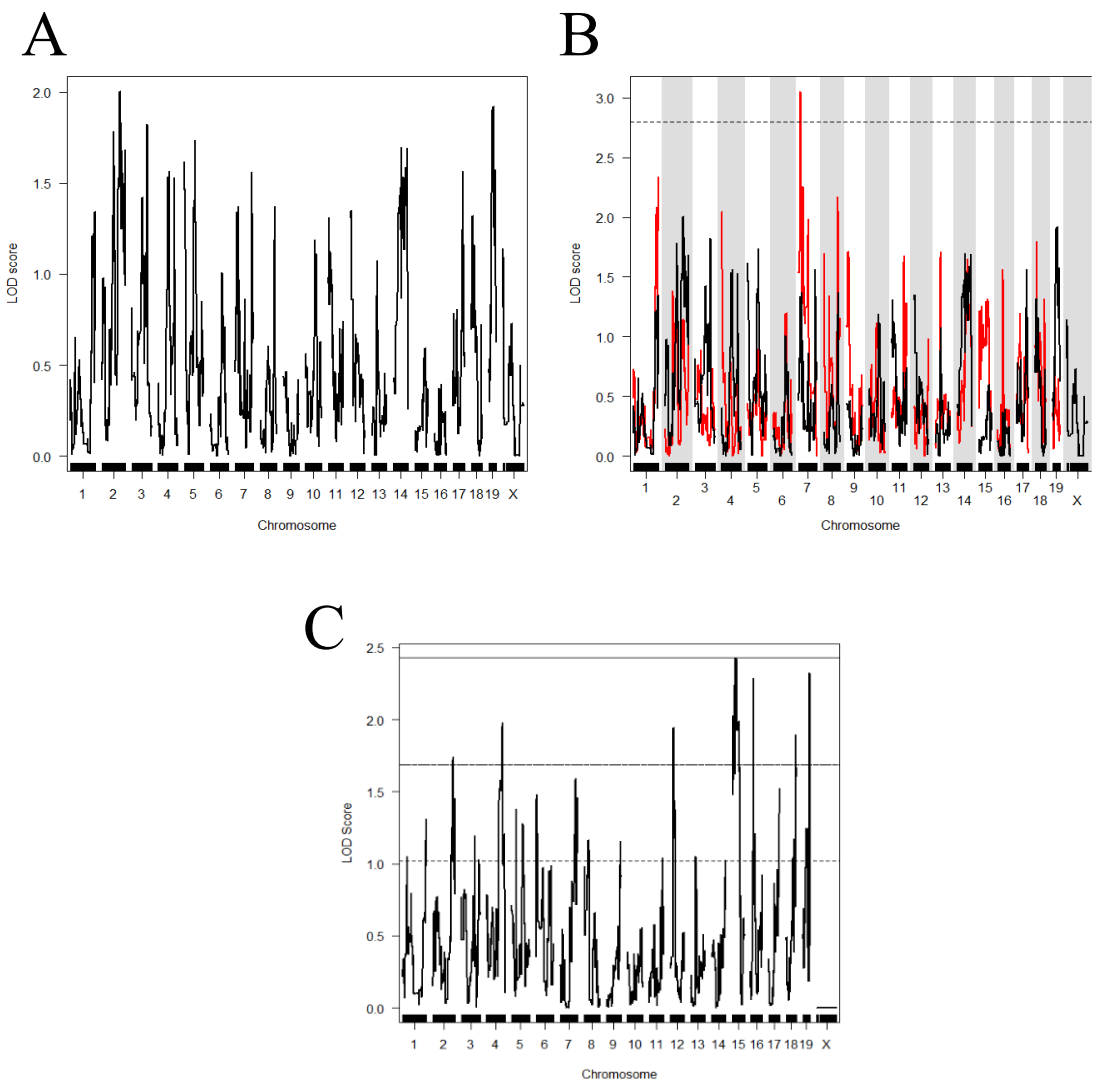

Figure 27: QTL Results from the CASTD2F2 Protein C Cross. A) Whole QTL, with no significant or suggestive peaks seen. B) QTL with sex as an additive covariate. Chr 7 reaches suggestive threshold LOD 3.054308, Suggestive threshold 2.80, p=0.339. C) QTL with sex as an interactive covariate, with no peaks reaching significance. Nearly all Chrs reach the 50% suggestive threshold (bottom dotted line), and 7 Chrs reach the 20% threshold (middle dotted/dashed line).

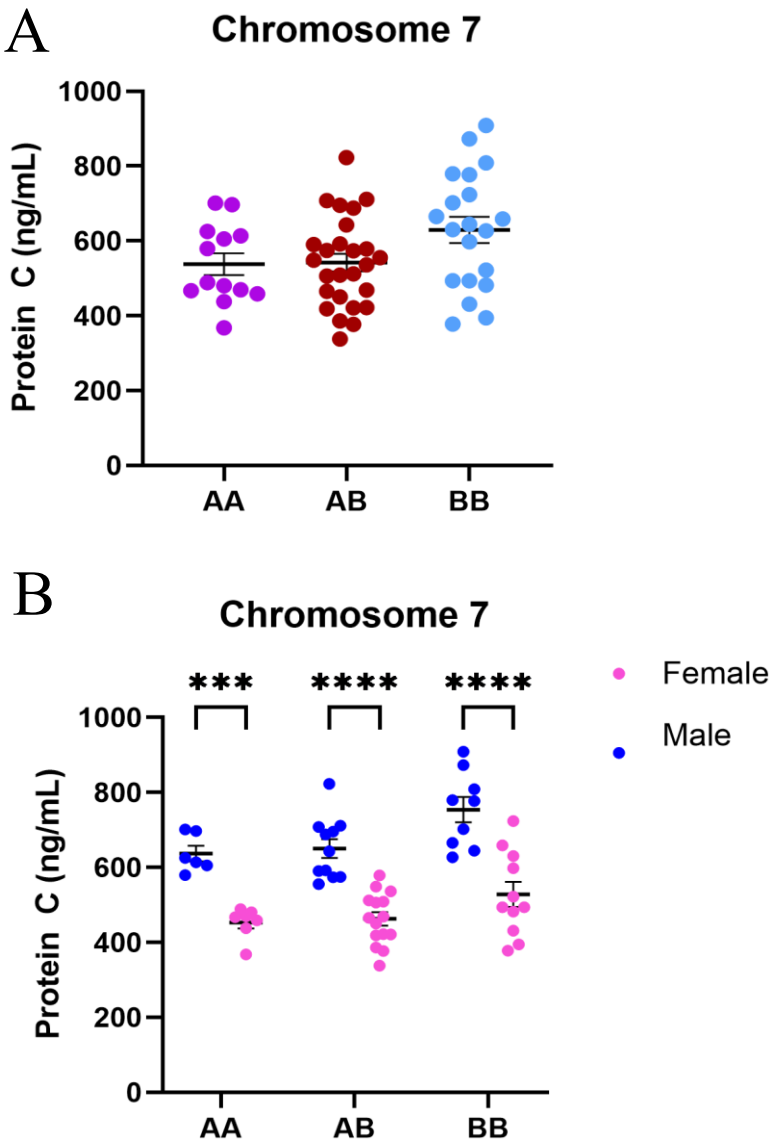

Figure 28: Effect Plots from Chr 7 Peak in CAST x DBA Cross. A) Those homozygous for CAST (BB) have higher Protein C antigen levels than those homozygous for DBA (AA), which is different from what was seen in the parental strain data. This difference is not significant, though. B) There is still a strong Male/Female sex difference in all genotypes (AA: $p=0.0006$, AB & BB: $p<0.0001$).

4.3.6 *Proc* RNA Expression Differences

RT-qPCR analysis of lung tissue RNA collected from 36 individuals revealed a significant difference between expression of the *Proc* gene in B6 wildtype and DBA mice ($p=0.0135$), as seen in Figure 29A. Additionally, liver RNA analysis from 37 individuals demonstrated a significant difference in *Proc* expression between A/J and CAST mice ($p=0.0362$) as seen in Figure 29B. The expression difference in A/J and DBA mice is also trending towards significance ($p=0.0511$). Analyzing additional mice with these genotypes would likely provide more compelling results. We examined the sex differences within each strain and tissue type and discovered no statistically significant differences in *Proc* gene expression between male and female mice. Identical RNA analysis was performed on heart tissue collected from 30 individuals. Interestingly, RT-qPCR showed negligible expression of the *Proc* gene across all strains in the heart. This is likely due to the composition of heart tissue, where cardiomyocytes comprise approximately 80% of the heart by volume[115]. Protein C is activated on the surface of endothelial cells[116], so the reduced number of these cells could lead to virtually no observable expression found in the heart within normal RT-qPCR parameters. Furthermore, we found that 129S1 ($p=0.0117$) and A/J ($p=0.0050$) had greater *Proc* expression in the liver compared to the lungs, as seen in Figure 30. The difference in expression of *Proc* between the liver and the lung is also trending towards significance in DBA mice ($p=0.1376$). This could indicate a regulatory mechanism that acts in a tissue-specific manner that could be explored in future studies.

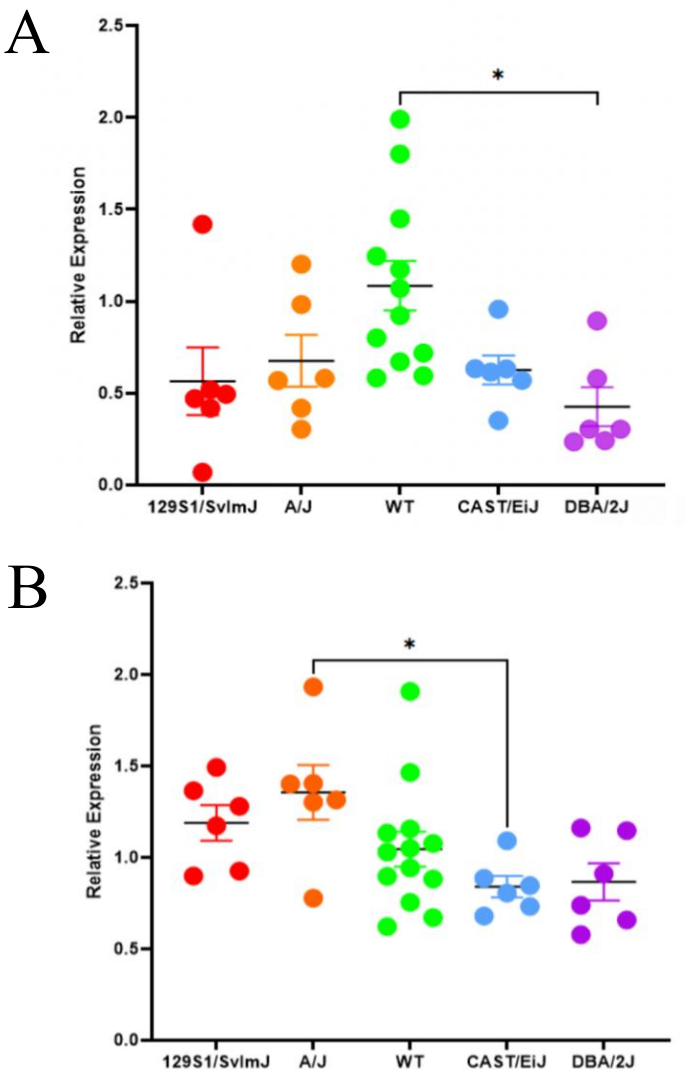

Figure 29: *Proc* Gene Analysis. A) Relative expression of lung tissues obtained from RT-qPCR by normalizing to both reference genes (*Actb*, *GusB*) and wild-type mice, showing significant differences between the wild type and DBA strains, p=0.01355. B) Relative expression of liver tissues obtained from RT-qPCR by normalizing to both reference genes (*Actb, GusB*) and wild-type mice, showing significant differences between the A/J and CAST strains, p=0.0362.

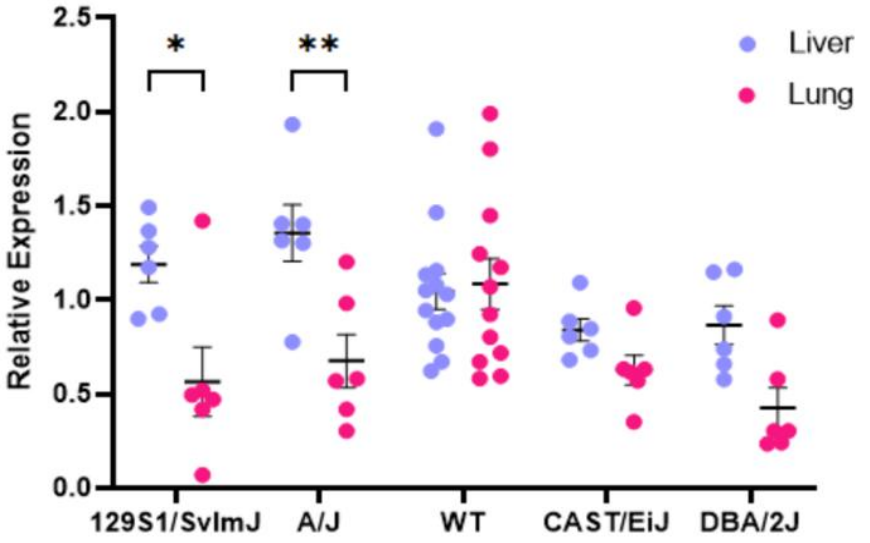

Figure 30: Tissue-Specific Expression Difference of *Proc*. The relative expression of *Proc* was measured to compare tissue-specific differences in the liver and lung, using RT-qPCR and normalization techniques. Significant differences were observed in the 129S1 strain (p=0.0117), and the A/J strain (p=0.0050), with liver tissues having greater *Proc* expression. This trend is consistent across all strains except wild-type, indicating the likelihood of a tissue-specific regulatory mechanism.

CHAPTER FIVE

DISCUSSION AND FINAL THOUGHTS

Thrombosis and medical maladies caused by thrombosis are the most common causes of death in the United States[1]. While blood clotting is an essential natural process, disruption of the complex process of coagulation can lead to thrombosis or hemorrhage[2,3]. The mechanisms of coagulation are well understood, but cell-type specific genetic control is not well studied. My work has uncovered novel insights into the genetic regulation of the important coagulation and fibrinolytic proteins FV, PAI-1, and PC.

While FV is a vital protein in the coagulation cascade, currently, only two genes have been implicated in the regulation of FV, *PLXDC2*[34] and *PSKH2*[35]. *PLXDC2* is located on Chr 2, but a significant distance away from our identified QTL peak. This doesn't entirely exclude it as a possible regulator based on our studies, as it isn't an absolute requirement that the minimal significant region houses the regulatory variant[117].

Additionally, since FV is not produced in megakaryocytes in humans, instead being taken up from the plasma[26,27], it would be interesting to assess additional strains to determine whether there are any that have no FV in the platelets. Another avenue of research for platelet FV includes analyzing whether full length FV is stored in the mouse platelets, or if the FV is partially cleaved and activated. In humans, platelet FV is packaged in a partially cleaved and activated form[26], so investigating whether this also holds for mouse platelets can help us better generalize from mice to humans. Since we have only assessed 5 of the 37 mouse strains[84], our investigations could reveal mice with varying levels of FV, possibly one or more that are human-like. This could provide more

information on the regulation of platelet FV, which is delivered directly to the site of growing thrombi.

PAI-1 is at the center of many diseases[52,56], but it is largely unknown how pPAI-1 (which accounts for ~90% of circulating PAI-1[67]) participates in blood clotting, even though it is delivered directly to the site of the thrombus. With the findings of my work, we can begin to address this gap in knowledge. We have identified the highly significant Chr 5 locus, serving as an "ON/OFF" switch for pPAI-, and have mouse strains with "high", "medium", and "low" levels of PAI-1 in the platelets. Allelic variation in pPAI-1 expression may modulate the balance between coagulation and fibrinolysis in a context-dependent manner. Understanding these allele specific effects is vital, particularly considering evidence suggesting that platelet hyperactivity and resistance to fibrinolysis are major contributors to the pathological thrombosis, MI, stroke, and pulmonary embolism[82].

Since PAI-1 is such an important molecule and involved in many diseases, it is not surprising that there has been development of potential inhibitors of this molecule[118]. Continuation of the research detailed in this manuscript could allow us to identify new drugs that can target pPAI-1 in a cell type specific manner. Small molecule screens can be completed on megakaryocytes to identify if there are any that can reduce the level of pPAI-1 to physiological levels in humans, thus reducing thrombosis risk.

PC deficiency is a severe phenotype[76], and also a promising target for treatment of hemophilia[104]. The drug Drotrecogin Alfa was used to treat patients with baseline PC deficiency in septic shock, and while initially promising[119], the drug was eventually removed from the market as the findings were not replicated in later studies[120]. While

there was consistent benefit to mortality when this drug was used, it was still removed from the market for reasons that may not be able to be answered. Investigating how this molecule is controlled in a cell-type specific manner could allow us to develop a more targeted drug to modulate the levels of PC when there is a deficiency.

In all three cases, further fine mapping is needed to investigate the precise genetic control of these important hemostasis molecules. One way to accomplish this is to use the R/MouseFM package[84] as we did for the PAI-1 crosses. This package uses data from the Mouse Genomes Project (https://www.sanger.ac.uk/data/mouse-genomes-project/). We can take strains with low levels of protein, intermediate levels, and high levels and input them as strains for comparison with the impact set as "high," "moderate" and "low". The output of this analysis is a single nucleotide polymorphism (SNPs) that are the same in "low" strains but different in "high" strains. This information could provide us with SNPs to investigate in the genomic loci found from our QTL analysis and lead us to the specific SNP responsible for the varying levels in the mouse strains. Adding markers and performing additional crosses could also help with mapping and/or identification of the causative variant.

Additionally, increasing the sample size in all cases can increase the power of our analysis. By increasing our sample size, we can potentially increase the number of significant loci[121]. This may help us resolve the loci of our already significant peaks to a narrower genetic range. Also, suggestive peaks may reach significance, allowing us to identify potential modifiers of our three proteins more precisely.

Overall, the results from our research give a better understanding of the cell-type specific genetic regulation of important coagulation molecules. Additional studies are

needed to identify specific genetic regulators and eventually apply our findings to help humans at risk for thrombosis.

.

APPENDIX A

IACUC APPROVAL FOR MOUSE STUDIES

OAKLAND UNIVERSITY
Powered by Google

Caitlyn Conley <conley@oakland.edu>

Committee Action Record – New or De Novo IACUC Protocol # 2022-1164 Approval

1 message

eSirius3GWebServer <no-reply@esirius.cayuse.com> Tue, Apr 5, 2022 at 4:17 PM
To: adamayoub@oakland.edu, ajurek@oakland.edu, arodionova@oakland.edu, cdschneider@oakland.edu, rjwestrick@oakland.edu

Reference: IACUC Protocol # 2022-1164

Protocol Title: Comparative Analysis of Platelet Gene Expression in Inbred and Pregnant Mice

Principal Investigator: Westrick, Randal

Approval Period: 04/04/2022 - 04/04/2025

Dear Professor Westrick, Randal:

The Institutional Animal Care and Use Committee (IACUC) has reviewed the original proposal, noted the required modifications provided by you upon committee's request (if applicable), and approved the project referenced above.

The proposed activities are approved for a period of three years, starting 04/04/2022 and ending 04/04/2025, and assigned the approval # IACUC-2022-1164. Please be aware that protocols expire at 12:01 AM on the expiration date. Ninety (90) days before the protocol approval expires, Cayuse will send you an alert email prompting you to submit a De Novo application to renew the project, if desired.
Any unanticipated problems, changes in, or halting of the activities proposed in the project, as described, must be promptly reported to the IACUC Administrator.

In addition, all faculty, staff, and students involved in the project must be trained and qualified to conduct the project in a responsible manner. Please note, in this regard, that you, the Principal Investigator, are fully responsible at all times.

Please let me know if you have any questions.

Sincerely,

Janet Schofding Animal Research Facility Manager and IACUC Administrator

**This protocol is currently expired, but was active during the completion of the experiments. Animals from this protocol were transferred to protocol 2023-1201 after the expiration of the protocol.

OAKLAND UNIVERSITY
Powered by Google

Caitlyn Conley <conley@oakland.edu>

Committee Action Record – New or De Novo IACUC Protocol # 2023-1201 Approval
1 message

eSirius3GWebServer <no-reply@esirius.cayuse.com> Tue, Aug 8, 2023 at 9:08 AM
To: rjwestrick@oakland.edu

cayuse Animal Oversight

Reference: IACUC Protocol # 2023-1201

Protocol Title: The Identification and Characterization of Thrombosis and Atherothrombosis Modifier Genes

Principal Investigator: Westrick, Randal

Approval Period: 08/08/2023 - 08/08/2026

Dear Professor Westrick, Randal:

The Institutional Animal Care and Use Committee (IACUC) has reviewed the original proposal, noted the required modifications provided by you upon committee's request (if applicable), and approved the project referenced above.

The proposed activities are approved for a period of three years, starting 08/08/2023 and ending 08/08/2026, and assigned the approval # IACUC-2023-1201. This is your formal approval notice; please save it for your records. Be aware that protocols expire at 12:01 AM on the expiration date. Ninety (90) days before the protocol approval expires, Cayuse will send you an alert email prompting you to submit a De Novo application to renew the project, if desired.

Any unanticipated problems, changes in, or halting of the activities proposed in the project, as described, must be promptly reported to the IACUC Administrator.

In addition, all faculty, staff, and students involved in the project must be trained and qualified to conduct the project in a responsible manner. Please note, in this regard, that you, the Principal Investigator, are fully responsible at all times.

Please let me know if you have any questions.

Sincerely,

Janet Schofding
Animal Research Facility Manager and IACUC Administrator

**This protocol is still active and houses all of our animals now.

REFERENCES

1. Ashorobi D, Ameer MA, Fernandez R. Thrombosis. In: *StatPearls*. Treasure Island (FL); 2025.
2. LaPelusa A, Dave HD. Physiology, Hemostasis. In: *StatPearls*. Treasure Island (FL); 2025.
3. Smith SA, Travers RJ, Morrissey JH. How it all starts: Initiation of the clotting cascade. *Crit Rev Biochem Mol Biol*. 2015;50:326-336. doi: 10.3109/10409238.2015.1050550
4. Chaudhry R, Killeen RB, Babiker HM. Physiology, Coagulation Pathways. In: *StatPearls*. Treasure Island (FL); 2025.
5. Bakker CM, Knot EA, Stibbe J, Wilson JH. Disseminated intravascular coagulation in liver cirrhosis. *J Hepatol*. 1992;15:330-335. doi: 10.1016/0168-8278(92)90064-v
6. Lisman T, Porte RJ. Pathogenesis, prevention, and management of bleeding and thrombosis in patients with liver diseases. *Res Pract Thromb Haemost*. 2017;1:150-161. doi: 10.1002/rth2.12028
7. Hou Y, Carrim N, Wang Y, Gallant RC, Marshall A, Ni H. Platelets in hemostasis and thrombosis: Novel mechanisms of fibrinogen-independent platelet aggregation and fibronectin-mediated protein wave of hemostasis. *J Biomed Res*. 2015;29:437-444. doi: 10.7555/JBR.29.20150121
8. Noh JY. Megakaryopoiesis and Platelet Biology: Roles of Transcription Factors and Emerging Clinical Implications. *Int J Mol Sci*. 2021;22. doi: 10.3390/ijms22179615

9. Verhamme P, Hoylaerts MF. The pivotal role of the endothelium in haemostasis and thrombosis. *Acta Clin Belg*. 2006;61:213-219. doi: 10.1179/acb.2006.036

10. Keramati AR, Chen MH, Rodriguez BAT, Yanek LR, Bhan A, Gaynor BJ, Ryan K, Brody JA, Zhong X, Wei Q, et al. Genome sequencing unveils a regulatory landscape of platelet reactivity. *Nat Commun*. 2021;12:3626. doi: 10.1038/s41467-021-23470-9

11. Downes K, Zhao X, Gleadall NS, McKinney H, Kempster C, Batista J, Thomas PL, Cooper M, Michael JV, Kreuzhuber R, et al. G protein-coupled receptor kinase 5 regulates thrombin signaling in platelets via PAR-1. *Blood Adv*. 2022;6:2319-2330. doi: 10.1182/bloodadvances.2021005453

12. Stefanucci L, Frontini M. Non-coding genetic variation in regulatory elements determines thrombosis and hemostasis phenotypes. *J Thromb Haemost*. 2022;20:1759-1765. doi: 10.1111/jth.15754

13. Johnsen JM, Levy GG, Westrick RJ, Tucker PK, Ginsburg D. The endothelial-specific regulatory mutation, Mvwf1, is a common mouse founder allele. *Mamm Genome*. 2008;19:32-40. doi: 10.1007/s00335-007-9079-4

14. Fang C, Huang F, Yao M, Wang Z, Ma J, Wu D, Guo T, Zhang F, Mo J. Advances in microRNA regulation of deep vein thrombosis through venous vascular endothelial cells (Review). *Mol Med Rep*. 2024;29. doi: 10.3892/mmr.2024.13220

15. Briet E, Bertina RM, van Tilburg NH, Veltkamp JJ. Hemophilia B Leyden: a sex-linked hereditary disorder that improves after puberty. *N Engl J Med*. 1982;306:788-790. doi: 10.1056/NEJM198204013061306

16. Kida M, Souri M, Yamamoto M, Saito H, Ichinose A. Transcriptional regulation of cell type-specific expression of the TATA-less A subunit gene for human coagulation factor XIII. *J Biol Chem*. 1999;274:6138-6147. doi: 10.1074/jbc.274.10.6138

17. Gyurina K, Karai B, Ujfalusi A, Hevessy Z, Barna G, Jakso P, Palfi-Meszaros G, Poliska S, Scholtz B, Kappelmayer J, et al. Coagulation FXIII-A Protein Expression Defines Three Novel Sub-populations in Pediatric B-Cell Progenitor Acute Lymphoblastic Leukemia Characterized by Distinct Gene Expression Signatures. *Front Oncol*. 2019;9:1063. doi: 10.3389/fonc.2019.01063

18. Mignotte V, Deveaux S, Filipe A. Transcriptional regulation in megakaryocytes: the thrombopoietin receptor gene as a model. *Stem Cells*. 1996;14 Suppl 1:232-239. doi: 10.1002/stem.5530140730

19. Block KL, Shou Y, Thorton M, Poncz M. The regulated expression of a TATA-less, platelet-specific gene, alphaIIb. *Stem Cells*. 1996;14 Suppl 1:38-47. doi: 10.1002/stem.5530140705

20. Shifman S, Darvasi A. Mouse inbred strain sequence information and yin-yang crosses for quantitative trait locus fine mapping. *Genetics*. 2005;169:849-854. doi: 10.1534/genetics.104.032474

21. Nicolaes GA, Dahlback B. Factor V and thrombotic disease: description of a janus-faced protein. *Arterioscler Thromb Vasc Biol*. 2002;22:530-538. doi: 10.1161/01.atv.0000012665.51263.b7

22. Dahlback B. Novel insights into the regulation of coagulation by factor V isoforms, tissue factor pathway inhibitoralpha, and protein S. *J Thromb Haemost*. 2017;15:1241-1250. doi: 10.1111/jth.13665

23. Santamaria S, Reglinska-Matveyev N, Gierula M, Camire RM, Crawley JTB, Lane DA, Ahnstrom J. Factor V has an anticoagulant cofactor activity that targets the early phase of coagulation. *J Biol Chem*. 2017;292:9335-9344. doi: 10.1074/jbc.M116.769570

24. Huang JN, Koerper MA. Factor V deficiency: a concise review. *Haemophilia*. 2008;14:1164-1169. doi: 10.1111/j.1365-2516.2008.01785.x

25. Rowley JW, Oler AJ, Tolley ND, Hunter BN, Low EN, Nix DA, Yost CC, Zimmerman GA, Weyrich AS. Genome-wide RNA-seq analysis of human and mouse platelet transcriptomes. *Blood*. 2011;118:e101-111. doi: 10.1182/blood-2011-03-339705

26. Gould WR, Simioni P, Silveira JR, Tormene D, Kalafatis M, Tracy PB. Megakaryocytes endocytose and subsequently modify human factor V in vivo to form the entire pool of a unique platelet-derived cofactor. *J Thromb Haemost*. 2005;3:450-456. doi: 10.1111/j.1538-7836.2005.01157.x

27. Camire RM, Pollak ES, Kaushansky K, Tracy PB. Secretable human platelet-derived factor V originates from the plasma pool. *Blood*. 1998;92:3035-3041.

28. Yang TL, Pipe SW, Yang A, Ginsburg D. Biosynthetic origin and functional significance of murine platelet factor V. *Blood*. 2003;102:2851-2855. doi: 10.1182/blood-2003-04-1224

29. Ren M, Li R, Chen N, Pang N, Li Y, Deng X, Wang L, Luo M, Liu Y, Hao H, et al. Platelet-Derived Factor V Is a Critical Mediator of Arterial Thrombosis. *J Am Heart Assoc*. 2017;6. doi: 10.1161/JAHA.117.006345

30. Mohapatra AK, Todaro AM, Castoldi E. Factor V variants in bleeding and thrombosis. *Res Pract Thromb Haemost*. 2024;8:102330. doi: 10.1016/j.rpth.2024.102330

31. Lam W, Moosavi L. Physiology, Factor V. In: *StatPearls*. Treasure Island (FL); 2025.

32. Wood JP, Bunce MW, Maroney SA, Tracy PB, Camire RM, Mast AE. Tissue factor pathway inhibitor-alpha inhibits prothrombinase during the initiation of blood coagulation. *Proc Natl Acad Sci U S A*. 2013;110:17838-17843. doi: 10.1073/pnas.1310444110

33. Lutsey PL, Zakai NA. Epidemiology and prevention of venous thromboembolism. *Nat Rev Cardiol*. 2023;20:248-262. doi: 10.1038/s41569-022-00787-6

34. Thibord F, Hardy L, Ibrahim-Kosta M, Saut N, Pulcrano-Nicolas AS, Goumidi L, Civelek M, Eriksson P, Deleuze JF, Le Goff W, et al. A Genome Wide Association Study on plasma FV levels identified PLXDC2 as a new modifier of the coagulation process. *J Thromb Haemost*. 2019;17:1808-1814. doi: 10.1111/jth.14562

35. Gendre B, Martinez-Perez A, Kleber ME, van Hylckama Vlieg A, Boland A, Olaso R, Germain M, Munsch G, Moissl AP, Suchon P, et al. Genome-Wide Search for Nonadditive Allele Effects Identifies PSKH2 as Involved in the

Variability of Factor V Activity. *J Am Heart Assoc*. 2024;13:e034943. doi: 10.1161/JAHA.124.034943

36. Brake MA, Ivanciu L, Maroney SA, Martinez ND, Mast AE, Westrick RJ. Assessing Blood Clotting and Coagulation Factors in Mice. *Curr Protoc Mouse Biol*. 2019;9:e61. doi: 10.1002/cpmo.61

37. Morgan AP, Fu CP, Kao CY, Welsh CE, Didion JP, Yadgary L, Hyacinth L, Ferris MT, Bell TA, Miller DR, et al. The Mouse Universal Genotyping Array: From Substrains to Subspecies. *G3 (Bethesda)*. 2015;6:263-279. doi: 10.1534/g3.115.022087

38. Broman KW, Wu H, Sen S, Churchill GA. R/qtl: QTL mapping in experimental crosses. *Bioinformatics*. 2003;19:889-890. doi: 10.1093/bioinformatics/btg112

39. Abiola O, Angel JM, Avner P, Bachmanov AA, Belknap JK, Bennett B, Blankenhorn EP, Blizard DA, Bolivar V, Brockmann GA, et al. The nature and identification of quantitative trait loci: a community's view. *Nat Rev Genet*. 2003;4:911-916. doi: 10.1038/nrg1206

40. Lander E, Kruglyak L. Genetic dissection of complex traits: guidelines for interpreting and reporting linkage results. *Nat Genet*. 1995;11:241-247. doi: 10.1038/ng1195-241

41. Peters LL, Cheever EM, Ellis HR, Magnani PA, Svenson KL, Von Smith R, Bogue MA. Large-scale, high-throughput screening for coagulation and hematologic phenotypes in mice. *Physiol Genomics*. 2002;11:185-193. doi: 10.1152/physiolgenomics.00077.2002

42. Dekker J, Heard E. Structural and functional diversity of Topologically Associating Domains. *FEBS Lett*. 2015;589:2877-2884. doi: 10.1016/j.febslet.2015.08.044

43. Westrick RJ, Rojkjaer LP, Yang AY, Roh MH, Siebert AE, Ginsburg D. Deficiency of plasminogen activator inhibitor-2 results in accelerated tumor growth. *J Thromb Haemost*. 2020;18:2968-2975. doi: 10.1111/jth.15054

44. Dougherty KM, Pearson JM, Yang AY, Westrick RJ, Baker MS, Ginsburg D. The plasminogen activator inhibitor-2 gene is not required for normal murine development or survival. *Proc Natl Acad Sci U S A*. 1999;96:686-691. doi: 10.1073/pnas.96.2.686

45. Silverman GA, Whisstock JC, Bottomley SP, Huntington JA, Kaiserman D, Luke CJ, Pak SC, Reichhart JM, Bird PI. Serpins flex their muscle: I. Putting the clamps on proteolysis in diverse biological systems. *J Biol Chem*. 2010;285:24299-24305. doi: 10.1074/jbc.R110.112771

46. Huang X, Rezaie AR, Broze GJ, Jr., Olson ST. Heparin is a major activator of the anticoagulant serpin, protein Z-dependent protease inhibitor. *J Biol Chem*. 2011;286:8740-8751. doi: 10.1074/jbc.M110.188375

47. Mast AE, Ruf W. Regulation of coagulation by tissue factor pathway inhibitor: Implications for hemophilia therapy. *J Thromb Haemost*. 2022;20:1290-1300. doi: 10.1111/jth.15697

48. Johnstone CP, Wang NB, Sevier SA, Galloway KE. Understanding and Engineering Chromatin as a Dynamical System across Length and Timescales. *Cell Syst*. 2020;11:424-448. doi: 10.1016/j.cels.2020.09.011

49. Eitzman DT, Westrick RJ, Nabel EG, Ginsburg D. Plasminogen activator inhibitor-1 and vitronectin promote vascular thrombosis in mice. *Blood*. 2000;95:577-580.

50. Collen D, Lijnen HR. Basic and clinical aspects of fibrinolysis and thrombolysis. *Blood*. 1991;78:3114-3124.

51. Gils A, Declerck PJ. The structural basis for the pathophysiological relevance of PAI-I in cardiovascular diseases and the development of potential PAI-I inhibitors. *Thromb Haemost*. 2004;91:425-437. doi: 10.1160/TH03-12-0764

52. Sillen M, Declerck PJ. A Narrative Review on Plasminogen Activator Inhibitor-1 and Its (Patho)Physiological Role: To Target or Not to Target? *Int J Mol Sci*. 2021;22. doi: 10.3390/ijms22052721

53. Fay WP, Shapiro AD, Shih JL, Schleef RR, Ginsburg D. Brief Report - Complete Deficiency of Plasminogen-Activator Inhibitor Type-1 Due to a Frame-Shift Mutation. *New Engl J Med*. 1992;327:1729-1733. doi: Doi 10.1056/Nejm199212103272406

54. Hamsten A, Wiman B, Defaire U, Blomback M. Increased Plasma-Levels of a Rapid Inhibitor of Tissue Plasminogen-Activator in Young Survivors of Myocardial-Infarction. *New Engl J Med*. 1985;313:1557-1563. doi: Doi 10.1056/Nejm198512193132501

55. Wiman B, Hamsten A. The Fibrinolytic Enzyme-System and Its Role in the Etiology of Thromboembolic Disease. *Semin Thromb Hemost*. 1990;16:207-216. doi: DOI 10.1055/s-2007-1002671

56. Altalhi R, Pechlivani N, Ajjan RA. PAI-1 in Diabetes: Pathophysiology and Role as a Therapeutic Target. *Int J Mol Sci*. 2021;22. doi: 10.3390/ijms22063170

57. Eddy AA. Plasminogen activator inhibitor-1 and the kidney. *Am J Physiol Renal Physiol*. 2002;283:F209-220. doi: 10.1152/ajprenal.00032.2002

58. Urano T, Suzuki Y, Iwaki T, Sano H, Honkura N, Castellino FJ. Recognition of Plasminogen Activator Inhibitor Type 1 as the Primary Regulator of Fibrinolysis. *Curr Drug Targets*. 2019;20:1695-1701. doi: 10.2174/1389450120666190715102510

59. Baker SK, Strickland S. A critical role for plasminogen in inflammation. *J Exp Med*. 2020;217. doi: 10.1084/jem.20191865

60. Eriksson P, Reynisdottir S, Lonnqvist F, Stemme V, Hamsten A, Arner P. Adipose tissue secretion of plasminogen activator inhibitor-1 in non-obese and obese individuals. *Diabetologia*. 1998;41:65-71. doi: 10.1007/s001250050868

61. Czekay RP, Wilkins-Port CE, Higgins SP, Freytag J, Overstreet JM, Klein RM, Higgins CE, Samarakoon R, Higgins PJ. PAI-1: An Integrator of Cell Signaling and Migration. *Int J Cell Biol*. 2011;2011:562481. doi: 10.1155/2011/562481

62. Heissig B, Dhahri D, Eiamboonsert S, Salama Y, Shimazu H, Munakata S, Hattori K. Role of mesenchymal stem cell-derived fibrinolytic factor in tissue regeneration and cancer progression. *Cell Mol Life Sci*. 2015;72:4759-4770. doi: 10.1007/s00018-015-2035-7

63. Harada K, Yahata T, Onizuka M, Ibrahim AA, Kikkawa E, Miyata T, Ando K. Plasminogen activator inhibitor type-1 is a negative regulator of hematopoietic

regeneration in the adipocyte-rich bone marrow microenvironment. *Biochem Biophys Res Commun*. 2021;557:180-186. doi: 10.1016/j.bbrc.2021.04.017

64. Ibrahim AA, Yahata T, Onizuka M, Dan T, Van Ypersele De Strihou C, Miyata T, Ando K. Inhibition of plasminogen activator inhibitor type-1 activity enhances rapid and sustainable hematopoietic regeneration. *Stem Cells*. 2014;32:946-958. doi: 10.1002/stem.1577

65. Sillen M, Declerck PJ. Targeting PAI-1 in Cardiovascular Disease: Structural Insights Into PAI-1 Functionality and Inhibition. *Front Cardiovasc Med*. 2020;7. doi: ARTN 622473
10.3389/fcvm.2020.622473

66. Brogren H, Karlsson L, Andersson M, Wang L, Erlinge D, Jern S. Platelets synthesize large amounts of active plasminogen activator inhibitor 1. *Blood*. 2004;104:3943-3948. doi: 10.1182/blood-2004-04-1439

67. Booth NA, Robbie LA, Croll AM, Bennett B. Lysis of platelet-rich thrombi: the role of PAI-1. *Ann N Y Acad Sci*. 1992;667:70-80. doi: 10.1111/j.1749-6632.1992.tb51599.x

68. Blair P, Flaumenhaft R. Platelet alpha-granules: basic biology and clinical correlates. *Blood Rev*. 2009;23:177-189. doi: 10.1016/j.blre.2009.04.001

69. Brogren H, Sihlbom C, Wallmark K, Lonn M, Deinum J, Karlsson L, Jern S. Heterogeneous glycosylation patterns of human PAI-1 may reveal its cellular origin. *Thromb Res*. 2008;122:271-281. doi: 10.1016/j.thromres.2008.04.008

70. Lawrence DA, Olson ST, Palaniappan S, Ginsburg D. Engineering plasminogen activator inhibitor 1 mutants with increased functional stability. *Biochemistry*. 1994;33:3643-3648. doi: 10.1021/bi00178a022

71. Komissarov AA, Declerck PJ, Shore JD. Mechanisms of conversion of plasminogen activator inhibitor 1 from a suicide inhibitor to a substrate by monoclonal antibodies. *J Biol Chem*. 2002;277:43858-43865. doi: 10.1074/jbc.M204110200

72. Sharp AM, Stein PE, Pannu NS, Carrell RW, Berkenpas MB, Ginsburg D, Lawrence DA, Read RJ. The active conformation of plasminogen activator inhibitor 1, a target for drugs to control fibrinolysis and cell adhesion. *Structure*. 1999;7:111-118. doi: 10.1016/S0969-2126(99)80018-5

73. Conlan MG, Tomasini BR, Schultz RL, Mosher DF. Plasma vitronectin polymorphism in normal subjects and patients with disseminated intravascular coagulation. *Blood*. 1988;72:185-190.

74. Vakeva A, Laurila P, Meri S. Regulation of complement membrane attack complex formation in myocardial infarction. *Am J Pathol*. 1993;143:65-75.

75. Tjarnlund-Wolf A, Brogren H, Lo EH, Wang X. Plasminogen activator inhibitor-1 and thrombotic cerebrovascular diseases. *Stroke*. 2012;43:2833-2839. doi: 10.1161/STROKEAHA.111.622217

76. Kindell DG, Keck RW, Jankun J. Comparison between the clot-protecting activity of a mutant plasminogen activator inhibitor-1 with a very long half-life and 6-aminocaproic acid. *Exp Ther Med*. 2015;9:2339-2343. doi: 10.3892/etm.2015.2399

77. Alessi MC, Poggi M, Juhan-Vague I. Plasminogen activator inhibitor-1, adipose tissue and insulin resistance. *Curr Opin Lipidol*. 2007;18:240-245. doi: 10.1097/MOL.0b013e32814e6d29

78. Jung RG, Motazedian P, Ramirez FD, Simard T, Di Santo P, Visintini S, Faraz MA, Labinaz A, Jung Y, Hibbert B. Association between plasminogen activator inhibitor-1 and cardiovascular events: a systematic review and meta-analysis. *Thromb J*. 2018;16:12. doi: 10.1186/s12959-018-0166-4

79. Ambrosi TH, Scialdone A, Graja A, Gohlke S, Jank AM, Bocian C, Woelk L, Fan H, Logan DW, Schurmann A, et al. Adipocyte Accumulation in the Bone Marrow during Obesity and Aging Impairs Stem Cell-Based Hematopoietic and Bone Regeneration. *Cell Stem Cell*. 2017;20:771-784 e776. doi: 10.1016/j.stem.2017.02.009

80. Luo Y, Chen GL, Hannemann N, Ipseiz N, Kronke G, Bauerle T, Munos L, Wirtz S, Schett G, Bozec A. Microbiota from Obese Mice Regulate Hematopoietic Stem Cell Differentiation by Altering the Bone Niche. *Cell Metab*. 2015;22:886-894. doi: 10.1016/j.cmet.2015.08.020

81. Heissig B, Lund LR, Akiyama H, Ohki M, Morita Y, Romer J, Nakauchi H, Okumura K, Ogawa H, Werb Z, et al. The plasminogen fibrinolytic pathway is required for hematopoietic regeneration. *Cell Stem Cell*. 2007;1:658-670. doi: 10.1016/j.stem.2007.10.012

82. Morrow GB, Mutch NJ. Past, Present, and Future Perspectives of Plasminogen Activator Inhibitor 1 (PAI-1). *Semin Thromb Hemost*. 2023;49:305-313. doi: 10.1055/s-0042-1758791

83. Carmona P, Mendez N, Ili CG, Brebi P. The Role of Clock Genes in Fibrinolysis Regulation: Circadian Disturbance and Its Effect on Fibrinolytic Activity. *Front Physiol*. 2020;11. doi: ARTN 129 10.3389/fphys.2020.00129

84. Munz M, Khodaygani M, Aherrahrou Z, Busch H, Wohlers I. In silico candidate variant and gene identification using inbred mouse strains. *PeerJ*. 2021;9:e11017. doi: 10.7717/peerj.11017

85. Siebert AE, Brake MA, Verbeek SC, Johnston AJ, Morgan AP, Cleuren AC, Jurek AM, Schneider CD, Germain DM, Battistuzzi FU, et al. Identification of Genomic Loci Regulating Platelet Plasminogen Activator Inhibitor-1 in Mice. *J Thromb Haemost*. 2023. doi: 10.1016/j.jtha.2023.06.018

86. Morgan AP, Didion JP, Doran AG, Holt JM, McMillan L, Keane TM, de Villena FPM. Whole Genome Sequence of Two Wild-Derived Mus musculus domesticus Inbred Strains, LEWES/EiJ and ZALENDE/EiJ, with Different Diploid Numbers. *G3-Genes Genom Genet*. 2016;6:4211-4216. doi: 10.1534/g3.116.034751

87. Munz M, Khodaygani M, Aherrahrou Z, Busch H, Wohlers I. In silico candidate variant and gene identification using inbred mouse strains. *Peerj*. 2021;9. doi: ARTN e11017 10.7717/peerj.11017

88. Keele GR, Crouse WL, Kelada SNP, Valdar W. Determinants of QTL Mapping Power in the Realized Collaborative Cross. *G3 (Bethesda)*. 2019;9:1707-1727. doi: 10.1534/g3.119.400194

89. Li XM, Quigg RJ, Zhou J, Xu SZ, Masinde G, Mohan S, Baylink DJ. A critical evaluation of the effect of population size and phenotypic measurement on QTL detection and localization using a large F2 murine mapping population. *Genet Mol Biol*. 2006;29:166-173. doi: Doi 10.1590/S1415-47572006000100030

90. Binder BR, Christ G, Gruber F, Grubic N, Hufnagl P, Krebs M, Mihaly J, Prager GW. Plasminogen activator inhibitor 1: physiological and pathophysiological roles. *News Physiol Sci*. 2002;17:56-61. doi: 10.1152/nips.01369.2001

91. Barnard SA, Pieters M, De Lange Z. The contribution of different adipose tissue depots to plasma plasminogen activator inhibitor-1 (PAI-1) levels. *Blood Rev*. 2016;30:421-429. doi: 10.1016/j.blre.2016.05.002

92. Ishikawa A. A Strategy for Identifying Quantitative Trait Genes Using Gene Expression Analysis and Causal Analysis. *Genes-Basel*. 2017;8. doi: ARTN 347 10.3390/genes8120347

93. Shockley KR, Churchill GA. Gene expression analysis of mouse chromosome substitution strains. *Mamm Genome*. 2006;17:598-614. doi: 10.1007/s00335-005-0176-y

94. Prows DR, Gibbons WJ, Jr., Burzynski BB. Synchronizing allelic effects of opposing quantitative trait loci confirmed a major epistatic interaction affecting acute lung injury survival in mice. *PLoS One*. 2012;7:e38177. doi: 10.1371/journal.pone.0038177

95. Mehic D, Colling M, Pabinger I, Gebhart J. Natural anticoagulants: A missing link in mild to moderate bleeding tendencies. *Haemophilia*. 2021;27:701-709. doi: 10.1111/hae.14356

96. Raife TJ, Lentz SR. The benefits of excess EPCR. *J Thromb Haemost*. 2005;3:1349-1350. doi: 10.1111/j.1538-7836.2005.01462.x

97. Rezaie AR. Regulation of the protein C anticoagulant and antiinflammatory pathways. *Curr Med Chem*. 2010;17:2059-2069. doi: 10.2174/092986710791233706

98. Dahlback B. Advances in Understanding Mechanisms of Thrombophilic Disorders. *Hamostaseologie*. 2020;40:12-21. doi: 10.1055/s-0040-1701612

99. Burstyn-Cohen T, Heeb MJ, Lemke G. Lack of Protein S in mice causes embryonic lethal coagulopathy and vascular dysgenesis. *Journal of Clinical Investigation*. 2009;119:2942-2953. doi: 10.1172/Jci39325

100. Jalbert LR, Rosen ED, Moons L, Chan JC, Carmeliet P, Collen D, Castellino FJ. Inactivation of the gene for anticoagulant protein C causes lethal perinatal consumptive coagulopathy in mice. *J Clin Invest*. 1998;102:1481-1488. doi: 10.1172/JCI3011

101. Gu JM, Crawley JTB, Ferrell G, Zhang FJ, Li WH, Esmon NL, Esmon CT. Disruption of the endothelial cell protein C receptor gene in mice causes placental thrombosis and early embryonic lethality. *Journal of Biological Chemistry*. 2002;277:43335-43343. doi: 10.1074/jbc.M207538200

102. Westrick RJ, Ginsburg D. Modifier genes for disorders of thrombosis and hemostasis. *J Thromb Haemost*. 2009;7 Suppl 1:132-135. doi: 10.1111/j.1538-7836.2009.03362.x

103. Arbini AA, Mannucci PM, Bauer KA. Low-Prevalence of the Factor-V Leiden Mutation among Severe Hemophiliacs with a Milder Bleeding Diathesis. *Thromb Haemostasis*. 1995;74:1255-1258.

104. Zhao YK, Weyand AC, Shavit JA. Novel treatments for hemophilia through rebalancing of the coagulation cascade. *Pediatr Blood Cancer*. 2021;68. doi: ARTN e28934
10.1002/pbc.28934

105. Toomey JR, Kratzer KE, Lasky NM, Stanton JJ, Broze GJ, Jr. Targeted disruption of the murine tissue factor gene results in embryonic lethality. *Blood*. 1996;88:1583-1587.

106. Eitzman DT, Westrick RJ, Bi X, Manning SL, Wilkinson JE, Broze GJ, Ginsburg D. Lethal perinatal thrombosis in mice resulting from the interaction of tissue factor pathway inhibitor deficiency and factor V Leiden. *Circulation*. 2002;105:2139-2142.

107. Jalbert LR, Rosen ED, Moons L, Chan JC, Carmeliet P, Collen D, Castellino FJ. Inactivation of the gene for anticoagulant protein C causes lethal perinatal consumptive coagulopathy in mice. *J Clin Invest*. 1998;102:1481-1488. doi: 10.1172/JCI3011

108. Westrick RJ, Tomberg K, Siebert AE, Zhu G, Winn ME, Dobies SL, Manning SL, Brake MA, Cleuren AC, Hobbs LM, et al. Sensitized mutagenesis screen in Factor V Leiden mice identifies thrombosis suppressor loci. *Proc Natl Acad Sci U S A*. 2017;114:9659-9664. doi: 10.1073/pnas.1705762114

109. Tomberg K, Westrick RJ, Kotnik EN, Cleuren AC, Siemieniak DR, Zhu G, Saunders TL, Ginsburg D. Whole exome sequencing of ENU-induced thrombosis modifier mutations in the mouse. *PLoS Genet*. 2018;14:e1007658. doi: 10.1371/journal.pgen.1007658

110. Cordes SP. N-ethyl-N-nitrosourea mutagenesis: boarding the mouse mutant express. *Microbiol Mol Biol Rev*. 2005;69:426-439. doi: 10.1128/MMBR.69.3.426-439.2005

111. Westrick RJ, Winn ME, Eitzman DT. Murine models of vascular thrombosis (Eitzman series). *Arterioscler Thromb Vasc Biol*. 2007;27:2079-2093. doi: 10.1161/ATVBAHA.107.142810

112. Westrick RJ, Winn ME, Eitzman DT. Murine models of vascular thrombosis (Eitzman series). *Arterioscler Thromb Vasc Biol*. 2007;27:2079-2093. doi: 10.1161/ATVBAHA.107.142810

113. Cui J, Eitzman DT, Westrick RJ, Christie PD, Xu ZJ, Yang AY, Purkayastha AA, Yang TL, Metz AL, Gallagher KP, et al. Spontaneous thrombosis in mice carrying the factor V Leiden mutation. *Blood*. 2000;96:4222-4226.

114. Manichaikul A, Moon JY, Sen S, Yandell BS, Broman KW. A model selection approach for the identification of quantitative trait loci in experimental crosses, allowing epistasis. *Genetics*. 2009;181:1077-1086. doi: 10.1534/genetics.108.094565

115. Zhou P, Pu WT. Recounting Cardiac Cellular Composition. *Circ Res*. 2016;118:368-370. doi: 10.1161/CIRCRESAHA.116.308139

116. Navarro S, Bonet E, Estelles A, Montes R, Hermida J, Martos L, Espana F, Medina P. The endothelial cell protein C receptor: its role in thrombosis. *Thromb Res*. 2011;128:410-416. doi: 10.1016/j.thromres.2011.08.001

117. Broekema RV, Bakker OB, Jonkers IH. A practical view of fine-mapping and gene prioritization in the post-genome-wide association era. *Open Biol*. 2020;10:190221. doi: 10.1098/rsob.190221

118. Miyata T. Overview: PAI-1 inhibitors and clinical applications. *Biomed J*. 2025:100874. doi: 10.1016/j.bj.2025.100874

119. Ranieri VM, Thompson BT, Barie PS, Dhainaut JF, Douglas IS, Finfer S, Gardlund B, Marshall JC, Rhodes A, Artigas A, et al. Drotrecogin alfa (activated) in adults with septic shock. *N Engl J Med*. 2012;366:2055-2064. doi: 10.1056/NEJMoa1202290

120. Lai PS, Thompson BT. Why activated protein C was not successful in severe sepsis and septic shock: are we still tilting at windmills? *Curr Infect Dis Rep*. 2013;15:407-412. doi: 10.1007/s11908-013-0358-9

121. Chitre AS, Polesskaya O, Munro D, Cheng R, Mohammadi P, Holl K, Gao J, Bimschleger H, Martinez AG, George AM, et al. An exponential increase in QTL detection with an increased sample size. *Genetics*. 2023;224. doi: 10.1093/genetics/iyad054